Eur. Phys. J. C (2017) 77:381
DOI 10.1140/epjc/s10052-017-4921-7

THE EUROPEAN PHYSICAL JOURNAL C

Regular Article - Theoretical Physics

Top–down holographic G-structure glueball spectroscopy at (N)LO in N and finite coupling

Karunava Sil[a], **Vikas Yadav**[b], **Aalok Misra**[c]

Department of Physics, Indian Institute of Technology, Roorkee, Uttaranchal 247 667, India

Received: 25 April 2017 / Accepted: 15 May 2017 / Published online: 9 June 2017

Abstract The top–down type IIB holographic dual of large-N thermal QCD as constructed in Mia et al. (Nucl Phys B 839:187, 2010) involving a fluxed resolved warped deformed conifold, its delocalized type IIA Strominger–Yau–Zaslow-mirror (SYZ-mirror) as well as its M-theory uplift constructed in Dhuria and Misra (JHEP 1311:001, 2013) – both in the finite coupling ($g_s \overset{<}{\sim} 1$)/'MQGP' limit of Dhuria and Misra (JHEP 1311:001, 2013) – were shown explicitly to possess a local $SU(3)/G_2$-structure in Sil and Misra (Nucl Phys B 910:754, 2016). Glueballs spectra in the *finite-gauge-coupling limit* (and not just large 't Hooft coupling limit) – a limit expected to be directly relevant to strongly coupled systems at finite temperature such as QGP (Natsuume in String theory and quark–gluon plasma, 2007) – has thus far been missing in the literature. In this paper, we fill this gap by calculating the masses of the $0^{++}, 0^{-+}, 0^{--}, 1^{++}, 2^{++}$ ('glueball') states (which correspond to fluctuations in the dilaton or complexified two-forms or appropriate metric components) in the aforementioned backgrounds of G-structure in the 'MQGP' limit of Dhuria and Misra (JHEP 1311:001, 2013). We use WKB quantization conditions on one hand and impose Neumann/Dirichlet boundary conditions at an IR cut-off ('r_0')/horizon radius ('r_h') on the solutions to the equations of motion on the other hand. We find that the former technique produces results closer to the lattice results. We also discuss the $r_h = 0$ limits of all calculations. In this context we also calculate the $0^{++}, 0^{--}, 1^{++}, 2^{++}$ glueball masses up to Next to Leading Order (NLO) in N and find a $\frac{g_s M^2}{N}(g_s N_f)$-suppression similar to and further validating semi-universality of NLO corrections to transport coefficients, observed in Sil and Misra (Eur Phys J C 76(11):618, 2016).

[a] e-mail: krusldph@iitr.ac.in

[b] e-mail: viitr.dph2015@iitr.ac.in

[c] e-mail: aalokfph@iitr.ac.in

1 Introduction

The AdS/CFT correspondence [1] remarkably establishes an equivalence between the partition functions of a five-dimensional gravitational theory (bulk theory) and a four-dimensional supersymmetric and scale invariant gauge theory (boundary theory). A generalization of the AdS/CFT correspondence is necessary to explore more realistic gauge theories (less supersymmetric and non-conformal) such as QCD with $SU(3)$ gauge group. The top–down model that we have considered in this work is motivated by the desire to capture QCD-like gauge theories from a suitable gravitational background. QCD is a strongly coupled theory at low energies. The low energy dynamics of QCD involves the color-neutral bound states of gluons, known as glueballs. Hence, the non-perturbative aspects of QCD can be largely understood from the glueball sector of the theory. Moreover, the plasma phase of QCD (QGP) occurs at high temperatures $T > T_c$. In a QGP medium the quarks and the gluons stay in a deconfined state due to Debye screening. However, the recent RHIC experiments indicate strongly that non-perturbative effects of QCD are present in the plasma phase. In fact the lattice results of [2] conclude that QGP must be non-perturbative in the temperature regime $T_c \leq T \leq 5T_c$. This is precisely the reason why we concentrate on the glueball spectra in the *finite-gauge-coupling limit* (and not just large 't Hooft coupling limit) – a limit expected to be directly relevant to strongly coupled systems at finite temperature such as QGP [3].

QCD is a non-abelian gauge theory, in which gauge fields play the role of dynamical degrees of freedom. Non-abelian nature of QCD allows the gauge bosons to form color-neutral bound states of gluons known as glueballs (gg, ggg, etc.). Therefore, the study of glueballs and their spectra enables us to gain a better understanding of the non-perturbative regime of QCD. The glueball state is represented by quantum numbers J^{PC}, where J, P and C correspond to total angular momentum, parity and charge conjugation, respectively.

Different generalized versions of the AdS/CFT correspondence has thus far been proposed to study non-supersymmetric field theories with a running gauge coupling constant. The original proposal was given by Witten to obtain a gravity dual for non-supersymmetric field theories. As per Witten's formalism, non-supersymmetric Yang–Mills theory can be obtained by compactifying one of the spatial direction on a circle and imposing antiperiodic boundary conditions on the fermions around this circle. This makes the fermions and scalars massive and they get decoupled leaving only gauge fields as degrees of freedom. The gravity dual of this compactified theory was asymptotically AdS. In a particular case of $\mathcal{N} = 4$ SU(N) super-Yang–Mills theory dual to type IIB string theory on $AdS_5 \times S^5$, the procedure described above gives an effective model of three-dimensional Yang–Mills theory, i.e., QCD_3.

The gravity dual of non-supersymmetric theories in the low energy limit is typically given by supergravity backgrounds involving $AdS_p \times M_q$ where AdS is the anti de Sitter space with dimension p and M_q is the internal manifold with dimension q. In supergravity theory the Kaluza–Klein modes on M_q can be classified according to the spherical harmonics of M_q, which forms representations of the isometry group of M_q. The states carrying the non-trivial isometry group quantum numbers are heavier and do not couple to the pure gluonic operators on the boundary. Thus the glueballs are identified with singlet states of the isometry group.

In the past decade, glueballs have been studied extensively to gain new insight into the non-perturbative regime of QCD. Various holographic setups such as soft-wall model, hard-wall model, modified soft wall model, etc. have been used to obtain the glueball's spectra. In [4,5] a soft wall holographic model was used to study the glueball spectrum. In [4] glueballs and scalar mesons were studied at finite temperature. It was found that the masses of the hadronic states decreases and the widths become broader as T increases. But for a temperature range of the order of 40–60 MeV, states disappear from the glueball and meson spectral function. Both hard-wall and soft-wall holographic models were considered [6,7] to obtain the glueball correlation functions to study the dynamics of QCD. Decay rates were obtained for glueballs in both models. Dynamical content of the correlators was investigated [7] by obtaining their spectral density and relating it with various other quantities to obtain the estimates for three lowest-dimensional gluon condensates. In [8] a two-flavor quenched dynamical holographic QCD model was considered with two different forms for the dilaton field given as $\Phi = \mu_G^2 z^2$ and $\Phi = \mu_G^2 z^2 \tanh(\mu_G^4 z^2/\mu_G^2)$, ($z$ being a radial coordinate). In [9] an AdS_5 mass renormalization was implemented in a modified holographic soft-wall model to obtain the spectrum of scalar and higher even glueball spin states with $P = C = +1$. In [10,11] a bottom–up approach was used to obtain the mass spectra of the scalar and vector glueballs. In this case, the vector glueball masses were found to be heavier than that of the scalar glueballs while higher values for both were reported in other approaches. In [12] a holographic description was used for supersymmetric and non-supersymmetric, non-commutative dipole gauge theory in 4D. The WKB approximation was used to obtain the mass by solving the dilaton and antisymmetric tensor field equations in the bulk. For the supersymmetric theory, dipole length plays the role of an intrinsic scale while for non-supersymmetric theory the same role is played by the temperature Two different phases for baryons were found, a big baryon dual to the static string and a small baryon dual to a moving string. In [13] spectrum for scalar, vector and tensor two-gluon and trigluon glueballs were obtained in 5-D holographic QCD model with a metric structure deformed by the dilaton field. The spectrum was compared with the results obtained from both soft-wall and hard-wall holographic QCD models. Here, the spectra of the two-gluon glueball was found to be in agreement with the lattice data. For trigluon glueballs, the masses for $1^{\pm-}, 2^{--}$ were matched while masses for $0^{--}, 0^{+-}$ and 2^{+-} were lighter than lattice data which indicates that the latter glueballs are dominated by the three-gluon condensate. In [14] a holographic glueball spectrum was obtained in the singlet sector of $\mathcal{N} = 1$ supersymmetric Klebanov–Strassler model. States containing the bifundamental A_i and B_i fields were not considered. Comparison with the lattice data showed a nice agreement for 1^{+-} and 1^{--} states, while 0^{+-} results were different because of its fermionic component.

Glueballs appear in the meson spectra of QCD and the difficulty in their identification in the meson spectra is largely due to lack of information as regards their coupling with mesons in strongly coupled QCD. Lattice QCD gives an estimate for the masses but it does not give any information as regards the glueball couplings and their decay widths both of which are required for identification of glueballs. Holographic approach gives a better understanding of glueball decay rates than lattice QCD. Various holographic models such as Witten–Sakai–Sugimoto model, Soft wall model and supersymmetric Klebanov–Strassler model, etc. have been used to obtain the coupling between mesons and glueballs to obtain expressions for the glueball decay widths.

In [15–20] top–down Witten–Sakai–Sugimoto model was used as a holographic setup for low energy QCD to obtain the coupling of scalar glueballs to mesons and subsequently obtain their decay widths. Results obtained were compared with the experimental data available for lattice counterparts $f_0(1500)$ and $f_0(1710)$ of scalar glueballs. In [15] results obtained for decay widths and branching ratios for scalar glueball decays were found to be consistent with experimental data for $f_0(1500)$ state in [15] while in [17] results favored $f_0(1710)$ as scalar glueball candidate instead of $f_0(1500)$. Decay patterns were obtained for scalar glueball candidate

$f_0(1710)$ in top–down holographic Witten–Sakai–Sugimoto model for low energy QCD in [16]. It was shown that there exists a narrow pseudoscalar glueball heavier than the scalar glueball whose decay pattern involves η and η' mesons. In [18–20] Witten–Sakai–Sugimoto model was used to study the phenomenology of scalar glueball states. A dilaton and an exotic mode were obtained as two sets of scalar glueball states in [18,19]. Calculation of mass spectra showed that out of two modes, dilaton mass is quite close to both $f_0(1710)$ and $f_0(1500)$ scalar glueball candidates while calculation of decay width showed that $f_0(1710)$ is the favored glueball candidate corresponding to dilaton mode. In [21] the holographic top–down Witten–Sakai–Sugimoto model was used to study the tensor 2^{++} glueball mass spectrum and decay width. Decay width was found to be above 1 GeV for glueball mass $M_T = 2400$ MeV while for $M_T = 2000$ MeV it was reduced to 640 MeV. In [22] modified holographic soft-wall model was used to calculate the mass spectrum and Regge trajectories of lightest scalar glueball and higher spin glueball states. Results were obtained for both even and odd spins glueball states.

In this paper, we use a large-N top–down holographic dual of QCD to obtain the spin $2^{++}, 1^{++}, 0^{++}, 0^{--}, 0^{-+}$ glueball spectrum explicitly for QCD_3 from type IIB, type IIA and M-theory perspectives. Now for the computation of the glueball masses, we need to introduce a scale in our theory. In other words, the conformal invariance has to be broken. This can be done in two different ways. The first approach, after Witten [23], corresponds to the compactification of the time direction on a circle of finite radius, forming a black hole in the background. In this case the masses are determined in units of the horizon radius r_h of the black hole. The other approach is to consider a cut-off at $r = r_0$ in the gravitational background (r being the non-compact radial direction) [24]. This forbids the arbitrary low energy excitations of the boundary field theory and hence breaks the conformal invariance. So, in this case the required scale to address strong interaction is introduced by the IR cut-off r_0. From a top–down perspective this IR cut-off will in fact be proportional to two-third power of the Ouyang embedding parameter obtained from the minimum radial distance (corresponding to the lightest quarks) requiring one to be at the South Poles in the $\theta_{1,2}$ coordinates, in the holomorphic Ouyang embedding of flavor $D7$-branes. In the spirit of [23], the time direction for both cases will be compact with fermions obeying antiperiodic boundary conditions along this compact direction, and hence we will be evaluating three-dimensional glueball masses.

Glueball masses can be obtained by evaluating the correlation functions of gauge invariant local operator. The first step to obtain the glueball spectrum in QCD_3 is to identify the operators in the gauge theory that have quantum number corresponding to the glueballs of interest. According to the gauge/gravity duality each supergravity mode corresponds to a gauge-theory operator. This operator couples to the supergravity mode at the boundary of the AdS space, for example, the lowest dimension operator with quantum numbers $J^{PC} = 0^{++}$ is $\mathrm{Tr}F^2 = \mathrm{Tr}F_{\mu\nu}F^{\mu\nu}$ and this operator couples to the dilaton mode on the boundary. To calculate 0^{++} glueball mass we need to evaluate the correlator $\langle \mathrm{Tr}F^2(x)\mathrm{Tr}F^2(y)\rangle = \Sigma_i c_i e^{-m_i|x-y|}$, where m_i give the value for glueball mass. However, the masses can also be obtained by solving the wave equations for supergravity modes which couples to the gauge-theory operators on the boundary. The latter approach is used in this paper.

The 11D metric obtained as the uplift of the delocalized Strominger–Yau–Zaslow (SYZ) type IIA metric, up to LO in N, can be interpreted as a black $M5$-brane wrapping a two-cycle, i.e. a black $M3$-brane [25,26]. Taking this as the starting point, compactifying again along the M-theory circle, we land up at the type IIA metric and then compactifying again along the periodic temporal circle (with the radius given by the reciprocal of the temperature), one obtains QCD_3 corresponding to the three non-compact directions of the black $M3$-brane world volume. The Type IIB background of [27], in principle, involves $M_4\times$ RWDC(≡Resolved Warped Deformed Conifold); asymptotically the same becomes $AdS_5 \times T^{1,1}$. To determine the gauge-theory fields that would couple to appropriate supergravity fields à la gauge-gravity duality, ideally one should work the same out for the $M_4\times$ RWDC background (which would also involve solving for the Laplace equation for the internal RWDC). We do not attempt to do the same here. Motivated, however, by, e.g.,

(a) asymptotically the type IIB background of [27] and its delocalized type IIA mirror of [28] consist of AdS_5 and
(b) terms of the type $\mathrm{Tr}(F^2(AB)^k)$, $(F^4(AB)^k)$ where $F^2 = F_{\mu\nu}F^{\mu\nu}$, $F^4 = F_{\mu_1}^{\mu_2}F_{\mu_2}^{\mu_3}F_{\mu_3}^{\mu_4}F_{\mu_4}^{\mu_1} - \frac{1}{4}\left(F_{\mu_1}^{\mu_2}F_{\mu_2}^{\mu_1}\right)^2$, A, B being the bifundamental fields that appear in the gauge-theory superpotential corresponding to $AdS_5 \times T^{1,1}$ in [29], form part of the gauge-theory operators corresponding to the solution to the Laplace equation on $T^{1,1}$ [30] (the operator $\mathrm{Tr}F^2$, which shares the quantum numbers of the 0^{++} glueball, couples to the dilaton and $\mathrm{Tr}F^4$ which also shares the quantum numbers of the 0^{++} glueball couples to trace of metric fluctuations and the four-form potential, both in the internal angular directions),

we calculate in this paper:

- type IIB dilaton fluctuations, which we refer to as 0^{++} glueball
- type IIB complexified two-form fluctuations that couple to $d^{abc}\mathrm{Tr}(F^a_{\mu\rho}F^{b\ \rho}_{\lambda}F^{c\ \lambda}_{\nu})$, which we refer to as 0^{--} glueball

- type IIA one-form fluctuations that couple to $\mathrm{Tr}(F \wedge F)$, which we refer to as 0^{-+} glueball
- M-theory metric's scalar fluctuations which we refer to as another (lighter) 0^{++} glueball
- M-theory metric's vector fluctuations which we refer to as 1^{++} glueball,
  and
- M-theory metric's tensor fluctuations which we refer to as 2^{++} glueball.

All holographic glueball spectra calculations done thus far, have only considered a large 't Hooft coupling limit: $g^2_{\mathrm{YM}}N \gg 1,\ N \gg 1$. However, holographic duals of thermal QCD laboratories like sQGP also require a finite gauge coupling [3]. This was addressed as part of the 'MQGP limit' in [28]. It is in this regard that results of this paper – which discusses supergravity glueball spectra at finite string coupling – are particularly significant. Also, the recent observation – see, e.g., [31] – that the non-perturbative properties of quark–gluon plasma can be related to the change of properties of scalar and pseudoscalar glueballs, makes the study of glueballs quite important.

The rest of the paper is organized as follows. In Sect. 2, via five subsections, we summarize the top–down type IIB holographic dual of large-N thermal QCD of [27], its delocalized SYZ type IIA mirror and its M-theory uplift of [25,28]. In Sect. 3, we discuss a supergravity calculation of the spectrum of 0^{++} glueball at finite horizon radius r_h (Sect. 3.1) and setting $r_h = 0$ (Sect. 3.2). The $r_h \neq 0$ computations are given in Sect. 3.1, corresponding to use of WKB quantization conditions using coordinate/field redefinitions of [32]. The $r_h = 0$ calculations are subdivided into Sect. 3.2.1 corresponding to solving the 0^{++} equation of motion up to LO in N and imposing the Neumann/Dirichlet boundary condition at the horizon, and Sect. 3.2.2 corresponding to WKB quantization conditions inclusive of non-conformal/NLO-in-N corrections using the redefinitions of [32]. Section 4 has to do with the 0^{-+} glueball spectrum. Further therein, Sects. 4.1.1 and 4.1.2, respectively, are on obtaining the $r_h \neq 0$ spectrum and its $r_h = 0$ limit using Neumann/Dirichlet boundary conditions on the solutions up to LO in N, respectively, at the horizon and the IR cut-off. Then Sects. 4.1.3 and 4.1.4, respectively, are on WKB quantization at finite and zero r_h up to LO in N, using the redefinitions of [32]. Section 5 is on 0^{--} glueball spectrum. Therein, Sects. 5.1 and 5.2 are on getting the spectrum by imposing Neumann/Dirichlet boundary condition on the solutions up to LO in N to the EOM, respectively, at the horizon and the IR cut-off. Section 5.3 has to do with obtaining the spectrum using WKB quantization up to LO in N at $r_h \neq 0$ using the redefinitions of [32]; Sect. 5.4 has to do with a similar calculation in the $r_h = 0$ limit at LO in N in Sect. 5.4.1 and up to NLO in N in Sect. 5.4.2. Section 6 has to do with M-theory calculations of 0^{++}, 1^{++}, 2^{++} glueballs arising from appropriate metric fluctuations. Section 6.1 is on such a 0^{++} glueball spectrum, whereas in Sect. 6.1.1 and Sect. 6.1.2 we obtain the same with a finite horizon radius r_h and an IR cut-off r_0, respectively, both by imposing Neumann/Dirichlet boundary conditions (at the horizon/IR cut-off) and using WKB quantization conditions and the redefinitions of [32]. Section 6.2 is on such a 2^{++} glueball spectrum with a finite horizon radius r_h in Sect. 6.2.1 and an IR cut-off r_0 in Sect. 6.2.2. The results are obtained by imposing Neumann/Dirichlet boundary conditions at the horizon/IR cut-off and also via WKB quantization conditions using redefinitions of [32] at LO in N in Sect. 6.2.1 ($r_h \neq 0$) and both at LO as well as up to NLO in N in Sect. 6.2.1 ($r_h = 0$ limit). Section 6.3 is on such a 1^{++} glueball spectrum, where similar to the previous sections, we have imposed Neumann/Dirichlet boundary conditions (at the horizon/IR cut-off) and used WKB quantization conditions and the redefinitions of [32]. The spectrum corresponding to the finite horizon radius r_h at LO in N is discussed in Sect. 6.3.1. On the other hand, the results corresponding to that with an IR cut-off r_0 both at LO and up to NLO in N is given in Sect. 6.3.2. From the point of view of comparing the string theory and the M-theory glueball spectrum calculations, we obtain the 2^{++} glueball spectrum arising from tensor mode of metric fluctuations in the type IIB background of [27] in Sect. 7. Section 7.1 has to do with a supergravity calculation (via Neumann/Dirichlet boundary conditions at the horizon in Sect. 7.1.1 and WKB quantization condition using redefinitions of [32] in Sect. 7.1.2), and Sect. 7.2 has to do with zero-horizon radius limit calculation (WKB quantization condition using redefinitions of [32] at LO in N in Sect. 7.2.1 and up to NLO in N in Sect. 7.2.2). Section 8 contains a summary and discussion of the results obtained in this paper. There a Appendix A on the square of different fluxes that appear in EOM relevant to spin-two perturbations of the type IIB metric.

2 Background: a top–down type IIB holographic large-N thermal QCD and its M-theory uplift in the 'MQGP' limit

In this section, via five subsections we will:

- provide a short review of the type IIB background of [27] which is supposed to provide a UV complete holographic dual of large-N thermal QCD, as well as their precursors in Sect. 2.1,
- discuss the 'MQGP' limit of [28] and the motivation for considering the same in Sect. 2.2,
- briefly review issues as discussed in [28] pertaining to construction of delocalized S(trominger) Y(au) Z(aslow) mirror and approximate supersymmetry, in Sect. 2.3,

- briefly review the new results of [25,33] pertaining to construction of explicit $SU(3)$ and G_2 structures, respectively, of type IIB/IIA and M-theory uplift,
- briefly discuss the new Physics-related results of [25,33], in Sect. 2.4.

2.1 Type IIB dual of large-N thermal QCD

In this subsection, we will discuss a UV complete holographic dual of large-N thermal QCD as given in Dasgupta–Mia et al. [27]. As mentioned in Sect. 1, this was inspired by the zero-temperature Klebanov–Witten model [29], the non-conformal Klebanov–Tseytlin model [34], its IR completion as given in the Klebanov–Strassler model [35] and Ouyang's inclusion [36] of flavor in the same,[1] as well as the non-zero temperature/non-extremal version of [37] (the solution, however, was not regular as the non-extremality/black-hole function and the ten-dimensional warp factor vanished simultaneously at the horizon radius) [38,39] (valid only at high temperatures) of the Klebanov–Tseytlin model and [40] (addressing the IR region), in the absence of flavors.

(a) Brane construction
In order to include fundamental quarks at non-zero temperature in the context of type IIB string theory, to the best of our knowledge, the following model proposed in [27] is the closest to a UV complete holographic dual of large-N thermal QCD. The KS model (after a duality cascade) and QCD have similar IR behavior: $SU(M)$ gauge group and IR confinement. However, they differ drastically in the UV as the former yields a logarithmically divergent gauge coupling (in the UV) – Landau pole. This necessitates modification of the UV sector of the KS model apart from inclusion of non-extremality factors. With this in mind and building up on all of the above, the type IIB holographic dual of [27] was constructed. The setup of [27] is summarized below.

- From a gauge-theory perspective, the authors of [27] considered N black $D3$-branes placed at the tip of six-dimensional conifold, M $D5$-branes wrapping the vanishing two-cycle and M $\overline{D5}$-branes distributed along the resolved two-cycle and placed at the outer boundary of the IR–UV interpolating region/inner boundary of the UV region.
- More specifically, the M $\overline{D5}$ are distributed around the antipodal point relative to the location of M $D5$ branes on the blown-up S^2. If the $D5/\overline{D5}$ separation is given by $\mathcal{R}_{D5/\overline{D5}}$, then this provides the boundary common to the outer UV–IR interpolating region and the inner UV region. The region $r > \mathcal{R}_{D5/\overline{D5}}$ is the UV. In other words, the radial space, in [27] is divided into the IR region, the IR–UV interpolating region and the UV. To summarize the above:
  - $r_0/r_h < r < |\mu_{\text{Ouyang}}|^{\frac{2}{3}}(r_h = 0)/\mathcal{R}_{D5/\overline{D5}}(r_h \neq 0)$: the IR/IR–UV interpolating regions with $r \sim \Lambda$: deep IR where the $SU(M)$ gauge theory confines
  - $r > |\mu_{\text{Ouyang}}|^{\frac{2}{3}}(r_h = 0)/\mathcal{R}_{D5/\overline{D5}}(r_h \neq 0)$: the UV region.
- N_f $D7$-branes, via Ouyang embedding, are holomorphically embedded in the UV (asymptotically $AdS_5 \times T^{1,1}$), the IR–UV interpolating region and dipping into the (confining) IR (up to a certain minimum value of r corresponding to the lightest quark) and N_f $\overline{D7}$-branes present in the UV and the UV–IR interpolating (not the confining IR). This is to ensure turning off of three-form fluxes, constancy of the axion–dilaton modulus and hence conformality and absence of Landau poles in the UV region.
- The resultant ten-dimensional geometry hence involves a resolved warped deformed conifold. Back-reactions are included, e.g., in the ten-dimensional warp factor. Of course, the gravity dual, as in the Klebanov–Strassler construct, at the end of the Seiberg-duality cascade will have no $D3$-branes and the $D5$-branes are smeared/dissolved over the blown-up S^3 and thus replaced by fluxes in the IR region.

The delocalized S(trominger) Y(au) Z(aslow) type IIA mirror of the aforementioned type IIB background of [27] and its M-theory uplift had been obtained in [25,28,33].

(b) Seiberg-duality cascade, IR confining $SU(M)$ gauge theory at finite temperature and $N_c = N_{\text{eff}}(r) + M_{\text{eff}}(r)$

1. *IR Confinement after Seiberg Duality Cascade*: Footnote numbered 3 shows that one effectively adds on to the number of $D3$-branes in the UV and hence, one has $SU(N+M) \times SU(N+M)$ color gauge group (implying an asymptotic AdS_5) and $SU(N_f) \times SU(N_f)$ flavor gauge group, in the UV: $r \geq \mathcal{R}_{D5/\overline{D5}}$. It is expected that there will be a partial Higgsing of $SU(N+M) \times SU(N+M)$ to $SU(N+M) \times SU(N)$ at $r = \mathcal{R}_{D5/\overline{D5}}$ [42]. The two gauge couplings, $g_{SU(N+M)}$ and $g_{SU(N)}$ flow logarithmically and oppositely in the IR region:

$$4\pi^2 \left(\frac{1}{g^2_{SU(N+M)}} + \frac{1}{g^2_{SU(N)}} \right) e^{\phi} \sim \pi;$$
$$4\pi^2 \left(\frac{1}{g^2_{SU(N+M)}} - \frac{1}{g^2_{SU(N)}} \right) e^{\phi} \sim \frac{1}{2\pi\alpha'} \int_{S^2} B_2. \quad (1)$$

[1] See [41] for earlier attempts at studying back-reacted $D3/D7$ geometry at zero temperature; we thank Zayas for bringing [40,41] to our attention.

Had it not been for $\int_{S^2} B_2$, in the UV region, one could have set $g^2_{SU(M+N)} = g^2_{SU(N)} = g^2_{YM} \sim g_s \equiv$ constant (implying conformality) which is the reason for inclusion of M $\overline{D5}$-branes at the common boundary of the UV–IR interpolating and the UV regions, to annul this contribution. In fact, the running also receives a contribution from the N_f flavor $D7$-branes which needs to be annulled via N_f $\overline{D7}$-branes. The gauge coupling $g_{SU(N+M)}$ flows towards strong coupling and the $SU(N)$ gauge coupling flows towards weak coupling. Upon application of Seiberg duality, $SU(N+M)_{\text{strong}} \overset{\text{Seiberg Dual}}{\longrightarrow} SU(N-(M-N_f))_{\text{weak}}$ in the IR region; assuming after repeated Seiberg dualities or duality cascade, N decreases to 0 and there is a finite M, one will be left with $SU(M)$ gauge theory with N_f flavors that confines in the IR region – the finite temperature version of the same is what was looked at by [27].

2. *Obtaining $N_c = 3$, and color-flavor enhancement of length scale in the IR region*: So, in the IR region, at the end of the duality cascade, what gets identified with the number of colors N_c is M, which in the 'MQGP limit' to be discussed below, can be tuned to equal 3. One can identify N_c with $N_{\text{eff}}(r) + M_{\text{eff}}(r)$, where $N_{\text{eff}}(r) = \int_{\text{Base of Resolved Warped Deformed Conifold}} F_5$ and $M_{\text{eff}} = \int_{S^3} \tilde{F}_3$ (the S^3 being dual to $e_\psi \wedge (\sin\theta_1 \mathrm{d}\theta_1 \wedge \mathrm{d}\phi_1 - B_1 \sin\theta_2 \wedge \mathrm{d}\phi_2)$, wherein B_1 is an asymmetry factor defined in [27], and $e_\psi \equiv \mathrm{d}\psi + \cos\theta_1\, \mathrm{d}\phi_1 + \cos\theta_2\, \mathrm{d}\phi_2$) where $\tilde{F}_3 (\equiv F_3 - \tau H_3) \propto M(r) \equiv 1 - \frac{\mathrm{e}^{\alpha(r-\mathcal{R}_{D5/\overline{D5}})}}{1+\mathrm{e}^{\alpha(r-\mathcal{R}_{D5/\overline{D5}})}}$, $\alpha \gg 1$ [43]. The effective number N_{eff} of $D3$-branes varies between $N \gg 1$ in the UV and 0 in the deep IR, and the effective number M_{eff} of $D5$-branes varies between 0 in the UV and M in the deep IR (i.e., at the end of the duality cascade in the IR region). Hence, the number of colors N_c varies between M in the deep IR and a large value [even in the MQGP limit of (11) (for a large value of N)] in the UV region. Hence, at very low energies, the number of colors N_c can be approximated by M, which in the MQGP limit is taken to be finite and can hence be taken to be equal to three. However, in this discussion, the low energy or the IR region is relative to the string scale. But these energies which are much less than the string scale, can still be much larger than T_c. Therefore, for all practical purposes, as regard the energy scales relevant to QCD, the number of colors can be tuned to three.

   In the IR region in the MQGP limit, with the inclusion of terms higher order in $g_s N_f$ in the RR and NS–NS three-form fluxes and the NLO terms in the angular part of the metric, there occurs an IR color-flavor enhancement of the length scale as compared to a Planckian length scale in KS for $\mathcal{O}(1)$ M, thereby showing that quantum corrections will be suppressed. Using [27]:

$$
\begin{aligned}
N_{\text{eff}}(r) &= N\left[1 + \frac{3g_s M_{\text{eff}}^2}{2\pi N} \times \left(\log r + \frac{3g_s N_f^{\text{eff}}}{2\pi}(\log r)^2\right)\right],\\
M_{\text{eff}}(r) &= M + \frac{3g_s N_f M}{2\pi}\log r + \sum_{m\geq 1}\sum_{n\geq 1} N_f^m M^n f_{mn}(r),\\
N_f^{\text{eff}}(r) &= N_f + \sum_{m\geq 1}\sum_{n\geq 0} N_f^m M^n g_{mn}(r).
\end{aligned}
\tag{2}
$$

   it was argued in [25] that the length scale of the OKS-BH metric in the IR region will be given by

$$
\begin{aligned}
L_{\text{OKS-BH}} &\sim \sqrt{M} N_f^{\frac{3}{4}} \sqrt{\left(\sum_{m\geq 0}\sum_{n\geq 0} N_f^m M^n f_{mn}(\Lambda)\right)} \times \left(\sum_{l\geq 0}\sum_{p\geq 0} N_f^l M^p g_{lp}(\Lambda)\right)^{\frac{1}{4}} g_s^{\frac{1}{4}}\sqrt{\alpha'}\\
&\equiv N_f^{\frac{3}{4}} \sqrt{\left(\sum_{m\geq 0}\sum_{n\geq 0} N_f^m M^n f_{mn}(\Lambda)\right)} \times \left(\sum_{l\geq 0}\sum_{p\geq 0} N_f^l M^p g_{lp}(\Lambda)\right)^{\frac{1}{4}} L_{\text{KS}}\Big|_{\Lambda:\log\Lambda < \frac{2\pi}{3g_s N_f}},
\end{aligned}
\tag{3}
$$

   which implies that in the IR region, relative to KS, there is a color-flavor enhancement of the length scale in the OKS-BH metric. Hence, in the IR region, even for $N_c^{\text{IR}} = M = 3$ and $N_f = 2$ (light flavors) upon inclusion of $n, m > 1$ terms in M_{eff} and N_f^{eff} in (2), $L_{\text{OKS-BH}} \gg L_{\text{KS}} (\sim L_{\text{Planck}})$ in the MQGP limit involving $g_s \overset{\sim}{<} 1$, implying that the stringy corrections are suppressed and one can trust supergravity calculations. As a reminder: one will generate higher powers of M and N_f in the double summation in M_{eff} in (2), e.g., from the terms higher order in $g_s N_f$ in the RR and NS–NS three-form fluxes that become relevant for the aforementioned values of g_s, N_f.

3. Further, the global flavor group in the UV–IR interpolating and UV regions, due to presence of N_f $D7$ and N_f $\overline{D7}$-branes, is $SU(N_f) \times SU(N_f)$, which is

broken in the IR region to $SU(N_f)$ as the IR case has only N_f $D7$-branes.

Hence, the following features of the type IIB model of [27] make it an ideal holographic dual of thermal QCD:

- the theory having quarks transforming in the fundamental representation, is UV conformal and IR confining with the required chiral symmetry breaking in the IR region and restoration at high temperatures;
- the theory is UV complete with the gauge coupling remaining finite in the UV (absence of Landau poles),
- the theory is not just defined for high temperatures but for low and high temperatures;
- with the inclusion of a finite baryon chemical potential (as will become evident in Sect. 3), the theory provides a lattice-compatible QCD confinement–deconfinement temperature T_c for the right number of light quark flavors and masses, and is also thermodynamically stable; given the IR proximity of the value of the lattice-compatible T_c, after the end of the Seiberg-duality cascade, the number of quark flavors approximately equals M, which in the 'MQGP' limit of (11) can be tuned to equal 3;
- in the MQGP limit (11) which requires considering a finite gauge coupling and hence string coupling, the theory was shown in [28] to be holographically renormalizable from an M-theory perspective with the M-theory uplift also being thermodynamically stable.

(d) Supergravity solution on resolved warped deformed conifold

The working metric is given by

$$\begin{aligned} \mathrm{d}s^2 = &\frac{1}{\sqrt{h}}(-g_1\mathrm{d}t^2 + \mathrm{d}x_1^2 + \mathrm{d}x_2^2 + \mathrm{d}x_3^2) \\ &+ \sqrt{h}[g_2^{-1}\mathrm{d}r^2 + r^2\mathrm{d}\mathcal{M}_5^2]. \end{aligned} \tag{4}$$

The g_i are black-hole functions in a modified OKS (Ouyang–Klebanov–Strassler)-BH (Black-Hole) background and are assumed to be $g_{1,2}(r,\theta_1,\theta_2) = 1 - \frac{r_h^4}{r^4} + \mathcal{O}\left(\frac{g_sM^2}{N}\right)$ where r_h is the horizon, and the (θ_1,θ_2) dependence come from the $\mathcal{O}\left(\frac{g_sM^2}{N}\right)$ corrections. The h_i are expected to receive corrections of $\mathcal{O}\left(\frac{g_sM^2}{N}\right)$ [42]. We assume the same to be true of the 'black-hole functions' $g_{1,2}$. The compact five-dimensional metric in (4) is given as

$$\begin{aligned} \mathrm{d}\mathcal{M}_5^2 = &h_1(\mathrm{d}\psi + \cos\theta_1\,\mathrm{d}\phi_1 + \cos\theta_2\,\mathrm{d}\phi_2)^2 \\ &+ h_2(\mathrm{d}\theta_1^2 + \sin^2\theta_1\,\mathrm{d}\phi_1^2) + h_4(h_3\mathrm{d}\theta_2^2 + \sin^2\theta_2\,\mathrm{d}\phi_2^2) \\ &+ h_5\,\cos\psi(\mathrm{d}\theta_1\mathrm{d}\theta_2 - \sin\theta_1\sin\theta_2\mathrm{d}\phi_1\mathrm{d}\phi_2) \\ &+ h_5\,\sin\psi(\sin\theta_1\,\mathrm{d}\theta_2\mathrm{d}\phi_1 + \sin\theta_2\,\mathrm{d}\theta_1\mathrm{d}\phi_2), \end{aligned} \tag{5}$$

$r \gg a, h_5 \sim \frac{(\text{deformation parameter})^2}{r^3} \ll 1$ for $r \gg (\text{deformation parameter})^{\frac{2}{3}}$, i.e. in the UV/IR–UV interpolating region. The h_i appearing in internal metric as well as M, N_f are not constant and up to linear order depend on g_s, M, N_f are given as follows:

$$\begin{aligned} &h_1 = \frac{1}{9} + \mathcal{O}\left(\frac{g_sM^2}{N}\right), \quad h_2 = \frac{1}{6} + \mathcal{O}\left(\frac{g_sM^2}{N}\right), \\ &h_4 = h_2 + \frac{a^2}{r^2}, \\ &h_3 = 1 + \mathcal{O}\left(\frac{g_sM^2}{N}\right), \quad h_5 \neq 0, \quad L = (4\pi g_sN)^{\frac{1}{4}}. \end{aligned} \tag{6}$$

One sees from (5) and (6) that one has a non-extremal resolved warped deformed conifold involving an S^2-blowup (as $h_4 - h_2 = \frac{a^2}{r^2}$), an S^3-blowup (as $h_5 \neq 0$) and squashing of an S^2 (as h_3 is not strictly unity). The horizon (being at a finite $r = r_h$) is warped squashed $S^2 \times S^3$. In the deep IR, in principle, one ends up with a warped squashed $S^2(a) \times S^3(\epsilon)$, ϵ being the deformation parameter. Assuming $\epsilon^{\frac{2}{3}} > a$ and given that $a = \mathcal{O}\left(\frac{g_sM^2}{N}\right)r_h$ [42], in the IR and in the MQGP limit, $N_{\text{eff}}(r \in \text{IR}) = \int_{\text{warped squashed } S^2(a)\times S^3(\epsilon)} F_5(r \in \text{IR}) \ll M = \int_{S^3(\epsilon)} F_3(r \in \text{IR})$; we have a confining $SU(M)$ gauge theory in the IR region.

The warp factor that includes the back-reaction in the IR region is given as

$$\begin{aligned} h = \frac{L^4}{r^4}\Bigg[1 + \frac{3g_sM_{\text{eff}}^2}{2\pi N}\log r\Bigg\{1 + \frac{3g_sN_f^{\text{eff}}}{2\pi}\left(\log r + \frac{1}{2}\right) \\ + \frac{g_sN_f^{\text{eff}}}{4\pi}\log\left(\sin\frac{\theta_1}{2}\sin\frac{\theta_2}{2}\right)\Bigg\}\Bigg], \end{aligned} \tag{7}$$

where, in principle, $M_{\text{eff}}/N_f^{\text{eff}}$ are not necessarily the same as M/N_f; we, however, will assume that, up to $\mathcal{O}\left(\frac{g_sM^2}{N}\right)$, they are. Proper UV behavior requires [42]

$$\begin{aligned} &h = \frac{L^4}{r^4}\left[1 + \sum_{i=1}\frac{\mathcal{H}_i(\phi_{1,2},\theta_{1,2},\psi)}{r^i}\right], \quad \text{large } r; \\ &h = \frac{L^4}{r^4}\left[1 + \sum_{i,j;(i,j)\neq(0,0)}\frac{h_{ij}(\phi_{1,2},\theta_{1,2},\psi)\log^i r}{r^j}\right], \\ &\quad \text{small } r. \end{aligned} \tag{8}$$

In the IR region, up to $\mathcal{O}(g_sN_f)$ and setting $h_5 = 0$, the three-forms are given in [27]:

$$\begin{aligned} \text{(a) } \widetilde{F}_3 = &2MA_1\left(1 + \frac{3g_sN_f}{2\pi}\log r\right)e_\psi \\ &\wedge\frac{1}{2}(\sin\theta_1\,\mathrm{d}\theta_1 \wedge \mathrm{d}\phi_1 - B_1\,\sin\theta_2\,\mathrm{d}\theta_2 \wedge \mathrm{d}\phi_2) \\ &-\frac{3g_sMN_f}{4\pi}A_2\,\frac{\mathrm{d}r}{r} \wedge e_\psi \wedge \left(\cot\frac{\theta_2}{2}\,\sin\theta_2\,\mathrm{d}\phi_2\right. \\ &\left. - B_2\,\cot\frac{\theta_1}{2}\,\sin\theta_1\,\mathrm{d}\phi_1\right) \end{aligned}$$

$$
\begin{aligned}
&- \frac{3g_sMN_f}{8\pi} A_3 \ \sin\theta_1 \ \sin\theta_2 \\
&\times \left(\cot\frac{\theta_2}{2}\, \mathrm{d}\theta_1 + B_3 \ \cot\frac{\theta_1}{2}\, \mathrm{d}\theta_2 \right) \wedge \mathrm{d}\phi_1 \wedge \mathrm{d}\phi_2, \\
\text{(b) } H_3 = {} & 6g_sA_4M \left(1 + \frac{9g_sN_f}{4\pi} \ \log r \right. \\
&\left. + \frac{g_sN_f}{2\pi} \ \log\sin\frac{\theta_1}{2} \ \sin\frac{\theta_2}{2} \right) \frac{\mathrm{d}r}{r} \\
&\wedge \frac{1}{2}(\sin\theta_1 \, \mathrm{d}\theta_1 \wedge \mathrm{d}\phi_1 - B_4 \ \sin\theta_2 \, \mathrm{d}\theta_2 \wedge \mathrm{d}\phi_2) \\
&+ \frac{3g_s^2MN_f}{8\pi} A_5 \left(\frac{\mathrm{d}r}{r} \wedge e_\psi - \frac{1}{2}\mathrm{d}e_\psi \right) \\
&\wedge \left(\cot\frac{\theta_2}{2}\, \mathrm{d}\theta_2 - B_5 \ \cot\frac{\theta_1}{2}\, \mathrm{d}\theta_1 \right). \qquad (9)
\end{aligned}
$$

The asymmetry factors in (9) are given by $A_i = 1 + \mathcal{O}\big(\frac{a^2}{r^2}$ or $\frac{a^2\log r}{r}$ or $\frac{a^2\log r}{r^2}\big) + \mathcal{O}\big(\frac{\text{deformation parameter}^2}{r^3}\big)$, $B_i = 1+\mathcal{O}\big(\frac{a^2\log r}{r}$ or $\frac{a^2\log r}{r^2}$ or $\frac{a^2\log r}{r^3}\big)+\mathcal{O}\big(\frac{(\text{deformation parameter})^2}{r^3}\big)$. As in the UV region, $\frac{(\text{deformation parameter})^2}{r^3} \ll \frac{(\text{resolution parameter})^2}{r^2}$, we will assume the same three-form fluxes for $h_5 \neq 0$.

Further, to ensure UV conformality, it is important to ensure that the axion–dilaton modulus approaches a constant implying a vanishing beta function in the UV region. This was discussed in detail in Appendix B of [25], wherein in particular, assuming an F-theory uplift involving, locally, an elliptically fibered $K3$, it was shown that UV conformality and the Ouyang embedding are mutually consistent.

2.2 The 'MQGP limit'

In [28], we had considered the following two limits:

(i) weak(g_s)coupling−large 't Hooft coupling limit:

$$
\begin{aligned}
& g_s \ll 1, \, g_sN_f \ll 1, \, \frac{g_sM^2}{N} \ll 1, \, g_sM \gg 1, \, g_sN \gg 1 \\
& \text{effected by: } g_s \sim \epsilon^d, \, M \sim (\mathcal{O}(1)\epsilon)^{-\frac{3d}{2}}, \\
& \quad N \sim (\mathcal{O}(1)\epsilon)^{-19d}, \epsilon \ll 1, d > 0 \qquad (10)
\end{aligned}
$$

(the limit in the first line though not its realization in the second line, considered in [27]);

(ii) MQGP limit: $\frac{g_sM^2}{N} \ll 1, \, g_sN \gg 1$, finite g_s, M

$$
\begin{aligned}
& \text{effected by: } g_s \sim \epsilon^d, \, M \sim (\mathcal{O}(1)\epsilon)^{-\frac{3d}{2}}, \\
& \quad N \sim (\mathcal{O}(1)\epsilon)^{-39d}, \epsilon \lesssim 1, d > 0. \qquad (11)
\end{aligned}
$$

Let us enumerate the motivations for considering the MQGP limit which was discussed in detail in [25]. There are principally two.

1. Unlike the AdS/CFT limit wherein $g_{\rm YM} \to 0$, $N \to \infty$ such that $g_{\rm YM}^2N$ is large, for strongly coupled thermal systems like sQGP, what is relevant is $g_{\rm YM} \sim \mathcal{O}(1)$ and $N_c = 3$. From the discussion in the previous paragraphs, specially the one in point (c) of Sect. 2.1, one sees that in the IR region after the Seiberg-duality cascade, effectively $N_c = M$, which in the MQGP limit of (11) can be tuned to 3. Further, in the same limit, the string coupling $g_s \overset{<}{\sim} 1$. The finiteness of the string coupling necessitates addressing the same from an M-theory perspective. This is the reason for coining the name: 'MQGP limit'. In fact this is the reason why one is required to first construct a type IIA mirror, which was done in [28] à la delocalized Strominger–Yau–Zaslow mirror symmetry, and then take its M-theory uplift.
2. From the perspective of calculational simplification in supergravity, the following are examples of the same and constitute therefore the second set of reasons for looking at the MQGP limit of (11):
   - In the UV–IR interpolating region and the UV, $(M_{\rm eff}, N_{\rm eff}, N_f^{\rm eff}) \overset{\rm MQGP}{\approx} (M, N, N_f)$.
   - Asymmetry factors A_i, B_j (in three-form fluxes) $\overset{MQGP}{\to} 1$ in the UV–IR interpolating region and the UV.
   - Simplification of ten-dimensional warp factor and non-extremality function in the MQGP limit.

With $\mathcal{R}_{D5/\overline{D5}}$ denoting the boundary common to the UV–IR interpolating region and the UV region, $\tilde{F}_{lmn}$, $H_{lmn} = 0$ for $r \geq \mathcal{R}_{D5/\overline{D5}}$ is required to ensure conformality in the UV region. Near the $\theta_1 = \theta_2 = 0$-branch, assuming $\theta_{1,2} \to 0$ as $\epsilon^{\gamma_\theta > 0}$ and $r \to \mathcal{R}_{\rm UV} \to \infty$ as $\epsilon^{-\gamma_r < 0}$, $\lim_{r\to\infty} \tilde{F}_{lmn} = 0$ and $\lim_{r\to\infty} H_{lmn} = 0$ for all components except $H_{\theta_1\theta_2\phi_{1,2}}$; in the MQGP limit and near the $\theta_{1,2} = \pi/0$-branch, $H_{\theta_1\theta_2\phi_{1,2}} = 0/\ \frac{3g_s^2MN_f}{8\pi}\Big|_{N_f=2, g_s=0.6, M=\left(\mathcal{O}(1)g_s\right)^{-\frac{3}{2}}} \ll 1$. So, the UV nature too is captured near $\theta_{1,2} = 0$-branch in the MQGP limit. This mimics addition of $\overline{D5}$-branes in [27] to ensure cancellation of $\tilde{F}_3$.

2.3 Approximate supersymmetry, construction of the delocalized SYZ IIA mirror and its M-theory uplift in the MQGP limit

A central issue to [26,28] has been the implementation of delocalized mirror symmetry via the Strominger–Yau–Zaslow prescription according to which the mirror of a Calabi–Yau can be constructed via three T-dualities along a special Lagrangian T^3 fibered over a large base in the Calabi–Yau. This subsection is a quick review of precisely this.

To implement the quantum mirror symmetry à la Strominger–Yau–Zaslow [44], one needs a special Lagrangian (sLag) T^3 fibered over a large base (to nullify contributions from open-string disc instantons with boundaries as non-contractible one-cycles in the sLag). Defining delocalized T-duality coordinates, $(\phi_1, \phi_2, \psi) \to (x, y, z)$ valued in $T^3(x, y, z)$ [28]:

$$x = \sqrt{h_2} h^{\frac{1}{4}} \sin\langle\theta_1\rangle\langle r\rangle\phi_1, \quad y = \sqrt{h_4} h^{\frac{1}{4}} \sin\langle\theta_2\rangle\langle r\rangle\phi_2,$$
$$z = \sqrt{h_1}\langle r\rangle h^{\frac{1}{4}}\psi, \tag{12}$$

using the results of [45] it was shown in [26,33] that the following conditions are satisfied:

$$i^*J\big|_{\mathrm{RC/DC}} \approx 0,$$
$$\Im m(i^*\Omega)\big|_{\mathrm{RC/DC}} \approx 0, \tag{13}$$
$$\Re e(i^*\Omega)\big|_{\mathrm{RC/DC}} \sim \text{volume form } (T^3(x, y, z)),$$

for the T^2-invariant sLag of [45] for a deformed conifold. Hence, if the resolved warped deformed conifold is predominantly either resolved or deformed, the local T^3 of (12) is the required sLag to effect SYZ-mirror construction.

Interestingly, in the 'delocalized limit' [46] $\psi = \langle\psi\rangle$, under the coordinate transformation:

$$\begin{pmatrix} \sin\theta_2 \mathrm{d}\phi_2 \\ \mathrm{d}\theta_2 \end{pmatrix} \to \begin{pmatrix} \cos\langle\psi\rangle & \sin\langle\psi\rangle \\ -\sin\langle\psi\rangle & \cos\langle\psi\rangle \end{pmatrix} \begin{pmatrix} \sin\theta_2 \mathrm{d}\phi_2 \\ \mathrm{d}\theta_2 \end{pmatrix}, \tag{14}$$

and $\psi \to \psi - \cos\langle\bar{\theta}_2\rangle\phi_2 + \cos\langle\theta_2\rangle\phi_2 - \tan\langle\psi\rangle \ln\sin\bar{\theta}_2$, the h_5 term becomes $h_5[\mathrm{d}\theta_1\mathrm{d}\theta_2 - \sin\theta_1 \sin\theta_2 \mathrm{d}\phi_1\mathrm{d}\phi_2]$, $e_\psi \to e_\psi$, i.e., one introduces an isometry along ψ in addition to the isometries along $\phi_{1,2}$. This clearly is not valid globally – the deformed conifold does not possess a third global isometry.

To enable use of SYZ-mirror duality via three T-dualities, one also needs to ensure a large base (implying large complex structures of the aforementioned two two-tori) of the $T^3(x, y, z)$ fibration. This is effected via [47]:

$$\mathrm{d}\psi \to \mathrm{d}\psi + f_1(\theta_1)\cos\theta_1\mathrm{d}\theta_1 + f_2(\theta_2)\cos\theta_2\mathrm{d}\theta_2,$$
$$\mathrm{d}\phi_{1,2} \to \mathrm{d}\phi_{1,2} - f_{1,2}(\theta_{1,2})\mathrm{d}\theta_{1,2}, \tag{15}$$

for appropriately chosen large values of $f_{1,2}(\theta_{1,2})$. The three-form fluxes remain invariant. The fact that one can choose such large values of $f_{1,2}(\theta_{1,2})$, was justified in [28]. The guiding principle is that one requires the metric obtained after SYZ-mirror transformation applied to the non-Kähler resolved warped deformed conifold is like a non-Kähler warped resolved conifold at least locally. Then $G^{\mathrm{IIA}}_{\theta_1\theta_2}$ needs to vanish [28]. This was explicitly shown in [25].

As in the Klebanov–Strassler construction, a single T-duality along a direction orthogonal to the $D3$-brane world volume, e.g., z of (12), yields $D4$ branes straddling a pair of $NS5$-branes consisting of world-volume coordinates (θ_1, x) and (θ_2, y). Further, T-dualizing along x and then y would yield a Taub–NUT space from each of the two $NS5$-branes [48]. The $D7$-branes yield $D6$-branes which get uplifted to Kaluza–Klein monopoles in M-theory [49], which too involve Taub–NUT spaces. Globally, probably the 11-dimensional uplift would involve a seven-fold one of the G_2-structure, analogous to the uplift of $D5$-branes wrapping a two-cycle in a resolved warped conifold [50].

2.4 G-structures

The mirror type IIA metric after performing three T-dualities, first along x, then along y and finally along z, utilizing the results of [46] was worked out in [28]. The type IIA metric components were worked out in [28].

Now, any metric-compatible connection can be written in terms of the Levi-Civita connection and the contorsion tensor κ. Metric compatibility requires $\kappa \in \Lambda^1 \otimes \Lambda^2$, Λ^n being the space of n-forms. Alternatively, in d complex dimensions, since $\Lambda^2 \cong so(d)$, κ also can be thought of as $\Lambda^1 \otimes so(d)$. Given the existence of a G-structure, we can decompose $so(d)$ into a part in the Lie algebra g of $G \subset SO(d)$ and its orthogonal complement $g^\perp = so(d)/g$. The contorsion κ splits accordingly into $\kappa = \kappa^0 + \kappa^g$, where κ^0 – the intrinsic torsion – is the part in $\Lambda^1 \otimes g^\perp$. One can decompose κ^0 into irreducible G representations providing a classification of G-structures in terms of which representations appear in the decomposition. Let us consider the decomposition of T^0 in the case of $SU(3)$-structure. The relevant representations are $\Lambda^1 \sim 3 \oplus \bar{3}$, $g \sim 8$, $g^\perp \sim 1 \oplus 3 \oplus \bar{3}$. Thus the intrinsic torsion, an element of $\Lambda^1 \oplus su(3)^\perp$, can be decomposed into the following $SU(3)$ representations:

$$\begin{aligned} \Lambda^1 \otimes su(3)^\perp &= (3 \oplus \bar{3}) \otimes (1 \oplus 3 \oplus \bar{3}) \\ &= (1 \oplus 1) \oplus (8 \oplus 8) \oplus (6 \oplus \bar{6}) \oplus (3 \oplus \bar{3}) \oplus (3 \oplus \bar{3})' \\ &\equiv W_1 \oplus W_2 \oplus W_3 \oplus W_4 \oplus W_5. \end{aligned} \tag{16}$$

The $SU(3)$ structure torsion classes [51] can be defined in terms of J, Ω, $\mathrm{d}J$, $\mathrm{d}\Omega$ and the contraction operator $\lrcorner : \Lambda^k T^\star \otimes \Lambda^n T^\star \to \Lambda^{n-k} T^\star$, J being given by

$$J = \mathrm{e}^1 \wedge \mathrm{e}^2 + \mathrm{e}^3 \wedge \mathrm{e}^4 + \mathrm{e}^5 \wedge \mathrm{e}^6,$$

and the $(3, 0)$-form Ω being given by

$$\Omega = (\mathrm{e}^1 + i\mathrm{e}^2) \wedge (\mathrm{e}^3 + i\mathrm{e}^4) \wedge (\mathrm{e}^5 + i\mathrm{e}^6).$$

The torsion classes are defined in the following way:

- $W_1 \leftrightarrow [\mathrm{d}J]^{(3,0)}$, given by real numbers $W_1 = W_1^+ + W_1^-$ with $\mathrm{d}\Omega_+ \wedge J = \Omega_+ \wedge \mathrm{d}J = W_1^+ J \wedge J \wedge J$ and $\mathrm{d}\Omega_- \wedge J = \Omega_- \wedge \mathrm{d}J = W_1^- J \wedge J \wedge J$;
- $W_2 \leftrightarrow [\mathrm{d}\Omega]_0^{(2,2)}$: $(\mathrm{d}\Omega_+)^{(2,2)} = W_1^+ J \wedge J + W_2^+ \wedge J$ and $(\mathrm{d}\Omega_-)^{(2,2)} = W_1^- J \wedge J + W_2^- \wedge J$;
- $W_3 \leftrightarrow [\mathrm{d}J]_0^{(2,1)}$ is defined as $W_3 = \mathrm{d}J^{(2,1)} - [J \wedge W_4]^{(2,1)}$;

- $W_4 \leftrightarrow J \wedge \mathrm{d}J$: $W_4 = \frac{1}{2} J \lrcorner \mathrm{d}J$;
- $W_5 \leftrightarrow [\mathrm{d}\Omega]_0^{(3,1)}$: $W_5 = \frac{1}{2}\Omega_+ \lrcorner \mathrm{d}\Omega_+$ (the subscript 0 indicative of the primitivity of the respective forms).

In [26], we saw that the five $SU(3)$ structure torsion classes, in the MQGP limit, satisfied (schematically)

$$T^{\mathrm{IIB}}_{SU(3)} \in W_1 \oplus W_2 \oplus W_3 \oplus W_4 \oplus W_5 \sim \frac{\mathrm{e}^{-3\tau}}{\sqrt{g_s N}} \oplus (g_s N)^{\frac{1}{4}} \mathrm{e}^{-3\tau} \oplus \sqrt{g_s N}\mathrm{e}^{-3\tau} \oplus -\frac{2}{3} \oplus -\frac{1}{2} \tag{17}$$

($r \sim \mathrm{e}^{\frac{\tau}{3}}$), such that

$$\frac{2}{3} W_5^{\bar{3}} = W_4^{\bar{3}} \tag{18}$$

in the UV–IR interpolating region/UV, implying a Klebanov–Strassler-like supersymmetry [52]. Locally around $\theta_1 \sim \frac{1}{N^{\frac{1}{5}}}, \theta_2 \sim \frac{1}{N^{\frac{3}{10}}}$, the type IIA torsion classes of the delocalized SYZ type IIA mirror metric were shown in [25] to be

$$\begin{aligned} T^{\mathrm{IIA}}_{SU(3)} &\in W_2 \oplus W_3 \oplus W_4 \oplus W_5 \\ &\sim \gamma_2 g_s^{-\frac{1}{4}} N^{\frac{3}{10}} \oplus g_s^{-\frac{1}{4}} N^{-\frac{1}{20}} \oplus g_s^{-\frac{1}{4}} N^{\frac{3}{10}} \oplus g_s^{-\frac{1}{4}} N^{\frac{3}{10}} \\ &\approx \gamma W_2 \oplus W_4 \oplus W_5 \overset{\text{fine tuning:}\gamma \approx 0}{\longrightarrow} \approx W_4 \oplus W_5. \end{aligned} \tag{19}$$

Further,

$$W_4 \sim \Re e W_5 \tag{20}$$

indicative of supersymmetry after constructing the delocalized SYZ-mirror.

Apart from quantifying the departure from $SU(3)$ holonomy due to intrinsic contorsion supplied by the NS–NS three-form H, via the evaluation of the $SU(3)$ structure torsion classes, to the best of our knowledge for the first time in the context of holographic thermal QCD *at finite gauge coupling* in [25]:

(i) the existence of approximate supersymmetry of the type IIB holographic dual of [27] in the MQGP limit near the coordinate branch $\theta_1 = \theta_2 = 0$ was demonstrated, which apart from the existence of a special Lagrangian three-cycle (as shown in [25,26]) is essential for construction of the local SYZ type IIA mirror;
(ii) it was demonstrated that the large-N suppression of the deviation of the type IIB resolved warped deformed conifold from being a complex manifold, is lost on being duality-chased to type IIA – it was also shown that one further fine tuning $\gamma_2 = 0$ in W_2^{IIA} can ensure that the local type IIA mirror is complex;
(iii) for the local type IIA $SU(3)$ mirror, the possibility of a surviving approximate supersymmetry was demonstrated, which is essential from the point of view of the end result of the application of the SYZ-mirror prescription.

We can get a one-form type IIA potential from the triple T-dual (along x, y, z) of the type IIB $F_{1,3,5}$ in [28], using which the following $D = 11$ metric was obtained in [28] ($u \equiv \frac{r_h}{r}$):

$$\begin{aligned} \mathrm{d}s_{11}^2 &= \mathrm{e}^{-\frac{2\phi^{\mathrm{IIA}}}{3}} [g_{tt}\mathrm{d}t^2 + g_{\mathbb{R}^3}(\mathrm{d}x^2 + \mathrm{d}y^2 + \mathrm{d}z^2) \\ &\quad + g_{uu}\mathrm{d}u^2 + \mathrm{d}s^2_{\mathrm{IIA}}(\theta_{1,2}, \phi_{1,2}, \psi)] \\ &\quad + \mathrm{e}^{\frac{4\phi^{\mathrm{IIA}}}{3}} (\mathrm{d}x_{11} + A^{F_1} + A^{F_3} + A^{F_5})^2 \\ &\equiv \text{Black } M3 - \text{Brane} \\ &\quad + \mathcal{O}\left(\left[\frac{g_s M^2 \log N}{N}\right](g_s M) N_f\right). \end{aligned} \tag{21}$$

If V is a seven-dimensional real vector space, then a three-form φ is said to be positive if it lies in the $GL(7, \mathbb{R})$ orbit of φ_0, where φ_0 is a three-form on $\mathbb{R}^7$ which is preserved by the G_2-subgroup of $GL(7, \mathbb{R})$. The pair (φ, g) for a positive three-form φ and the corresponding metric g constitute a G_2-structure. The space of p-forms decomposes as the following irreps of G_2 [53]:

$$\begin{aligned} \Lambda^1 &= \Lambda^1_7, \\ \Lambda^2 &= \Lambda^2_7 \oplus \Lambda^2_{14}, \\ \Lambda^3 &= \Lambda^3_1 \oplus \Lambda^3_7 \oplus \Lambda^3_{27}, \\ \Lambda^4 &= \Lambda^4_1 \oplus \Lambda^4_7 \oplus \Lambda^4_{27}, \\ \Lambda^5 &= \Lambda^5_7 \oplus \Lambda^5_{14}, \\ \Lambda^6 &= \Lambda^6_7. \end{aligned} \tag{22}$$

The subscripts denote the dimension of the representation, and components of the same representation/dimensionality are isomorph. Let M be a 7-manifold with a G_2-structure (φ, g). Then the components of spaces of two-, three-, four-, and five-forms are given in [53,54]. The metric g defines a reduction of the frame bundle F to a principal $SO(7)$-sub-bundle Q, that is, a sub-bundle of oriented orthonormal frames. Now, g also defines a Levi-Civita connection ∇ on the tangent bundle TM, and hence on F. However, the G_2-invariant three-form φ reduces the orthonormal bundle further to a principal G_2-sub-bundle Q. The Levi-Civita connection can be pulled back to Q. On Q, ∇ can be uniquely decomposed as

$$\nabla = \bar{\nabla} + \mathcal{T} \tag{23}$$

where $\bar{\nabla}$ is a G_2-compatible canonical connection on P, taking values in the sub-algebra $\mathfrak{g}_2 \subset \mathfrak{so}(7)$, while $\mathcal{T}$ is a one-form taking values in $\mathfrak{g}_2^{\perp} \subset \mathfrak{so}(7)$; $\mathcal{T}$ is known as the intrinsic torsion of the G_2-structure – the obstruction to the Levi-Civita connection being G_2-compatible. Now $\mathfrak{so}(7)$ splits under G_2 as

$$\mathfrak{so}(7) \cong \Lambda^2 V \cong \Lambda^2_7 \oplus \Lambda^2_{14}. \tag{24}$$

But $\Lambda^2_{14} \cong \mathfrak{g}_2$, so the orthogonal complement $\mathfrak{g}_2^{\perp} \cong \Lambda^2_7 \cong V$. Hence $\mathcal{T}$ can be represented by a tensor T_{ab} which lies in $W \cong V \otimes V$. Now, since φ is G_2-invariant, it is $\bar{\nabla}$-parallel. So, the torsion is determined by $\nabla\varphi$ from Lemma 2.24 of [55]:

$$\nabla\varphi \in \Lambda^1_7 \otimes \Lambda^3_7 \cong W. \tag{25}$$

Due to the isomorphism between the $\Lambda^{a=1,\ldots,5}_7$s, $\nabla\varphi$ lies in the same space as T_{AB} and thus completely determines it. Equation (25) is equivalent to

$$\nabla_A \varphi_{BCD} = T_A{}^E \psi_{EBCD} \tag{26}$$

where T_{AB} is the full torsion tensor. Equation (26) can be inverted to yield

$$T_A{}^M = \frac{1}{24}(\nabla_A \varphi_{BCD})\psi^{MBCD}. \tag{27}$$

The tensor $T_A{}^M$, like the space W, possesses 49 components and hence fully defines $\nabla\varphi$. In general T_{AB} can be split into torsion components as

$$T = T_1 g + T_7 \lrcorner \varphi + T_{14} + T_{27} \tag{28}$$

where T_1 is a function and gives the **1** component of T. We also have T_7, which is a one-form and hence gives the **7** component, and $T_{14} \in \Lambda^2_{14}$ gives the **14** component. Further, T_{27} is traceless symmetric and gives the **27** component. Writing T_i as W_i, we can split W as

$$W = W_1 \oplus W_7 \oplus W_{14} \oplus W_{27}. \tag{29}$$

From [56], we see that a G_2 structure can be defined as

$$\varphi_0 = \frac{1}{3!} f_{ABC} e^{ABC} = e^{-\phi^{\mathrm{IIA}}} f_{abc} e^{abc} + e^{-\frac{2\phi^{\mathrm{IIA}}}{3}} J \wedge e^{x_{10}}, \tag{30}$$

where $A, B, C = 1, \ldots, 6, 10$; $a, b, c, = 1, \ldots, 6$ and f_{ABC} are the structure constants of the imaginary octonions. Using the same, the G_2-structure torsion classes were worked out around $\theta_1 \sim \frac{1}{N^{\frac{1}{5}}}, \theta_2 \sim \frac{1}{N^{\frac{3}{10}}}$ in [25] to be found to be

$$T_{G_2} \in W_2^{14} \oplus W_3^{27} \sim \frac{1}{(g_s N)^{\frac{1}{4}}} \oplus \frac{1}{(g_s N)^{\frac{1}{4}}}. \tag{31}$$

Hence, the approach of the seven-fold, locally, to having a G_2 holonomy ($W_1^{G_2} = W_2^{G_2} = W_3^{G_2} = W_4^{G_2} = 0$) is accelerated in the MQGP limit.

As stated earlier, the global uplift to M-theory of the type IIB background of [27] is expected to involve a seven-fold of the G_2 structure (not a G_2-holonomy due to the non-zero G_4). It is hence extremely important to be able to see this, at least locally. It is in this sense that the results of [28] are of great significance; as one explicitly sees, for the first time, in the context of holographic thermal QCD *at finite gauge coupling*, though locally, the aforementioned G_2 structure has been worked out in terms of the non-trivial G_2-structure torsion classes.

3 $0^{++(***\cdots}$ Glueball spectrum from type IIB supergravity background

In this section we discuss the 0^{++} glueball spectrum by solving the dilaton wave equation in the type IIB background discussed in Sect. 2. The type IIB metric as given in Eq. (4) with the warp factor h given in (7) can be simplified by working around a particular value of θ_1 and θ_2: $\{\theta_1 = \frac{1}{N^{1/5}}, \theta_2 = \frac{1}{N^{3/10}}\}$, then keeping terms up to NLO in N in the large N limit. The simplified type IIB metric is given as

$$\begin{aligned} ds^2 &= g_{tt} dt^2 + g_{x_1 x_1}(dx_1^2 + dx_2^2 + dx_3^2) \\ &\quad + g_{rr} dr^2 + \sqrt{h} r^2 d\mathcal{M}_5^2, \end{aligned} \tag{32}$$

with the components $g_{tt}, g_{x_1 x_1} (= g_{x_2 x_2} = g_{x_3 x_3}), g_{rr}$ as given now:

$$\begin{aligned} g_{tt} &= \frac{r^2(1 - B(r))\left(\frac{r_h^4}{r^4} - 1\right)}{2\sqrt{\pi}\sqrt{N}\sqrt{g_s}} \\ g_{x_1 x_1} &= \frac{r^2(1 - B(r))}{2\sqrt{\pi}\sqrt{N}\sqrt{g_s}} \\ g_{rr} &= \frac{2\sqrt{\pi}\sqrt{N}(r^2 - 3a^2)(B(r) + 1)\sqrt{g_s}}{r^4\left(1 - \frac{r_h^4}{r^4}\right)}, \end{aligned} \tag{33}$$

where $B(r) = \frac{3M^2 g_s \log(r)(12 N_f g_s \log(r) + 6 N_f g_s + N_f g_s(-\log(N)) - 2\log(4) N_f g_s + 8\pi)}{32\pi^2 N}$, and a being the resolution parameter is proportional to the horizon radius r_h. Hence while computing the spectrum with a cut-off in the radial direction and no horizon, we must put both r_h and a to zero in the above equation.

Moreover, the dilaton profiles with/without the black-hole are given below as

$$\begin{aligned} &\text{(a) } r_h \neq 0 : e^{-\Phi} = \frac{1}{g_s} - \frac{N_f}{8\pi}\log(r^6 + a^2 r^4) \\ &\quad - \frac{N_f}{2\pi}\log\left(\sin\frac{\theta_1}{2}\sin\frac{\theta_2}{2}\right), \quad r < \mathcal{R}_{D5/\overline{D5}}, \\ &\quad e^{-\Phi} = \frac{1}{g_s}, \quad r > \mathcal{R}_{D5/\overline{D5}}; \\ &\text{(b) } r_h = 0 : e^{-\Phi} = \frac{1}{g_s} - \frac{3N_f}{4\pi}\log r \\ &\quad - \frac{N_f}{2\pi}\log\left(\sin\frac{\theta_1}{2}\sin\frac{\theta_2}{2}\right), \quad r < \left|\mu_{\mathrm{Ouyang}}\right|^{\frac{2}{3}}, \\ &\quad e^{-\Phi} = \frac{1}{g_s}, \quad r > \left|\mu_{\mathrm{Ouyang}}\right|^{\frac{2}{3}}. \end{aligned} \tag{34}$$

Again working around the particular choices of θ_1 and θ_2 the above profile can be simplified up to NLO in N. The dilaton equation that has to be solved is given as

$$\partial_\mu\left(\mathrm{e}^{-2\Phi}\sqrt{g}g^{\mu\nu}\partial_\nu\phi\right)=0. \tag{35}$$

To solve the above dilaton equation we assume ϕ in (35) to be of the form $\phi=\mathrm{e}^{ik.x}\tilde{\phi}(r)$. Now, with this, we adopt the WKB method to get to the final result. The first step towards the WKB method is to convert the glueball equation of motion into a Schrödinger-like equation. Then the WKB quantization condition can be applied on the potential term obtained from the Schrödinger-like equation. For the (0^{++}) glueball spectrum with no horizon ($r_h=0$), one of the solutions was obtained by imposing the Neumann boundary condition at the cut-off.

3.1 $r_h\neq 0$ using WKB quantization method

In the following we discuss the spectrum of the 0^{++} glueball in the type IIB background with a black hole, implying a horizon of radius r_h in the geometry. The results corresponding to the coordinate and field redefinitions of [32] are discussed below.

Using the redefinitions of [32] with $r=\sqrt{y}$, $r_h=\sqrt{y_h}$ and finally $y=y_h(1+\mathrm{e}^z)$, the 0^{++} EOM (35), with $k^2=-m^2$, can be written as

$$\partial_z(E_z\partial_z\tilde{\phi})+y_h^2F_zm^2\tilde{\phi}=0, \tag{36}$$

where at leading order in N, E_z and F_z are given with $L=(4\pi g_sN)^{1/4}$ as

$$\begin{aligned}E_z=&\frac{1}{128\pi^2L^5g_s^2}(\mathrm{e}^z+2)y_h^2(8\pi+g_sN_f\log 256\\&+2N_fg_s\log N-3g_sN_f\log[(\mathrm{e}^z+1)y_h])\\&\times[2(3a^2\{4\pi+g_sN_f(\log 16-6)\}\\&+(\mathrm{e}^z+1)y_h\{8\pi+g_sN_f\log 256\})\\&+2g_sN_f\log N\{3a^2+2(\mathrm{e}^z+1)y_h\}\\&-3g_sN_f\{3a^2+2(\mathrm{e}^z+1)y_h\}\log[(\mathrm{e}^z+1)y_h]],\end{aligned} \tag{37}$$

$$\begin{aligned}F_z=&\frac{1}{128\pi^2g_s^2Ly_h(\mathrm{e}^z+1)}\mathrm{e}^z(4\pi+g_sN_f\log 16\\&+g_sN_f\log N-\frac{3}{2}g_sN_f\log[(\mathrm{e}^z+1)y_h])\\&\times[(\mathrm{e}^z+1)y_h(8\pi+2g_sN_f\log N+g_sN_f\log 256\\&-3g_sN_f\log[(\mathrm{e}^z+1)y_h])\\&-3a^2(4\pi+6g_sN_f+g_sN_f\log N\\&+g_sN_f\log 16-\frac{3}{2}g_sN_f\log[(\mathrm{e}^z+1)y_h])].\end{aligned} \tag{38}$$

Now, redefining the wave function $\tilde{\phi}$ as $\psi(z)=\sqrt{E_z}\tilde{\phi}(z)$ Eq. (36) reduces to a Schrödinger-like equation

$$\left(\frac{\mathrm{d}^2}{\mathrm{d}y^2}+V(z)\right)\psi(z)=0 \tag{39}$$

where the potential $V(z)$ has a rather cumbersome expression, which we will not explicitly write out. The WKB quantization condition becomes $\int_{z_1}^{z_2}\sqrt{V(z)}=\left(n+\frac{1}{2}\right)\pi$ where $z_{1,2}$ are the turning points of $V(z)$. We will work below with a dimensionless glueball mass $\tilde{m}$ assumed to be large and defined via $m=\tilde{m}\frac{r_h}{L^2}$. To determine the turning points of the potential $V(z)$, we consider two limits of the same – $r\in[r_h,\sqrt{3}a(r_h)\approx\sqrt{3}br_h]\cup[\sqrt{3}br_h,\infty)\equiv$ (IR, IR/UV interpolating $+$ UV). In the IR region, we have to take the limit $z\to-\infty$. Now in the large-$\tilde{m}$ and large-$\log N$ limit this potential at small z can be shown to be given as:

$$\begin{aligned}V(z\ll 0)=&\frac{1}{8}(1-3b^2)\mathrm{e}^z\tilde{m}^2\\&+\mathcal{O}\left(\mathrm{e}^{2z},\left(\frac{1}{\tilde{m}}\right)^2,\frac{1}{\log N}\right)<0\end{aligned} \tag{40}$$

Hence, there are no turning points in the IR region.

Now, in the UV region, apart from taking the large-z limit we also have to take $N_f=M=0$, to get

$$\begin{aligned}V(z\gg 1)=&-\frac{3(b^2+1)(y_h\tilde{m}^2+3)}{4y_h\mathrm{e}^{2z}}\\&+\frac{3b^2+y_h\tilde{m}^2+6}{4y_h\mathrm{e}^z}-1+\mathcal{O}(\mathrm{e}^{-3z}).\end{aligned} \tag{41}$$

The turning points of (41) are $z_1=\frac{1}{8}\big(3b^2-\sqrt{9b^4-6b^2\left(7y_h\tilde{m}^2+18\right)+y_h\tilde{m}^4-36y_h\tilde{m}^2-108}+y_h\tilde{m}^2+6\big)$, $z_2=\frac{1}{8}\big(3b^2+\sqrt{9b^4-6b^2\left(7y_h\tilde{m}^2+18\right)+y_h\tilde{m}^4-36y_h\tilde{m}^2-108}+y_h\tilde{m}^2+6\big)$, which in the large $\tilde{m}$ limit is given as $\{z_1=(3+3b^2)+\mathcal{O}(\frac{1}{\tilde{m}^2}),z_2=\frac{\tilde{m}^2}{4}-\frac{3(2+3b^2)}{4}+\mathcal{O}(\frac{1}{\tilde{m}^2})\}$.

To obtain a real spectrum, one first notes

$$\begin{aligned}&\sqrt{V(z\gg 1,N_f=M=0;b=0.6)}\\&=\sqrt{0.25\mathrm{e}^{-z}-1.02\mathrm{e}^{-2z}}\tilde{m}+\mathcal{O}\left(\mathrm{e}^{-3z},\frac{1}{\tilde{m}^2}\right)\end{aligned} \tag{42}$$

and

$$\int \sqrt{V(z)}\mathrm{d}z = \frac{\sqrt{\mathrm{e}^{-2z}(0.25\mathrm{e}^{z}-1.0023)}\tilde{m}\left(0.124856\mathrm{e}^{z}\tan^{-1}\left(\frac{0.124856\mathrm{e}^{z}-1.00115}{\sqrt{0.25\mathrm{e}^{z}-1.0023}}\right)-1.\sqrt{0.25\mathrm{e}^{z}-1.0023}\right)}{\sqrt{0.25\mathrm{e}^{z}-1.0023}}.$$
$$= \frac{\sqrt{\mathrm{e}^{-2z}(0.25\mathrm{e}^{z}-1.02)}\tilde{m}\left(0.123768\mathrm{e}^{z}\tan^{-1}\left(\frac{0.123768\mathrm{e}^{1.z}-1.00995}{\sqrt{0.25\mathrm{e}^{z}-1.02}}\right)-1.\sqrt{0.25\mathrm{e}^{z}-1.02}\right)}{\sqrt{0.25\mathrm{e}^{z}-1.02}}. \tag{43}$$

Therefore

$$\int_{4.08}^{0.25\tilde{m}^2-2.31}\sqrt{V(z)} = 0.39\tilde{m}-2 = \left(n+\frac{1}{2}\right)\pi, \tag{44}$$

yielding

$$m_n^{0^{++}} = 9.18+8.08n. \tag{45}$$

3.2 Glueball mass for $r_h = 0$ and an IR cut-off r_0

In this background the type IIB metric and the dilaton profile has to be modified by the limit $r_h \to 0$ and hence with $a \to 0$. This time also we have provided two solutions to the dilaton equation. The first solution was obtained by first following the redefinition of the variables in [64] and then imposing a Neumann boundary condition at the radial cut-off. For the other solution we again consider the WKB method after a redefinition of variables as given in [32].

3.2.1 Neumann boundary condition at r_0

Following [64], we redefine the radial coordinate as $z = \frac{1}{r}$. With this change of variable, the radial cut-off now maps to $z = z_0$, with $z_0 = \frac{1}{r_0}$. The dilaton equation using the metric and the dilaton background in the limit $(r_h, a) \to 0$ is given as

$$\mathrm{e}^{2U}\partial_z(\mathrm{e}^{-2U}\partial_z\tilde{\phi}) + \left(\frac{(4g_sN\pi)(B(z)+1)}{(1-B(z))}\right)(m^2)\tilde{\phi} = 0, \tag{46}$$

where up to NLO in N we have

$$\mathrm{e}^{U} = \frac{8\times 2^{1/4}g_s^{13/8}\pi^{13/8}N^{5/8}z^{3/2}}{4(\pi\log(4)N_fg_s+\pi)+2\pi N_fg_s\log(N)+3N_fg_s\log(z)}$$
$$-\frac{15M^2z^{3/2}g_s^{21/8}\log(z)(-12N_fg_s\log(z)+6N_fg_s+N_fg_s(-\log(N))-\log(16)N_fg_s+8\pi)}{8\,2^{3/4}\pi^{3/8}N^{3/8}(3N_fg_s\log(z)+2\pi N_fg_s\log(N)+4(\pi\log(4)N_fg_s+\pi))}. \tag{47}$$

Now to convert the above equation in a one-dimensional Schrödinger-like form we introduce a new field variable $\psi(z)$ by $\psi(z) = \mathrm{e}^{-U}\tilde{\phi}(z)$.

With this one can write the equation in the following Schrödinger-like form:

$$\frac{\partial^2\psi(z)}{\partial z^2} = V(z)\psi(z). \tag{48}$$

The potential $V(z)$, in the large-N large-log N limit is given as

$$V(z) = 4\pi g_sm^2N + \frac{6}{\pi z^2\log(N)} - \frac{15}{4z^2} + \mathcal{O}\left(\frac{1}{(\log N)^2}, \frac{g_sM^2}{N}\right). \tag{49}$$

Hence, the Schrödinger equation becomes

$$\psi''(z)+\psi(z)\left(4\pi g_sm^2N+\frac{6}{\pi z^2\log(N)}-\frac{15}{4z^2}\right) = 0, \tag{50}$$

whose solution is given as follows:

$$\psi(z) = c_1\sqrt{z}J_{\sqrt{\frac{2}{\pi}}\sqrt{\frac{2\pi\log(N)-3}{\log(N)}}}\left(2\sqrt{g_s}m\sqrt{N}\sqrt{\pi}z\right) + c_2\sqrt{z}Y_{\sqrt{\frac{2}{\pi}}\sqrt{\frac{2\pi\log(N)-3}{\log(N)}}}\left(2\sqrt{g_s}m\sqrt{N}\sqrt{\pi}z\right). \tag{51}$$

Finiteness of $\psi(z)$ at $z = 0$ requires setting $c_2 = 0$. Then imposing the Neumann boundary condition on $\tilde{\phi}(z)$ at $z = z_0$ implies

$$\tilde{\phi}'(z_0) = \frac{1}{\left(-2\pi g_sN_f\log\left(\frac{1}{N}\right)+3g_sN_f\log(z_0)+4(\pi g_sN_f\log(4)+\pi)\right)^2}$$
$$\times\left\{4\sqrt[4]{2}\pi^{13/8}g_s^{13/8}N^{5/8}z_0\left[3\left(-2\pi g_sN_f\log\left(\frac{1}{N}\right)\right.\right.$$
$$+3g_sN_f\log(z_0)-2g_sN_f+4\pi g_sN_f\log(4)+4\pi\Big)$$
$$\times J_{\sqrt{4-\frac{6}{\pi\log(N)}}}\left(2\sqrt{g_s}m\sqrt{N}\sqrt{\pi}z_0\right)+\left(-2\pi g_sN_f\log\left(\frac{1}{N}\right)\right.$$
$$+3g_sN_f\log(z_0)+4(\pi g_sN_f\log(4)+\pi)\Big)$$
$$\times\Big(2\sqrt{\pi}\sqrt{g_s}m\sqrt{N}z_0J_{\sqrt{4-\frac{6}{\pi\log(N)}}-1}\left(2\sqrt{g_s}m\sqrt{N}\sqrt{\pi}z_0\right)$$
$$-2\sqrt{\pi}\sqrt{g_s}m\sqrt{N}z_0J_{\sqrt{4-\frac{6}{\pi\log(N)}}+1}\left(2\sqrt{g_s}m\sqrt{N}\sqrt{\pi}z_0\right)$$
$$\left.\left.+J_{\sqrt{4-\frac{6}{\pi\log(N)}}}\left(2\sqrt{g_s}m\sqrt{N}\sqrt{\pi}z_0\right)\Big)\right]\right\} = 0, \tag{52}$$

implying in the large-N large-z (as the Neumann boundary condition will be implemented in the IR region) limit:

$$\frac{1}{2}x_0 J_{\sqrt{4-\frac{6}{\pi\log(N)}}-1}(x_0) - \frac{1}{2}x_0 J_{\sqrt{4-\frac{6}{\pi\log(N)}}+1}(x_0) + 2J_{\sqrt{4-\frac{6}{\pi\log(N)}}}(x_0) = 0, \tag{53}$$

where $x_0 \equiv 2\sqrt{g_s N\pi} m z_0$. The graphical solution points out that the ground state has a zero mass and the lightest (first excited state) glueball mass is approximately given by $3.71\frac{r_0}{L^2}$ (Fig. 1).

3.2.2 WKB method: including the non-conformal/NLO (in N) corrections

Again following the redefinition of variables as given in [32]: $r = \sqrt{y}$, $y = y_0(1 + e^z)$, where $r_0 = \sqrt{y_0}$ is the radial cut-off, and using the type IIB metric as well as the dilaton profile in the limit $(rh, a) \to 0$, the dilaton equation (35) can be written as

$$\partial_z(C_z\partial_z\tilde{\phi}) + y_h^2 D_z m^2\tilde{\phi} = 0, \tag{54}$$

where C_z and D_z are given up to NLO in N by

$$\begin{aligned} C_z = {} & \frac{1}{32768\sqrt{2}\,\pi^{21/4}N^{9/4}g_s^{13/4}}e^{-z}(e^z+1)^3 \\ & \times y_0^3(8\pi + 2g_sN_f\log N + 4g_sN_f\log 4 \\ & - 3g_sN_f\log[y_0(e^z+1)])^2(128\pi^2N \\ & + 15g_sM^2\{-8\pi + g_sN_f(\log 16 - 6) \\ & + g_sN_f\log N\}\log[(e^z+1)y_0] \\ & - 90M^2g_s^2N_f\log[(e^z+1)y_0]^2) \end{aligned} \tag{55}$$

$$\begin{aligned} D_z = {} & \frac{1}{32768\sqrt{2}\,\pi^{17/4}N^{5/4}g_s^{9/4}}e^z(8\pi + 2g_sN_f\log N \\ & + 4g_sN_f\log 4 - 3g_sN_f\log[y_0(e^z+1)])^2 \\ & \times (128\pi^2N + 3g_sM^2\{-8\pi + g_sN_f(\log 16 - 6) \\ & + g_sN_f\log N\}\log[(e^z+1)y_0] \\ & - 18M^2g_s^2N_f\log[(e^z+1)y_0]^2). \end{aligned} \tag{56}$$

Defining a new variable $\psi(z)$ such that $\psi(z) = \sqrt{C_z}\tilde{\phi}(z)$, the above equation can be converted into a Schrödinger-like equation,

$$\left(\frac{d^2}{dy^2} + V(z)\right)\psi(z) = 0, \tag{57}$$

where the potential is given up to NLO in N as

$$\begin{aligned} V(z) = {} & -\frac{1}{4} - \frac{3e^{2z}g_s{}^2\log N M^2\tilde{m}^2N_f\log(y_0)}{128\pi^2N} \\ & + \frac{e^{2z}(2(g_sN_f(\log N(\tilde{m}^2-3) + \tilde{m}^2\log(16) + 12 - 6\log(4)) + 4\pi(\tilde{m}^2-3)) - 3g_s(\tilde{m}^2-3)N_f\log(y_0))}{4(2g_sN_f(\log N + \log(16)) - 3g_sN_f\log(y_0) + 8\pi)} \\ & + \mathcal{O}\left(\frac{1}{N^2}\right). \end{aligned} \tag{58}$$

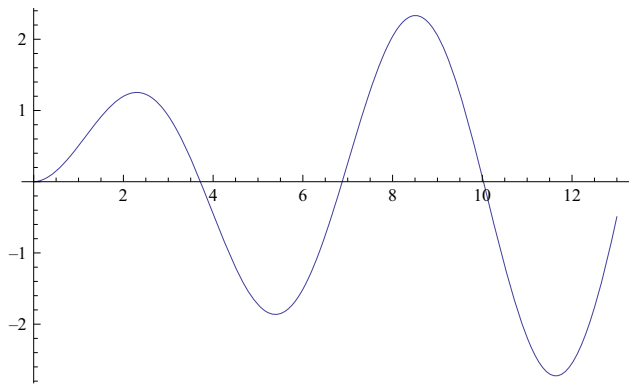

Fig. 1 $0^{++*,++**,++***}$ Masses obtained by graphical solution of the Neumann boundary condition in the $r_h = 0$ limit

The domain of integration over which $V(z) > 0$ can be shown to be $\{\log\left(\frac{3g_s{}^2M^2N_f\log(N)\log(y_0)}{64\pi^2\tilde{m}N} + \frac{1}{\tilde{m}}\right), \log(\delta^2-1)\}$, where $\mu^{\frac{2}{3}} = \delta\sqrt{y_0}$. Note that the IR cut-off r_0 or y_0 is not put in by hand but is proportional to the Ouyang embedding parameter (corresponding to the embedding of the flavor $D7$-branes) raised to the two-third power. The proportionality constant δ could be determined, as discussed in point number 5 in Sect. 8, by matching with lattice calculations and turns out to be $\mathcal{O}(1)$.

Expanding $\sqrt{V}$ first in N and then in $\tilde{m}$ and then integrating over the above mentioned domain, one gets the following quantization condition:

$$\begin{aligned} & \int_{z=\log\left(\frac{3M^2g_s{}^2N_f\log N\log y_0}{64\pi^2\tilde{m}N} + \frac{1}{\tilde{m}}\right)}^{\log(\delta^2-1)} \sqrt{V(z)} \\ & = \frac{1}{2}(\delta^2-1)\tilde{m}\left(\frac{3M^2g_s{}^2N_f\log N\log y_0}{64\pi^2N} + 1\right) - 0.75 \\ & \quad + \mathcal{O}\left(\frac{1}{\tilde{m}N}, \frac{1}{\tilde{m}^2}\right) = \left(n + \frac{1}{2}\right)\pi, \end{aligned} \tag{59}$$

yielding

$$m_n^{0^{++}} = \frac{(6.28319n + 4.64159)\left(1 - \frac{0.00474943g_s{}^2\log NM^2N_f\log(y_0)}{N}\right)}{\delta^2-1}. \tag{60}$$

4 Scalar glueball ($0^{-+(***\cdots)}$) masses

As $\mathrm{Tr}(F\tilde{F})$ has $P=-, C=+$ and it couples to A_1 in the Wess–Zumino term for the type IIA $D4-$brane: $\int_{\Sigma_{4,1}} A\wedge F\wedge F$, one considers A_1's EOM:

$$\partial_\nu\left(\sqrt{g^{\mathrm{IIA}}}g^{\mu\sigma}_{\mathrm{IIA}}g^{\nu\rho}_{\mathrm{IIA}}(\partial_{[\sigma}A_{\rho]})\right)=0, \tag{61}$$

where $\mu,\nu,\ldots=a(\equiv 0,1,2,3), r,\alpha(\equiv 5,\ldots,9)$. Like [57], assume $A_\mu=\delta^{\theta_2}_\mu a_{\theta_2}(r)e^{ik\cdot x}$, $k^2=-m^2$ as the fluctuation about the type IIA A_1 that was worked out in [28]. The 0^{-+} EOM then reduces to

$$\sqrt{g^{\mathrm{IIA}}}g^{\theta_2\theta_2}_{\mathrm{IIA}}g^{rr}_{\mathrm{IIA}}a''_{\theta_2}(r)+\partial_r\left(\sqrt{g^{\mathrm{IIA}}}g^{\theta_2\theta_2}_{\mathrm{IIA}}g^{rr}_{\mathrm{IIA}}\right)a'_{\theta_2}(r)+\sqrt{h}m^2\sqrt{g^{\mathrm{IIA}}}g^{\theta_2\theta_2}_{\mathrm{IIA}}a_{\theta_2}(r)=0. \tag{62}$$

4.1 Neumann/Dirichlet boundary conditions

4.1.1 $r_h\neq 0$

Then taking the large-N limit followed by a small-θ_1 small-θ_2 limit one can show that the equation of motion (62) yields

$$-\frac{8\pi(r^4-{r_h}^4)a''_{\theta_2}(r)}{\sqrt{3}}+\frac{32\pi(r^4-2{r_h}^4)a'_{\theta_2}(r)}{\sqrt{3}r}-32\sqrt[6]{3}\pi^2 g_s m^2 N a_{\theta_2}(r)=0. \tag{63}$$

Working near $r=r_h$, approximating (64) by

$$-\frac{32\pi {r_h}^3(r-r_h)a_{\theta_2}{}''(r)}{\sqrt{3}}+\left(\frac{160\pi {r_h}^2(r-r_h)}{\sqrt{3}}-\frac{32\pi {r_h}^3}{\sqrt{3}}\right)a_{\theta_2}{}'(r)-32\sqrt[6]{3}\pi^2 g_s m^2 N a_{\theta_2}(r)=0, \tag{64}$$

whose solution is given as follows:

$$a_{\theta_2}(r)=c_1 U\left(-\frac{3^{2/3}g_s m^2 N\pi}{5{r_h}^2},1,\frac{5r}{r_h}-5\right)+c_2 L_{\frac{3^{2/3}\pi g_s m^2 N}{5{r_h}^2}}\left(\frac{5r}{r_h}-5\right). \tag{65}$$

Imposing the Neumann boundary condition, $a'_{\theta_2}(r=r_h)=0$, utilizing

$$\begin{aligned}U\left(1-\frac{3^{2/3}\pi g_s m^2 N}{5|r_h|^2},2,\frac{5r}{r_h}-5\right)&=-\frac{{r_h}^3}{3^{2/3}\pi g_s m^2 N(r-r_h)\Gamma\left(-\frac{3^{2/3}g_s m^2 N\pi}{5{r_h}^2}\right)}\\&+\frac{\psi^{(0)}\left(1-\frac{3^{2/3}g_s m^2 N\pi}{5{r_h}^2}\right)+\log\left(\frac{5r}{r_h}-5\right)+2\gamma-1}{\Gamma\left(-\frac{3^{2/3}g_s m^2 N\pi}{5{r_h}^2}\right)}\\&+\frac{(r-r_h)(5{r_h}^2-3^{2/3}\pi g_s m^2 N)\left(2\psi^{(0)}\left(2-\frac{3^{2/3}g_s m^2 N\pi}{5{r_h}^2}\right)+2\log(r-r_h)+2\log\left(\frac{5}{r_h}\right)+4\gamma-5\right)}{4{r_h}^3\Gamma\left(-\frac{3^{2/3}g_s m^2 N\pi}{5{r_h}^2}\right)}\\&+\mathcal{O}((r-r_h)^2),\end{aligned} \tag{66}$$

$r_h=T\sqrt{4\pi g_s N}$ – up to LO in N – requires $c_2=0$ and

$$\frac{3^{2/3}m^2}{20T^2}=n, \tag{67}$$

implying

$$m^{0^{-+}}_n=\frac{2\sqrt{5}\sqrt{n}T}{\sqrt[3]{3}}. \tag{68}$$

One can show that imposing the Dirichlet boundary condition $a_{\theta_2}(r=r_h)=0$ yields the same spectrum as (68). If the temperature T gets identified with a of [57], then the ground state, unlike [57], is massless; the excited states for lower n are closer to $a=0$ and the higher excited states are closer to $a\to\infty$ in [57].

4.1.2 $r_h=0$ *Limit of (63)*

The $r_h=0$ limit of (63) gives

$$\sqrt{3}r^4 a_{\theta_2}{}''(r)-4\sqrt{3}r^3 a_{\theta_2}{}'(r)+3\sqrt[6]{3}\tilde{m}^2 r_0^2 a_{\theta_2}(r)=0, \tag{69}$$

which near $r=r_0$ yields

$$a_{\theta_2}(r)=(4r-3\tilde{m})^{5/4}\left(c_1 U\left(\frac{5}{4}-\frac{\tilde{m}^2}{4\sqrt[3]{3}},\frac{9}{4},\frac{3r}{\tilde{m}}-\frac{9}{4}\right)+c_2 L^{\frac{5}{4}}_{\frac{1}{12}(3^{2/3}\tilde{m}^2-15)}\left(\frac{3r}{\tilde{m}}-\frac{9}{4}\right)\right). \tag{70}$$

Imposing the Neumann boundary condition on (70) yields

$$\begin{aligned}&m^{0^{-+}}(r_h=0)=0,\\&m^{0^{-+*}}(r_h=0)\approx 3.4\frac{r_0}{L^2},\\&m^{0^{-+**}}(r_h=0)\approx 4.35\frac{r_0}{L^2}.\end{aligned} \tag{71}$$

One can similarly show that imposing the Dirichlet boundary condition on (70) for $c_2 = 0$ yields

$$m^{0^{-+}}(r_h = 0) = 0,$$
$$m^{0^{-+*}}(r_h = 0) \approx 3.06\frac{r_0}{L^2},$$
$$m^{0^{-+**}}(r_h = 0) \approx 4.81\frac{r_0}{L^2}. \tag{72}$$

4.1.3 WKB Quantization for $r_h \neq 0$

The potential corresponding to the Schrödinger-like equation à la [32], substituting $m = \tilde{m}\frac{\sqrt{y_h}}{L^2}$, is given by

$$V = \frac{e^z(4\,3^{2/3}\tilde{m}^2(3e^z + e^{2z} + 2) - 64e^z - 108e^{2z} - 25e^{3z} + 96)}{16(e^z + 1)^2(e^z + 2)^2}. \tag{73}$$

Therefore, in the IR region:

$$V(z \ll 0) = \left(-\frac{3}{16}3^{2/3}\tilde{m}^2 - \frac{11}{2}\right)e^{2z} + \left(\frac{1}{8}3^{2/3}\tilde{m}^2 + \frac{3}{2}\right)e^z + \mathcal{O}(e^{-3z}), \tag{74}$$

the turning points being given by $-\infty$ and $\log\left(\frac{2\,3^{2/3}\tilde{m}^2+24}{3\,3^{2/3}\tilde{m}^2+88}\right) \approx -0.405$. But only $z \in (-\infty, -2.526]$ corresponds to the IR region in our calculations. So,

$$\int_{-\infty}^{-2.526}\sqrt{V} = 0.283\tilde{m} = \left(n + \frac{1}{2}\right)\pi, \tag{75}$$

from which one obtains

$$m_n^{0^{-+}}(T, \mathrm{IR}) = 5.56(1 + 2n)\frac{r_h}{L^2}. \tag{76}$$

Similarly, in the UV region

$$V(\mathrm{UV}, T) = \left(\frac{1}{4}3^{2/3}\tilde{m}^2 + \frac{21}{8}\right)e^{-z} + \left(\frac{9}{16} - \frac{3}{4}3^{2/3}\tilde{m}^2\right)e^{-2z} - \frac{25}{16} + \mathcal{O}(e^{-3z}), \tag{77}$$

whose turning points are $\log\left(\frac{1}{25}\left(2\quad 3^{2/3}\tilde{m}^2 \pm \sqrt{6}\sqrt{2\sqrt[3]{3}\tilde{m}^4 - 36\,3^{2/3}\tilde{m}^2 + 111} + 21\right)\right) = \log(3 + \mathcal{O}(\frac{1}{\tilde{m}^2}))$, $\log\left(0.33\tilde{m}^2 - 1.32 + \mathcal{O}(\frac{1}{\tilde{m}^2})\right)$. Now $\sqrt{V(\mathrm{UV}, T)} = \frac{1}{2}\sqrt[3]{3}\tilde{m}\,e^{-z}\sqrt{e^z - 3} + \mathcal{O}(\frac{1}{\tilde{m}})$. Therefore,

$$\int_{\log 3}^{\log(0.33\tilde{m}^2 - 1.32)}\sqrt{V(\mathrm{UV}, T)} = 0.654\tilde{m} - 2.5 = \left(n + \frac{1}{2}\right)\pi, \tag{78}$$

from which one obtains

$$m_n^{0^{-+}}(\mathrm{UV}, T) = (6.225 + 4.804n)\pi T. \tag{79}$$

4.1.4 WKB quantization at $r_h = 0$

The 'potential' is given by

$$V(0^{-+}, r_h = 0) = \frac{43^{2/3}\tilde{m}^2e^{2z} + \frac{e^{2z}(e^z+1)(5e^z+12)^2}{(e^z+2)^2} - 2(e^z + 1)(14e^z + 25e^{2z} + 4)}{16(e^z + 1)^3} + \mathcal{O}\left(\frac{g_sM^2}{N}\right). \tag{80}$$

Therefore, in the IR region

$$V(\mathrm{IR}, r_h = 0) = -\frac{1}{2} - \frac{3}{4}e^z + \left(\frac{9}{8} + \frac{3^{\frac{2}{3}}}{4}\tilde{m}^2\right)e^{2z} + \mathcal{O}(e^{3z}), \tag{81}$$

and in the IR region, the domain of integration becomes $[\log\left(\frac{\sqrt{2}}{3^{\frac{1}{3}}\tilde{m}}\right), \log(\delta^2 - 1)]$: $\int_{\log\left(\frac{\sqrt{2}}{3^{\frac{1}{3}}\tilde{m}}\right)}^{\log(\delta^2-1)}\sqrt{V(\mathrm{IR}, r_h = 0)} = \frac{3^{\frac{1}{3}}(\delta^2-1)}{2}\tilde{m} - 1.1126$, yielding

$$m_n^{0^{-+}}(\mathrm{IR}, r_h = 0) = \frac{(3.72 + 4.36n)}{(\delta^2 - 1)}\frac{r_0}{L^2}. \tag{82}$$

Also, in the UV region

$$V(\mathrm{UV}, r_h = 0) = \left(-\frac{3}{4}3^{2/3}\tilde{m}^2 - \frac{103}{16}\right)e^{-2z} + \left(\frac{1}{4}3^{2/3}\tilde{m}^2 + \frac{21}{8}\right)e^{-z} - \frac{25}{16}, \tag{83}$$

whose turning points are $\frac{1}{25}\left(23^{2/3}\tilde{m}^2 \pm \sqrt{12\sqrt[3]{3}\tilde{m}^4 - 2163^{2/3}\tilde{m}^2 - 2134} + 21\right) = \left(3 + \mathcal{O}(\frac{1}{\tilde{m}^2}), \frac{4}{25}3^{\frac{2}{3}}\tilde{m}^2 - \frac{33}{25}\right)$, yielding $\int_3^{\frac{4}{25}3^{2/3}\tilde{m}^2 - \frac{33}{25}}\sqrt{V(\mathrm{UV}, r_h = 0)} = \frac{\pi}{43^{\frac{1}{6}}} = \left(n + \frac{1}{2}\right)\pi$, from which one obtains

$$m_n^{0^{-+}}(\mathrm{UV}, r_h = 0) = 4.804\left(n + \frac{1}{2}\right)\frac{r_0}{L^2}. \tag{84}$$

5 Glueball ($0^{-(***\cdots)}$) masses

5.1 $r_h \neq 0$ and Neumann/Dirichlet boundary conditions at $r = r_h$

Given the Wess–Zumino term $A^{\mu\nu}d^{abc}\mathrm{Tr}\left(F^a_{\mu\rho}F^{b\ \rho}_{\lambda}F^{c\ \lambda}_{\nu}\right)$ and the two-form potential $A_{\mu\nu}$ being dual to a pseudoscalar, for $r_h \neq 0$, corresponding to QCD_3, one writes down the EOM for the fluctuation δA^{23}. The B_{MN}, C_{MN} EOMs are

$$D^M H_{MNP} = \frac{2}{3}F_{NPQRS}F^{QRS},$$
$$D^M F_{MNP} = -\frac{2}{3}F_{NPQRS}H^{QRS}, \tag{85}$$

or defining $A_{MN} = B_{MN} + iC_{MN}$, (85) can be rewritten as

$$D^M \partial_{[M} A_{NP]} = -\frac{2i}{3} F_{NPQRS} \partial^{[Q} A^{RS]}. \tag{86}$$

Now, $A_{MN} \to A^{(0)}_{MN} + \delta A_{MN}$ with $\delta A^{MN} = \delta^M_2 \delta^N_3 \delta A_{23}$, the EOM satisfied by $\delta A_{23}(x^{0,1,2,3}, r) = \int \frac{d^4k}{(2\pi)^4} e^{ik\cdot x} g_{22} G(r)$ reduces to

$$\partial_\mu \left(\sqrt{-g} g^{22} g^{33} g^{\mu\nu} \partial_\nu \delta A_{23}\right) = 0. \tag{87}$$

Assuming $a = \left(\alpha + \beta \frac{g_s M^2}{N} + \gamma \frac{g_s M^2}{N} \log r_h\right) r_h$ [33,42] for $(\alpha, \beta, \gamma) = (0.6, 4, 4)$ [33] and $k^\mu = (\omega, k_1, 0, 0) : k^2 = -m^2$, and defining $\mathcal{G}(r) \equiv g_{22} G(r)$ the EOM for $G(r)$ is

$$\begin{aligned}
&\mathcal{G}''(r) + \mathcal{G}'(r) \left(\frac{3 g_s M^2 (g_s N_f (\log N - 6 + \log(16)) - 24 g_s N_f \log(r) - 8\pi)}{64\pi^2 N r} \right. \\
&\left. - \frac{75 . {r_h}^2 (4 . g_s M^2 \log(r_h) + 4 . g_s M^2 + 0.6N)^2}{N^2 r^3} + \frac{5r^4 - {r_h}^4}{r^5 - r {r_h}^4} \right) \\
&- \frac{g_s m^2 \mathcal{G}(r)}{4\pi r^2 (r^4 - {r_h}^4)} \left(\frac{3 {r_h}^2 (4 . g_s M^2 \log(r_h) + 4 . g_s M^2 + 0.6N)^2}{N^2} - r^2 \right) \\
&\times [36 {g_s}^2 M^2 N_f \log^2(r) - 3 g_s M^2 \log(r) \\
&\times (g_s N_f (\log N - 6 + \log(16)) - 8\pi) + 16\pi^2 N] = 0.
\end{aligned} \tag{88}$$

The EOM (88) near $r = r_h$ can be approximated by

$$\mathcal{G}''(r) + \left(b_1 + \frac{1}{r - r_h}\right) \mathcal{G}'(r) + \mathcal{G}(r) \left(\frac{a_2}{r - r_h} + b_2\right) = 0, \tag{89}$$

where

$$\begin{aligned}
b_1 &= \frac{g_s M^2 (g_s (0.005 \log N - 0.015) N_f + (-0.114 g_s N_f - 360.) \log(r_h) - 360.119)}{N r_h} - \frac{24.5}{r_h}, \\
a_2 &= \frac{0.02 {g_s}^2 m^2 M^2 (\log(r_h) (g_s (0.24 \log N - 0.775) N_f - 2279.99) - 2.88 g_s N_f \log^2(r_h) - 2273.96)}{{r_h}^3} - \frac{0.251 g_s m^2 N}{{r_h}^3}, \\
b_2 &= \frac{0.04 {g_s}^2 m^2 M^2 (\log(r_h) (g_s N_f (8.158 - 3.42 \log N) + 4065.38) + g_s (0.12 \log N - 0.387) N_f + 41.04 g_s N_f \log^2(r_h) + 3976.41)}{{r_h}^4} \\
&\quad + \frac{7.163 g_s m^2 N}{{r_h}^4}.
\end{aligned} \tag{90}$$

The solution to (89) is given by

$$\begin{aligned}
\mathcal{G}(r) = e^{\frac{1}{2} r \left(-\sqrt{{b_1}^2 - 4b_2} - b_1\right)} &\left[c_1 U \left(-\frac{2a_2 - b_1 - \sqrt{{b_1}^2 - 4b_2}}{2\sqrt{{b_1}^2 - 4b_2}}, \right. \right. \\
&\left. \times 1, \sqrt{{b_1}^2 - 4b_2} r - \sqrt{{b_1}^2 - 4b_2} r_h \right) \\
&+ c_2 L_{\frac{2a_2 - \sqrt{{b_1}^2 - 4b_2} - b_1}{2\sqrt{{b_1}^2 - 4b_2}}} \left(r\sqrt{{b_1}^2 - 4b_2} - r_h \sqrt{{b_1}^2 - 4b_2} \right) \Bigg],
\end{aligned} \tag{91}$$

implying

$$\begin{aligned}
G'(r) &= \left(\frac{\mathcal{G}(r)}{g_{22}}\right)' \\
&= \frac{1}{\Gamma\left(\frac{-2a_2 + b_1 + \sqrt{{b_1}^2 - 4b_2}}{2\sqrt{{b_1}^2 - 4b_2}}\right)} \\
&\quad \times \sum_{n=-1}^{\infty} a_n(N, M, N_f, g_s, r_h)(r - r_h)^n.
\end{aligned} \tag{92}$$

Assuming $c_2 = 0$, the Neumann boundary condition at $r = r_h$ can be satisfied by setting the argument of the gamma function to a negative integer n. It runs out setting $\frac{-2a_2 + b_1 + \sqrt{{b_1}^2 - 4b_2}}{2\sqrt{{b_1}^2 - 4b_2}} = -n \in \mathbb{Z}^- \cup \{0\}$ produces a negligible ground state 0^{--} mass. Hence, we consider $\frac{-2a_2 + b_1 + 3\sqrt{{b_1}^2 - 4b_2}}{2\sqrt{{b_1}^2 - 4b_2}} = -n \in \mathbb{Z}^- \cup \{0\}$, which gives a finite ground state mass. This condition up to LO in N yields

$$\begin{aligned}
&\frac{T^2 \left(1.5 \sqrt{\frac{1.82719 \times 10^{12} T^2 - 1.66774 \times 10^9 m^2}{T^2}} - 675867.\right) + 265.153 m^2}{T \sqrt{1.82719 \times 10^{12} T^2 - 1.66774 \times 10^9 m^2}} \\
&= -n \in \mathbb{Z}^- \cup \{0\},
\end{aligned} \tag{93}$$

the solutions to which are given now:

$$\begin{aligned}
m_{0^{--}} &= 32.461 T, \\
m^*_{0^{--}} &= 32.88 T, \\
m^{**}_{0^{--}} &= 32.989 T,
\end{aligned}$$

$$m_{0^{--}}^{***} = 33.033T,$$
$$m_{0^{--}}^{****} = 33.055T. \tag{94}$$

One can show that one obtains the same spectrum as in (94) after imposing the Dirichlet boundary condition $G(r = r_h) = 0$.

5.2 $r_h = 0$ Limit of (88)

We have

$$\mathcal{G}''(r) + \frac{\mathcal{G}'(r)\left(\frac{3g_s M^2(g_s N_f(\log N - 6 + \log(16)) - 24 g_s N_f \log(r) - 8\pi)}{\pi^2 N} + 320\right)}{64r} + \frac{g_s m^2\left(36 {g_s}^2 M^2 N_f \log^2(r) - 3 g_s M^2 \log(r)(g_s N_f(\log N - 6 + \log(16)) - 8\pi) + 16\pi^2 N\right)}{4\pi r^4}\mathcal{G}(r) = 0. \tag{95}$$

The EOM (95) near $r = r_0$ – IR cut-off at $r_h = 0$ – reduces to

$$\mathcal{G}''(r) + (\alpha_1 + \beta_1(r - r_0))\mathcal{G}'(r) + (\alpha_2 + \beta_2(r - r_0))\mathcal{G}(r) = 0 \tag{96}$$

where

$$\begin{aligned}
\alpha_1 &= \frac{\frac{3{g_s}^2 \log N M^2 N_f}{\pi^2 N} + 320}{64 r_0}, \\
\beta_1 &= -\frac{3{g_s}^2 M^2 N_f}{64\pi^2 N {r_0}^2} - \frac{5}{{r_0}^2}, \\
\alpha_2 &= \frac{4\pi g_s m^2 N}{{r_0}^4} - \frac{3{g_s}^3 m^2 M^2 N_f \log(r_0)}{4\pi {r_0}^4}, \\
\beta_2 &= \frac{3{g_s}^3 \log N m^2 M^2 N_f (4\log(r_0) - 1)}{4\pi {r_0}^5} \\
&\quad - \frac{16\pi g_s m^2 N}{{r_0}^5}.
\end{aligned} \tag{97}$$

The solution to (96) is given by

$$\begin{aligned}
\mathcal{G}(r) = {} & \mathrm{e}^{-\alpha_1 r + \frac{\beta_2 r}{\beta_1} - \frac{\beta_1 r^2}{2} + \beta_1 r r_0} \\
& \times \Bigg[c_2 \, {}_1F_1\left(\frac{{\beta_1}^3 - \alpha_2 {\beta_1}^2 + \alpha_1 \beta_2 \beta_1 - {\beta_2}^2}{2{\beta_1}^3}; \right. \\
& \left. \times \frac{1}{2}; \frac{((r - r_0){\beta_1}^2 + \alpha_1\beta_1 - 2\beta_2)^2}{2{\beta_1}^3} \right) \\
& + c_1 H_{\frac{-\alpha_1\beta_1\beta_2 + \alpha_2{\beta_1}^2 - {\beta_1}^3 + {\beta_2}^2}{{\beta_1}^3}} \\
& \times \left(\frac{\alpha_1\beta_1 + {\beta_1}^2(r - r_0) - 2\beta_2}{\sqrt{2}{\beta_1}^{3/2}} \right) \Bigg].
\end{aligned} \tag{98}$$

One can then work out $G'(r = r_0) = \left(\frac{\mathcal{G}(r)}{g_{22}}\right)'\Big|_{r=r_0}$. Now, setting $c_2 = 0$, defining $\tilde{m}$ via $m = \tilde{m}\frac{r_0}{L^2}$, and using the large-$\tilde{m}$ limit of Hermite functions:

$$H_{\frac{-\alpha_1\beta_1\beta_2 + \alpha_2{\beta_1}^2 - (1 \text{ or } 2){\beta_1}^3 + {\beta_2}^2}{{\beta_1}^3}}\left(\frac{\alpha_1\beta_1 - 2\beta_2}{\sqrt{2}{\beta_1}^{3/2}}\right) \longrightarrow H_{-\frac{16\tilde{m}^4}{125}}\left(\frac{2^{\frac{5}{2}}}{5^{\frac{3}{2}}}\tilde{m}^2\right) \tag{99}$$

and

$$H_n(x) \xrightarrow{n \gg 1} \frac{2^{\frac{n}{2} + \frac{1}{2}} \mathrm{e}^{\frac{x^2}{2}} \left(\frac{n}{e}\right)^{n/2} \cos\left(\frac{\pi n}{2} - x\sqrt{2n - \frac{x^2}{3} + 1}\right)}{\sqrt[4]{1 - \frac{x^2}{2n}}}, \tag{100}$$

one can show that the Neumann (/Dirichlet: $G(r = r_0) = 0$) boundary condition at $r = r_0$ is equivalent to the condition

$$\frac{8}{375}\left(\sqrt{6}\tilde{m}^2\sqrt{375 - 64\tilde{m}^4} - 6i\pi\tilde{m}^4\right) = i\pi(2n + 1), \tag{101}$$

yielding

$$\begin{aligned}
& m_n^{0^{--}}(r_h = 0) \\
& = \frac{1}{2}5^{3/4}\sqrt[4]{\frac{-2\left(\sqrt{6}\sqrt{\pi^2\left(16n^2 + 22n + 7\right) + 6} + 6\right) - 3\pi^2(2n + 1)}{3\pi^2 - 32}} \\
& \quad \times \frac{r_0}{L^2}.
\end{aligned} \tag{102}$$

5.3 0^{--} Glueball spectrum from WKB method for $r_h \neq 0$

Using the variables of [32], the potential in the IR region is given as

$$V(\mathrm{IR}, T) = (6 - 0.01\tilde{m}^2)\mathrm{e}^z + (0.15\tilde{m}^2 - 16.1875)\mathrm{e}^{2z} + \mathcal{O}(\mathrm{e}^{3z}), \tag{103}$$

where in the 'large' $\tilde{m}$ limit, $V(\mathrm{IR}, T) > 0$ for (i)z : $\mathrm{e}^z > \frac{2.31799\times10^{31} - 3.86332\times10^{28}\tilde{m}^2}{6.25374\times10^{31} - 5.79497\times10^{29}\tilde{m}^2} = 0.067 + \mathcal{O}\left(\frac{1}{\tilde{m}^2}\right)$ if $\tilde{m} > 24.495$ and (ii) $0 < \mathrm{e}^z < \frac{2.31799\times10^{31} - 3.86332\times10^{28}\tilde{m}^2}{6.25374\times10^{31} - 5.79497\times10^{29}\tilde{m}^2} = 0.067 + \mathcal{O}\left(\frac{1}{\tilde{m}^2}\right)$ if $10.388 < \tilde{m} < 24.495$. One can show that $\int_{\log(0.067)}^{-2.526}\sqrt{V(\mathrm{IR}, T)} = \int_{-\infty}^{\log(0.067)}\sqrt{V(\mathrm{IR}, T)} \approx 0$, implying there is no contribution to the WKB quantization condition in the IR region.

Now, consider:

$$V(\mathrm{UV},T) = (-1.02\tilde{m}^2 - 22.5)\mathrm{e}^{-2z} + (0.25\tilde{m}^2 + 8.25)\mathrm{e}^{-z} - 1 + \mathcal{O}(\mathrm{e}^{-3z}). \tag{104}$$

For $\tilde{m} > 4.29$ the turning points of $V(\mathrm{UV},T)$ are $0.125\tilde{m}^2 - 0.025\sqrt{25.\tilde{m}^4 + 18.\tilde{m}^2 - 8775.} + 4.125 = 4.08 + \mathcal{O}\left(\frac{1}{\tilde{m}^2}\right) < \mathrm{e}^z < 0.125\tilde{m}^2 + 0.025\sqrt{25.\tilde{m}^4 + 18.\tilde{m}^2 - 8775.} + 4.125 = 0.25\tilde{m}^2 + 4.17 + \mathcal{O}\left(\frac{1}{\tilde{m}^2}\right)$. Hence,

$$\begin{aligned}&\int_{\log(4.08)}^{\log(0.25\tilde{m}^2+4.17)} \sqrt{V(\mathrm{UV},T)} \\ &= \int_{\log(4.08)}^{\log(0.25\tilde{m}^2+4.17)} \mathrm{e}^{-z}\sqrt{0.25\mathrm{e}^z - 1.02} + \mathcal{O}\left(\frac{1}{\tilde{m}}\right) \\ &= 0.389\tilde{m} - 2 + \mathcal{O}\left(\frac{1}{\tilde{m}}\right) = \left(n+\frac{1}{2}\right)\pi. \end{aligned} \tag{105}$$

Hence one obtains isospectrality with 0^{++}; for large n, there is also isospectrality with 2^{++}.

5.4 WKB method at $r_h = 0$

In this section we will discuss obtaining the spectrum at $r_h = 0$ using WKB quantization condition at LO in N in Sect. 5.4.1 and up to NLO in N in Sect. 5.4.2.

5.4.1 LO in N

In the IR region, the WKB 'potential' can be shown to be given by

$$V(\mathrm{IR}, r_h = 0) = -\frac{1}{4} + \frac{1}{4}(-3 + \tilde{m}^2)\mathrm{e}^{2z} + \mathcal{O}(\mathrm{e}^{3z}), \tag{106}$$

with turning points: $\left(\log\left(\frac{1}{m_0} + \mathcal{O}\left(\frac{1}{m_0^3}\right)\right) \approx -\log(m_0), \log\left(\delta^2 - 1\right)\right)$. Further dropping $\mathcal{O}\left(\frac{1}{m_0^3}\right)$ terms, $\int_{-\log m_0}^{-2.526}\sqrt{V(\mathrm{IR}, r_h = 0)} = \frac{\left(\delta^2-1\right)}{2}\tilde{m} - 0.785 = \left(n+\frac{1}{2}\right)\pi$ yielding

$$\begin{aligned} m_n^{0^{--}}(\mathrm{IR}, r_h = 0) &= \frac{(3+4n)\pi}{2\left(\delta^2-1\right)}\frac{r_0}{L^2} \\ &= \left(\frac{4.71 + 6.28n}{\delta^2 - 1}\right)\frac{r_0}{L^2}. \end{aligned} \tag{107}$$

In the UV region,

$$V(\mathrm{UV}, r_h = 0) = -\frac{3}{4}(\tilde{m}^2 + 3)\mathrm{e}^{-2z} + \frac{1}{4}(\tilde{m}^2 + 6)\mathrm{e}^{-z} - 1, \tag{108}$$

with turning points: $\left(\log\left(3 + \mathcal{O}\left(\frac{1}{\tilde{m}^2}\right)\right), \log\left(\frac{\tilde{m}^2}{4} - \frac{3}{2} + \mathcal{O}\left(\frac{1}{\tilde{m}^2}\right)\right)\right)$, and $\sqrt{V(\mathrm{UV}, r_h = 0)} = \frac{\mathrm{e}^{-z}}{2}\sqrt{\mathrm{e}^z - 3}\tilde{m} + \mathcal{O}\left(\frac{1}{\tilde{m}}\right)$:

$$\int_{\log 3}^{\log\left(\frac{\tilde{m}^2}{4} - \frac{3}{2}\right)} \frac{\mathrm{e}^{-z}}{2}\sqrt{\mathrm{e}^z - 3}\tilde{m} = \left(n + \frac{1}{2}\right)\pi, \tag{109}$$

implying:

$$m_n^{0^{--}}(\mathrm{UV}, r_h = 0) = (7.87 + 6.93n)\frac{r_0}{L^2}. \tag{110}$$

5.4.2 NLO (in N)/non-conformal corrections

Up to NLO in N, in the IR region, the potential '$V(\mathrm{IR}, r_h = 0)$' is given by:

$$\begin{aligned} V(\mathrm{IR}, r_h = 0) = \frac{1}{256\pi^2 N}\{&\mathrm{e}^{2z}(-{g_s}^2 M^2 N_f(6\log N \\ &- 72 + \log(16777216)) + 36{g_s}^2 M^2\tilde{m}^2 N_f \log^2(y_0) \\ &+ g_s M^2\log(y_0) \times (g_s N_f(72 - \tilde{m}^2(6\log N - 36 \\ &+ \log(16777216))) + 48\pi\tilde{m}^2) + 48\pi g_s M^2 \\ &+ 64\pi^2(\tilde{m}^2 - 3)N)\} - \frac{1}{4} + \mathcal{O}(\mathrm{e}^{-3z}). \end{aligned} \tag{111}$$

The turning points of (111) up NLO in N are given by $\Bigg[\log\left(\frac{1}{\tilde{m}}\left[1 - \frac{g_s M^2\log(y_0)(-g_s N_f(6\log N - 36 + \log(16777216)) + 36 g_s N_f\log(y_0) + 48\pi)}{128\pi^2 N}\right]\right), \log(\delta^2 - 1)\Bigg]$. After evaluation of the integral of $\sqrt{V(\mathrm{IR}, r_h = 0)}$ between the aforementioned turning points, in the large-$\tilde{m}$ limit, one obtains the following quantization condition:

$$\begin{aligned}&\left(\frac{(\delta^2-1)}{2} - \frac{3(\delta^2-1)g_s M^2(g_s N_f)\log N\ \log r_0}{64\pi^2 N}\right)\tilde{m} \\ &- \frac{\pi}{4} = \left(n + \frac{1}{2}\right)\pi, \end{aligned} \tag{112}$$

which yields

$$\begin{aligned} m_n^{0^{--}}(r_h = 0) = &\frac{6.28319n + 4.71239}{\delta^2 - 1} \\ &\times\left(1 + \frac{0.01{g_s}^2\log N M^2 N_f\log(r_0)}{N}\right). \end{aligned} \tag{113}$$

6 Glueball masses from M-theory

The glueball spectrum for spin 0^{++}, 1^{++} and 2^{++} is calculated in this section from the M-theory perspective both by considering $r_h \neq 0$ and an IR radial cut-off (for $r_h = 0$) in the background. The 11-dimensional M-theory action is given as

$$S_M = \frac{1}{16\pi}\int_M \mathrm{d}^{11}x\sqrt{G}\,R - \frac{1}{4}\sqrt{G}\int_M \mathrm{d}^{11}x G_4\wedge *_{11}G_4, \tag{114}$$

where $G_4 = \mathrm{d}C_3 + A_1\wedge \mathrm{d}B_2 + \mathrm{d}x_{10}\wedge \mathrm{d}B_2$, and $C^M_{\mu\nu 10} = B^{\mathrm{IIA}}_{\mu\nu}, C^M_{\mu\nu\rho} = C^{\mathrm{IIA}}_{\mu\nu\rho}$. Now, as shown in [28], no F_4^{IIA} (to be obtained via a triple T-dual of type IIB $F_{1,3,5}$ where $F_1 \sim F_{x/y/z}$, $F_3 \sim F_{xyr/\theta_1/\theta_2}, F_{xzr/\theta_1/\theta_2}, F_{yzr/\theta_1/\theta_2}$ and $F_5 \sim F_{xyz\beta_1\beta_2}$ where $\beta_i = r/\theta_i$) can be generated.[2] Thus, the four-form flux $G_4 = \mathrm{d}(C_{\mu\nu 10}\mathrm{d}x^\mu\wedge\mathrm{d}x^\nu\wedge\mathrm{d}x_{10}) + (A_1^{F_1} + A_1^{F_3} + A_1^{F_5})\wedge H_3 = H_3\wedge\mathrm{d}x_{10} + A\wedge H_3$, where $C_{\mu\nu 10}\equiv B_{\mu\nu}$.

$$\int G_4\wedge *_{11}G_4 = \int (H_3\wedge \mathrm{d}x_{10} + A\wedge H_3)\wedge *_{11}(H_3\wedge \mathrm{d}x_{10} + A\wedge H_3). \tag{115}$$

Now, $H_3\wedge \mathrm{d}x_{10}\wedge *_{11}(H_3\wedge A) = 0$ as neither H_3 nor A has support along x_{10}. Hence,

$$\begin{aligned} &H_3\wedge \mathrm{d}x_{10}\wedge *_{11}(H_3\wedge \mathrm{d}x_{10})\\ &= \sqrt{G}H_{\mu\nu\rho 10}G^{\mu\mu_1}G^{\nu\nu_1}G^{\rho\rho_1}G^{10\lambda_1}H_{\mu_1\nu_1\rho_1\lambda_1}\mathrm{d}t\wedge\cdots\mathrm{d}x_{10}\\ &= \sqrt{G}H_{\mu\nu\rho 10}(-G^{\mu 10}G^{\nu\nu_1}G^{\rho\rho_1}G^{10\lambda_1}H_{\nu_1\rho_1\lambda_1}\\ &\quad + G^{\mu\mu_1}G^{\nu 10}G^{\rho\rho_1}G^{10\lambda_1}H_{\mu_1\rho_1\lambda_1}\\ &\quad - G^{\mu\mu_1}G^{\nu\nu_1}G^{\rho 10}G^{10\lambda_1}H_{\mu_1\nu_1\lambda_1}\\ &\quad + G^{\mu\mu_1}G^{\nu\nu_1}G^{\rho\rho_1}G^{10\ 10}H_{\mu_1\nu_1\rho_1})\mathrm{d}t\wedge\cdots\mathrm{d}x_{10}, \end{aligned} \tag{116}$$

where $H_{\mu\nu\rho 10} = H_{\mu\nu\rho}$, and

$$\begin{aligned} &(H\wedge A)\wedge *_{11}(H\wedge A)\\ &= \sqrt{G}H_{[\mu\nu\rho A_\lambda]}G^{\mu\mu_1}G^{\nu\nu_1}G^{\lambda\lambda_1}H_{[\mu_1\nu_1\rho_1 A_{\lambda_1}]}, \end{aligned} \tag{117}$$

with $H_{[\mu_1\mu_2\mu_3 A_{\mu_4}]} \equiv H_{\mu_1\mu_2\mu_3 A_{\mu_4}} - (H_{\mu_2\mu_3\mu_4 A_{\mu_1}} - H_{\mu_3\mu_4\mu_1 A_{\mu_2}} + H_{\mu_4\mu_1\mu_2 A_{\mu_3}})$.

It was shown in [28] that in the MQGP limit (11), in Eq. (116), contribution of $H_3\wedge \mathrm{d}x^{11}\wedge *_{11}(H_3\wedge \mathrm{d}x^{11})$ is always dominated by $\sqrt{G}H_{\mu\nu\omega}G^{\mu\sigma}G^{\nu\psi}G^{\omega\alpha}G^{10\ 10}H_{\sigma\psi\alpha}$ term and in Eq. (117), contribution of $(H\wedge A)\wedge *_{11}(H\wedge A)$ is dominated by $\sqrt{G}H_{\theta_1\theta_2 y}A_\psi G^{\theta_1\alpha}G^{\theta_2\rho}G^{y\sigma}G^{\psi\beta}H_{\alpha\rho\beta}$ term. Therefore, for simplicity in calculations, we assume that leading contribution in Eqs. (116) and (117) are governed by aforementioned terms.

The relevant inverse components of the 11-dimensional metric, in the MQGP limit (11), as worked out in [28] using which the most dominant contribution near $\theta_{1,2} = 0$ in the Eqs. (116) and (117), as shown in [28], are given by the following analytical expressions:

$$\begin{aligned} &H_3\wedge \mathrm{d}x^{11}\wedge *_{11}(H_3\wedge \mathrm{d}x^{11})\Big|_{\theta_1\sim\frac{\alpha_{\theta_1}}{N^{\frac{1}{5}}},\theta_2\sim\frac{\alpha_{\theta_2}}{N^{\frac{3}{10}}}}\\ &= \frac{\sqrt{3}(-4\alpha_{\theta_2}^2 + 27\alpha_{\theta_1}^6)r^3N^{\frac{9}{10}}}{2\alpha_{\theta_1}^3\alpha_{\theta_2}^6 g_s^{\frac{11}{4}}\pi^{\frac{3}{4}}} + \frac{\alpha_{\theta_1}(82r^4 - r_h^4)N^{\frac{1}{4}}}{2\sqrt{3}\alpha_{\theta_2}^4 g_s^{\frac{11}{4}}\pi^{\frac{3}{4}}r} \end{aligned} \tag{118}$$

and

$$\begin{aligned} &(H\wedge A)\wedge *_{11}(H\wedge A)|_{\theta_1\sim\frac{\alpha_{\theta_1}}{N^{\frac{1}{5}}},\theta_2\sim\frac{\alpha_{\theta_2}}{N^{\frac{3}{10}}}}\\ &= \mathcal{F}(\alpha_{\theta_1},\alpha_{\theta_2};a;g_s,M,N_f)N^{\frac{17}{20}}, \end{aligned} \tag{119}$$

where $\mathcal{F}(\alpha_{\theta_1},\alpha_{\theta_2};a;g_s,M,N_f)$ is a well-defined function of the parameters indicated. One hence notes that $\lim_{r_\Lambda\to\infty}\int_0^{\frac{\sqrt{4\pi g_s N}}{r_h}}\int_{r_h}^{r_\Lambda}(H\wedge A)\wedge *_{11}(H\wedge A) \sim \frac{r_\Lambda}{r_h}N^{\frac{27}{20}}$, and is UV-divergent. Also, this yields a large cosmological constant in the IR because: $\frac{G_4\wedge *G_4}{\sqrt{G}} \ni \frac{|H\wedge A|^2}{\sqrt{G}} \sim \frac{N^{\frac{17}{20}}}{r^3N^{\frac{17}{20}}} = \frac{1}{r^3}$. To take care of both these issues, from the discussion of holographic renormalizability of the $D = 11$ supergravity action in [28], one sees that this term can be cancelled by a boundary counter term: $\int_{r=r_\Lambda}\sqrt{G}|G_4|^2$.

Now, using:

$$\sqrt{G}\Big|_{\theta_1\sim\frac{\alpha_{\theta_1}}{N^{\frac{1}{5}}},\theta_2\sim\frac{\alpha_{\theta_2}}{N^{\frac{3}{10}}}} = \frac{2N^{17/20}r^3}{27\ 3^{5/6}\sqrt[4]{\pi}\alpha_{\theta_1}^4\alpha_{\theta_2}g_s^{35/12}}, \tag{120}$$

and (118), one sees that one obtains a large-N suppressed cosmological constant from the second term in $\frac{|H\wedge \mathrm{d}x^{10}|^2}{\sqrt{G}}$, which remains small $\forall r > r_h$. To ensure one does not generate an N-enhanced cosmological constant from the first term in (118), one imposes the condition: $-4\alpha_{\theta_2}^2 + 27\alpha_{\theta_1}^6 = 0$, i.e., $\alpha_{\theta_2} = \frac{3^{\frac{3}{4}}\alpha_{\theta_1}^{\frac{3}{2}}}{\sqrt{2}}$.

One hence obtains the following flux-generated cosmological constant (with a slight abuse of notation):

$$\frac{G_4\wedge *G_4}{\sqrt{G}}\Big|_{\theta_1\sim\frac{1}{N^{\frac{1}{5}}},\theta_2\sim\frac{1}{N^{\frac{3}{10}}}} = \frac{3^{\frac{13}{12}}\sqrt{\alpha_{\theta_1}}g_s^{\frac{1}{6}}(82r^4 - r_h^4)}{N^{\frac{3}{5}}\sqrt{2\pi}r^4}. \tag{121}$$

Metric fluctuations: The background metric $g^{(0)}_{\mu\nu}$ is linearly perturbed as $g_{\mu\nu} = g^{(0)}_{\mu\nu} + h_{\mu\nu}$. With this perturbation the equation of motion follows from the action (114) as

$$R^{(1)}_{\mu\nu} = \frac{-1}{12}\frac{G_4^2}{\sqrt{G}}h_{\mu\nu}, \tag{122}$$

Now we assume the perturbation to have the following form: $h_{\mu\nu} = \epsilon_{\mu\nu}(r)\mathrm{e}^{ikx_1}$. Clearly there is a $SO(2)$ rotational sym-

[2] Consider T_x followed by T_y followed by T_z where T_i means T-dualizing along the ith direction. As an example, $T_x F^{\mathrm{IIB}}_x \to$ non − dynamical zero − form field strength$^{\mathrm{IIA}}$ [58], $T_y T_x F^{\mathrm{IIB}}_x \to F^{\mathrm{IIB}}_y$, $T_z F^{\mathrm{IIB}}_y \to F^{\mathrm{IIA}}_{yz}$ implying one can never generate F_4^{IIA} from F_1^{IIB}. As also an example consider $T_x F^{\mathrm{IIB}}_{xy\beta_i} \to F^{\mathrm{IIA}}_{y\beta_i}$, $T_y F^{\mathrm{IIA}}_{y\beta_i} \to F^{\mathrm{IIB}}_{\beta_i}$, $T_z F^{\mathrm{IIB}}_{\beta_i} \to F^{\mathrm{IIA}}_{\beta_i z}$ again not generating F_4^{IIA}; $T_x F^{\mathrm{IIB}}_{xyz\beta_1\beta_2} \to F^{\mathrm{IIA}}_{yz\beta_1\beta_2}$, $T_y F^{\mathrm{IIA}}_{yz\beta_1\beta_2} \to F^{\mathrm{IIB}}_{z\beta_1\beta_2}$, $T_z F^{\mathrm{IIB}}_{z\beta_1\beta_2} \to F^{\mathrm{IIB}}_{\beta_1\beta_2}$; thus one cannot generate F_4^{IIA}.

metry in the $x_2 - x_3$ plane which allow us to classify different perturbations into three categories, namely tensor, vector and scalar type of metric perturbations.

The mass spectrum was obtained by (i) solving equation (122) and applying Neumann/Diriclet boundary condition near r_h/r_0, (ii) following the redefinition of variables in [32] and then considering the WKB quantization condition.

6.1 0^{++} Glueball spectrum

The 0^{++} glueball in M-theory corresponds to scalar metric perturbations [59]:

$$\begin{aligned} h_{tt} &= g_{tt} e^{iqx_1} q_1(r), \\ h_{x_1 r} &= h_{r x_1} = iq\ g_{x_1 x_1} e^{iqx_1} q_3(r), \\ h_{rr} &= g_{rr} e^{iqx_1} q_2(r), \end{aligned} \tag{123}$$

where g_{tt}, $g_{x_i x_i}$ and g_{rr} are the metric components of the M-theory and is given in Eq. (21).

6.1.1 M-theory background with $r_h \neq 0$

Considering these components at leading order in N, and taking into account the above perturbation, we get the following differential equation for $q_3(r)$ with $q^2 = -m^2$ from (122):

$$\begin{aligned} & q_3''(r) + \frac{q_3'(r)}{12\pi g_s N r^3 (r^4 - {r_h}^4)} \{[r^2 (16\pi^2 {g_s}^2 m^2 N^2 r^2 \\ & + 12\pi g_s N (9r^4 - {r_h}^4) - 3r(r^4 - {r_h}^4)^2) \\ & - 3a^2 (16\pi^2 {g_s}^2 m^2 N^2 r^2 + 36\pi g_s N (r^4 - {r_h}^4) \\ & + 3r(r^4 - {r_h}^4)^2)]\} + \frac{q_3(r)}{12\pi g_s N r^4 (r^4 - {r_h}^4)} \\ & \times \{[r^2 (32\pi^2 {g_s}^2 m^2 N^2 r^2 + 12\pi g_s N (15r^4 + {r_h}^4) \\ & - 3r(5r^8 - 6r^4 {r_h}^4 + {r_h}^8)) - 36a^2 (4\pi^2 {g_s}^2 m^2 N^2 r^2 \\ & + \pi g_s N (11r^4 + {r_h}^4) + r^9 - r^5 {r_h}^4)]\} = 0. \end{aligned} \tag{124}$$

(a) *Spectrum from Neumann/Dirichlet Boundary Condition*: Equation (124), for $a = 0.6 r_h$ near $r = r_h$ (writing $m = \tilde{m} \frac{r_h}{L^2}$) simplifies to

$$\begin{aligned} & q_3''(r) + \frac{(2 - 0.00666667\tilde{m}^2) q_3'(r)}{r - r_h} \\ & + \frac{(0.76 - 0.103333\tilde{m}^2) q_3(r)}{r_h (r - r_h)} = 0. \end{aligned} \tag{125}$$

Lets write the above equation of the following form:

$$h''(r) + \frac{p}{r - r_h} h'(r) + \frac{s}{r - r_h} h(r) = 0, \tag{126}$$

where we have, $p = (2 - 0.00666667\tilde{m}^2)$, $s = \frac{(0.76 - 0.103333\tilde{m}^2)}{r_h}$.

The solution to (126) is given by

$$\begin{aligned} h(r) = {} & c_1 (2r - 2r_h)^{p/2} (r - r_h)^{-p/2} \\ & \times (-s(r - r_h))^{\frac{1}{2} - \frac{p}{2}} I_{p-1}(2\sqrt{-s(r - r_h)}) \\ & + (-1)^{1-p} c_2 (2r - 2r_h)^{p/2} (r - r_h)^{-p/2} \\ & \times (-s(r - r_h))^{\frac{1}{2} - \frac{p}{2}} K_{p-1}(2\sqrt{-s(r - r_h)}). \end{aligned} \tag{127}$$

Setting $c_2 = 0$, one can verify that one satisfy the Neumann boundary condition: $h'(r = r_h) = 0$ provided:

$$p = -n \in \mathbb{Z}^- \cup \{0\}, \tag{128}$$

implying:

$$\tilde{m} = 12.25\sqrt{2 + n}. \tag{129}$$

One can similarly show that by imposing the Dirichlet boundary condition, $h(r = r_h) = 0$,

$$\tilde{m} = 12.25\sqrt{1 + n}. \tag{130}$$

(b) *Spectrum using the WKB method*: Following the redefinition of [32], Eq. (124) can be rewritten in a Schrödinger-like form, where for $a = 0.6 r_h$ and setting $g_s = 0.9$, $N \sim (g_s)^{-39} \sim 100$ – in the MQGP limit of [28] – the 'potential' in the IR region can be shown to be given by

$$\begin{aligned} V_{\rm IR}(z) = {} & e^z (-0.00576389\tilde{m}^4 - 0.0708333\tilde{m}^2 + 0.) \\ & + 0.00201389\tilde{m}^4 + 0.00333333\tilde{m}^2 \\ & - 0.25 + \mathcal{O}(e^{2z}). \end{aligned} \tag{131}$$

The potential (131) is positive for $z \in (-\infty, \log(0.349)]$, but to remain within the IR region, one truncates this domain to $z \in (-\infty, -2.526]$ and the same yields

$$\begin{aligned} \int_{-\infty}^{-2.626} \sqrt{V_{\rm IR}(z)} &= 0.0898\tilde{m}^2 \log(\tilde{m}) - 0.0439\tilde{m}^2 \\ &= \pi \left(n + \frac{1}{2}\right) = \left(n + \frac{1}{2}\right)\pi, \end{aligned} \tag{132}$$

or

$$m_n^{0^{++}} = \frac{\sqrt{70.0055n + 35.0027}}{\sqrt{\mathcal{PL}(26.3065n + 13.1533)}}. \tag{133}$$

In the UV region, one can show that

$$\begin{aligned} V_{\rm UV}(z) = {} & \frac{-0.00694444\tilde{m}^4 + 0.295\tilde{m}^2 + 1.62}{e^{2z}} \\ & + \frac{-0.0833333\tilde{m}^2 - 0.54}{e^z} - 0.25 < 0, \end{aligned} \tag{134}$$

implying no turning points in the UV region.

6.1.2 M-theory background with IR cut-off r_0

In this case, Eq. (124) is modified only by the limit $(r_h, a) \to 0$. The equation in this limit is given as

$$q_3''(r) + q_3'(r)\left(\frac{4\pi g_s m^2 N}{3r^3} - \frac{r^4}{4\pi g_s N} + \frac{9}{r}\right) + q_3(r)\left(\frac{8\pi g_s m^2 N}{3r^4} - \frac{5r^3}{4\pi g_s N} + \frac{15}{r^2}\right) = 0. \tag{135}$$

(a) *Spectrum from Neumann/Dirichlet boundary condition*: Near the cut-off at $r = r_0$, Eq. (135) is given by

$$q_3''(r) + \left(\frac{4\tilde{m}^2 + 108}{12r_0} - \frac{(\tilde{m}^2+9)(r-r_0)}{{r_0}^2}\right) q_3'(r) + q_3(r)\left(\frac{8\tilde{m}^2+180}{12{r_0}^2} - \frac{(32\tilde{m}^2+360)(r-r_0)}{12{r_0}^3}\right) = 0, \tag{136}$$

whose solution is given by

$$q_3(r) = \mathrm{e}^{-\frac{2(4\tilde{m}^2+45)r}{3(\tilde{m}^2+9)r_0}}\left[c_1 H_{-\frac{2\tilde{m}^6+71\tilde{m}^4+828\tilde{m}^2+2835}{9(\tilde{m}^2+9)^3}}\left(\frac{3(\tilde{m}^2+9)^2 r - 2(2\tilde{m}^4+37\tilde{m}^2+153)r_0}{3\sqrt{2}(\tilde{m}^2+9)^{3/2}r_0}\right) + c_2\, {}_1F_1\left(\frac{2\tilde{m}^6+71\tilde{m}^4+828\tilde{m}^2+2835}{18(\tilde{m}^2+9)^3}; \frac{1}{2}; \frac{(3(\tilde{m}^2+9)^2 r - 2(2\tilde{m}^4+37\tilde{m}^2+153)r_0)^2}{18(\tilde{m}^2+9)^3 {r_0}^2}\right)\right]. \tag{137}$$

Thus,

$$q_3'(r=r_0) = \frac{1}{27{r_0}^2}\left\{\mathrm{e}^{-\frac{2(4\tilde{m}^2+45)}{3(\tilde{m}^2+9)}}([2\tilde{m}^6+71\tilde{m}^4+828\tilde{m}^2+2835]\left[-\frac{3\sqrt{2}c_1 r_0 H_{-\frac{11\tilde{m}^6+314\tilde{m}^4+3015\tilde{m}^2+9396}{9(\tilde{m}^2+9)^3}}\left(-\frac{\tilde{m}^4+20\tilde{m}^2+63}{3\sqrt{2}(\tilde{m}^2+9)^{3/2}}\right)}{(\tilde{m}^2+9)^{5/2}} - \frac{c_2(\tilde{m}^4+20\tilde{m}^2+63)r_0\, {}_1F_1\left(\frac{2\tilde{m}^6+71\tilde{m}^4+828\tilde{m}^2+2835}{18(\tilde{m}^2+9)^3}+1; \frac{3}{2}; \frac{(\tilde{m}^4+20\tilde{m}^2+63)^2}{18(\tilde{m}^2+9)^3}\right)}{(\tilde{m}^2+9)^4}\right] - \frac{1}{\tilde{m}^2+9}\left\{18(4\tilde{m}^2+45)r_0\left(c_1 H_{-\frac{2\tilde{m}^6+71\tilde{m}^4+828\tilde{m}^2+2835}{9(\tilde{m}^2+9)^3}}\left(-\frac{\tilde{m}^4+20\tilde{m}^2+63}{3\sqrt{2}(\tilde{m}^2+9)^{3/2}}\right) + c_2\, {}_1F_1\left(\frac{2\tilde{m}^6+71\tilde{m}^4+828\tilde{m}^2+2835}{18(\tilde{m}^2+9)^3}; \frac{1}{2}; \frac{(\tilde{m}^4+20\tilde{m}^2+63)^2}{18(\tilde{m}^2+9)^3}\right)\right)\right\}\right\}. \tag{138}$$

Numerically/graphically we see that, for $c_1 = -0.509c_2$, one gets $q_3(r = r_0, \tilde{m} \approx 4.1) = 0$. We hence estimate the ground state of 0^{++} from metric fluctuations in M-theory to be $4.1\frac{r_0}{L^2}$.

(b) *Spectrum using the WKB method*: Defining $m = \tilde{m}\frac{\sqrt{y_0}}{L^2}$ and following [32], the potential term in the Schrödinger-like equation from (135) is given as

$$V(z) = \frac{1}{2304\pi^2 {g_s}^2 N^2 (\mathrm{e}^z+1)^4}\{-16\pi^2 {g_s}^2 N^2 \times(12(\tilde{m}^2+12)\mathrm{e}^{3z} + (\tilde{m}^4+12\tilde{m}^2+216)\mathrm{e}^{2z} + 144\mathrm{e}^z + 36\mathrm{e}^{4z} + 36) + 24\pi g_s N {y_0}^{5/2}\mathrm{e}^{2z} \times(\mathrm{e}^z+1)^{7/2}(\tilde{m}^2+9\mathrm{e}^z+9) - 9{y_0}^5\mathrm{e}^{2z}(\mathrm{e}^z+1)^7\}. \tag{139}$$

We hence see that in the large-N limit, $V(z) < 0$, and hence it has no turning points. The WKB method à la [32] does not work in this case.

6.2 2^{++} Glueball spectrum

To study the spectrum of a spin 2^{++} glueball, we consider the tensor type of metric perturbations where the non-zero perturbations are given as

$$h_{x_2x_3} = h_{x_3x_2} = g_{x_1x_1}H(r)\mathrm{e}^{ikx_1}$$
$$h_{x_2x_2} = h_{x_3x_3} = g_{x_1x_1}H(r)\mathrm{e}^{ikx_1}, \tag{140}$$

where $g_{x_1x_1}$ is given in (21).

6.2.1 M-theory background with $r_h \neq 0$

Considering the tensor modes of metric perturbations and the M-theory metric components corrected up to NLO in N, given in (21), we obtain a second order differential equation in $H(r)$ from (122),

$$H''(r)+H'(r)\left(-\frac{3a^2}{r^3}+\frac{15g_sM^2(g_sN_f\log(N)-24g_sN_f\log(r)-6g_sN_f+g_sN_f\log(16)-8\pi)}{64\pi^2Nr}+\frac{5r^4-{r_h}^4}{r^5-r{r_h}^4}\right)$$
$$+\left(\frac{1}{4\pi r^4(r^4-rh^4)}[8\pi\{3a^2\ (-2\pi g_sNm^2r^2-r^4+{r_h}^4)+2\pi g_sNm^2r^4+4r^6\}-3{g_s}^2M^2m^2r^2(r^2-3a^2)\right.$$
$$\left.\times\log(r)\{g_sN_f\log(N)+g_sN_f(\log(16)-6)-8\pi\}+36{g_s}^3M^2N_fm^2r^2(r^2-3a^2)\log^2(r)]\right)H(r)=0, \tag{141}$$

where we assume $k^2=-m^2$ with m being the mass of the corresponding glueball.

(a) *Spectrum from Neumann/Dirichlet boundary condition*: Near $r=r_h$, the solution to the above equation will be given along the same lines as Sect. 5.1 for 0^{--} glueballs, and the analog of (93) is

$$\frac{T^2\left(\frac{1.5\sqrt{0.0536698T^2-0.00186263m^2}}{T}-0.115834\right)+0.00018196m^2}{T\sqrt{0.0536698T^2-0.00186263m^2}}=-n, \tag{142}$$

the solutions to which are given as

$$\begin{aligned}
m_{2^{++}}&=5.086T,\\
m^{*}_{2^{++}}&=5.269T,\\
m^{**}_{2^{++}}&=5.318T,\\
m^{***}_{2^{++}}&=5.338T,\\
m^{****}_{2^{++}}&=5.348T.
\end{aligned} \tag{143}$$

One can impose Dirichlet boundary condition: $H(r=r_h)=0$, and one can show that

$$m_n^{2^{++}\text{ (Neumann)}}=m_{n+1}^{2^{++}\text{ (Dirichlet)}},\quad \text{for } n=0,1,2,\ldots$$

(b) *Spectrum from WKB method*: Using the variables of [32], the potential term in the Schrödinger-like equation for 2^{++} glueball can be obtained from (141) and in the IR region, written in terms of $m=\tilde{m}\frac{r_h}{L^2}=\tilde{m}\frac{\sqrt{y_h}}{L^2}$, can be shown to be given by

$$V_{\rm IR}(z)=e^z(0.52-0.01\tilde{m}^2)+(0.15\tilde{m}^2-1.0275)e^{2z}+\mathcal{O}\left(\frac{g_sM^2}{N},e^{3z}\right). \tag{144}$$

Now, negative z implies being closer to the IR region and the boundary would correspond to $r\leq\sqrt{3}a=0.6\sqrt{3}r_h$, corresponding to $z=-2.53$. It can be shown that for $\tilde{m}>7.211$ $V(z\in[-2.71,-2.53])>0$. Now $\int_{z=-2.71}^{z=-2.53}\sqrt{V_{\rm IR}(z)}\approx 0$. Hence, the IR region does not contribute to the 2^{++} glueball spectrum.

In the UV region we must consider the limit $(z\to\infty)$. Moreover, in the UV region $N_f=M=0$. We have

$$V_{\rm UV}(z)=e^{-2z}(6.56-1.02\tilde{m}^2)+(0.25\tilde{m}^2-2.77)e^{-z}+1.+\mathcal{O}\left(\frac{1}{\tilde{m}},e^{-3z}\right), \tag{145}$$

whose turning points are $\{\log\left(4.08+\mathcal{O}(\frac{1}{\tilde{m}^2})\right),\infty\}$, giving the WKB quantization as

$$\int_{\log 4.08}^{\infty}\sqrt{V_{\rm UV}(z)}=0.39\tilde{m}=\left(n+\frac{1}{2}\right)\pi, \tag{146}$$

implying

$$m_n^{2^{++}}(T)=8.08\left(n+\frac{1}{2}\right)\frac{r_h}{L^2}. \tag{147}$$

6.2.2 M-theory background with an IR cut-off r_0

Considering the limit $(r_h,a\to 0)$, Eq. (141) is given by

$$H''(r)+\left(\frac{5(3M^2g_s(-24N_fg_s\log(r)-6N_fg_s+N_fg_s\log(N)+\log(16)N_fg_s-8\pi)+64\pi^2N)}{64\pi^2Nr}\right)H'(r)$$
$$+\frac{1}{4\pi r^4}(36m^2M^2N_fg_s^3\log^2(r)-3m^2M^2g_s^2\log(r)(N_fg_s\log(N)$$
$$+(\log(16)-6)N_fg_s-8\pi)+16\pi(\pi m^2Ng_s+2r^2))H(r)=0. \tag{148}$$

(a) *Neumann/Dirichlet boundary condition at* $r = r_0$: Up to LO in N near $r = r_0$, the above equation is given by

$$H''(r) + \left(\frac{5}{r_0} - \frac{5(r-r_0)}{{r_0}^2}\right) H'(r) + H(r)\left(\frac{\tilde{m}^2+8}{{r_0}^2} - \frac{4(\tilde{m}^2+4)(r-r_0)}{{r_0}^3}\right) = 0. \quad (149)$$

The solution of (149) is given by

$$H(r) = \mathrm{e}^{-\frac{4(\tilde{m}^2+4)r}{5r_0}}\left(c_1 H_{\frac{1}{125}(16\tilde{m}^4+53\tilde{m}^2+56)} \times \left(\frac{2(4\tilde{m}^2-9)r_0+25r}{5\sqrt{10}r_0}\right) + c_2\, {}_1F_1\left(\frac{1}{250}(-16\tilde{m}^4-53\tilde{m}^2-56); \frac{1}{2}; \frac{(25r+2(4\tilde{m}^2-9)r_0)^2}{250{r_0}^2}\right)\right). \quad (150)$$

The Neumann boundary condition $H'(r = r_0) = 0$, numerically shows that, for $c_1 = -0.509c_2$, the lightest 2^{++} glueball has a mass $1.137\frac{r_0}{L^2}$. Similarly, by imposing the Dirichlet boundary condition: $H(r = r_h) = 0$, for $c_1 = -0.509c_2$, the lightest 2^{++} glueball has a mass $0.665\frac{r_0}{L^2}$.

(b) *Spectrum using the WKB method*: Following [32], the 'potential' term, in the IR region, up to leading order in N with $m = \tilde{m}\frac{r_0}{L^2} = \tilde{m}\frac{\sqrt{y_0}}{L^2}$, is given as

$$V_{\mathrm{IR}}(z) = \frac{1}{4}(\tilde{m}^2+5)\mathrm{e}^{2z} - \frac{1}{4} + \mathcal{O}(\mathrm{e}^{3z}), \quad (151)$$

and $V_{\mathrm{IR}}(z) > 0$ for $z \in [\log(\frac{1}{\tilde{m}} + \frac{1}{\tilde{m}^3}), \log(\delta^2-1)] \approx [-\log\tilde{m}, \log(\delta^2-1)]$. Hence the WKB quantization condition gives

$$\int_{-\log\tilde{m}}^{-2.526}\sqrt{\frac{1}{4}(\tilde{m}^2+5)\mathrm{e}^{2z} - \frac{1}{4}} = \frac{(\delta^2-1)}{2}\tilde{m} - 0.785 + \mathcal{O}\left(\frac{1}{\tilde{m}^3}\right) = \left(n+\frac{1}{2}\right)\pi, \quad (152)$$

implying

$$m_n^{2^{++}}(\mathrm{IR}, r_h = 0) = m_n^{0^{--}}(\mathrm{IR}, r_h = 0). \quad (153)$$

In the UV region, we have

$$V_{\mathrm{UV}}(z) = \frac{1}{4}(\tilde{m}^2-10)\mathrm{e}^{-z} - \frac{3}{4}(\tilde{m}^2-5)\mathrm{e}^{-2z} + 1 + \mathcal{O}(\mathrm{e}^{-3z}) = \frac{\mathrm{e}^{-z}}{2}\sqrt{\mathrm{e}^z-3}\tilde{m} + \mathcal{O}\left(\mathrm{e}^{-3z}, \frac{1}{\tilde{m}}\right) \quad (154)$$

and $V_{\mathrm{UV}}(z) > 0$ for $z > \log\left(\frac{1}{8}\left(-\tilde{m}^2 + \sqrt{\tilde{m}^4 + 28{m_0}^2 - 140} + 10\right)\right) = \log\left(3 + \mathcal{O}\left(\frac{1}{\tilde{m}^2}\right)\right)$. Further, $\int_{\log 3}^{\infty}\sqrt{V_{\mathrm{UV}}(z)} = \frac{\pi\tilde{m}}{8\sqrt{3}}$, implying

$$m_n^{2^{++}}(\mathrm{UV}) = (3.46 + 6.93)\frac{r_0}{L^2}. \quad (155)$$

(c) *NLO-in-N/non-conformal corrections using the WKB method*: The 'potential' inclusive of NLO-in-N terms, in the IR region in the $r_h = 0$ limit, is given by

$$V(\mathrm{IR}, r_h = 0) = \frac{1}{512\pi^2 N}\{\mathrm{e}^{2z}(-60{g_s}^2M^2N_f \times (\log N - 12 + \log(16)) + 72{g_s}^2M^2{m_0}^2N_f\log^2(y_0) + g_sM^2\log(y_0)\times(g_sN_f({m_0}^2(-12\log N + 72 + \log(4096) - 15\log(16)) + 720) + 96\pi{m_0}^2) + 480\pi g_sM^2 + 128\pi^2({m_0}^2+5)N)\} - \frac{1}{4} + \mathcal{O}(\mathrm{e}^{-3z}), \quad (156)$$

whose turning points are given by $\left[\log\left\{\frac{1-\frac{g_sM^2\log(y_0)(g_sN_f(-12\log N+72+\log(4096)-15\log(16))+72g_sN_f\log(y_0)+96\pi)}{256\pi^2N}}{m_0}\right\}, \log\left(\delta^2-1\right)\right]$. The integral of $\sqrt{V(\mathrm{IR}, r_h = 0)}$ between these turning points, in the large-$\tilde{m}$ limit, yields the same spectrum as 0^{--} up to NLO in N.

6.3 Spin-1^{++} glueball spectrum

Here we need to consider the vector type of metric perturbation with the non-zero components given as $h_{ti} = h_{it} = g_{x_1x_1}G(r)\mathrm{e}^{ikx_1}$, $i = x_2, x_3$.

6.3.1 M-theory background with $r_h \neq 0$

Substituting the above ansatz for the perturbation in (122), the differential equation in $G(r)$ is given with $k^2 = -m^2$ as

$$G''(r) + G'(r)\left(-\frac{3a^2}{r^3} - \frac{15g_sM^2(-g_sN_f\log(N) + 24g_sN_f\log(r) + 6g_sN_f - 2g_sN_f\log(4) + 8\pi)}{64\pi^2Nr} + \frac{5}{r}\right) + \frac{G(r)}{4\pi r^4({r^4} - {r_h}^4)}\{(36{g_s}^3M^2N_f{m^2}r^2(r^2-3a^2)\log^2(r) - 3{g_s}^2M^2m^2r^2(r^2-3a^2)\log(r)(g_sN_f\log(N) + g_sN_f(\log(16)-6) - 8\pi) + 8\pi(3a^2(-2\pi g_sNm^2r^2 - r^4 + {r_h}^4) + 2\pi g_sNm^2r^4 + 4r^6))\} = 0. \quad (157)$$

(a) *Neumann/Diriclet boundary condition at* $r = r_h$: Near $r = r_h$, Eq. (157) up to LO in N, is given by

$$G''(r) + \left(\frac{3.92}{r_h}\right) G'(r) + \left(\frac{2 - 0.02\tilde{m}^2}{r_h(r - r_h)} + \frac{-1.16 + 0.57\tilde{m}^2}{r_h^2}\right) G'(r) = 0, \tag{158}$$

whose solution is given by

$$G(r) = \mathrm{e}^{\left(\frac{0.5r(-2.\sqrt{5.0016-0.57\tilde{m}^2}-3.92)+r_h\log(r-r_h)}{r_h}\right)} \times \left[c_1 U\left(-\frac{-0.01\tilde{m}^2 - \sqrt{5.0016 - 0.57\tilde{m}^2} + 1}{\sqrt{5.0016 - 0.57\tilde{m}^2}}, 2, \frac{2.\sqrt{5.0016 - 0.57\tilde{m}^2}r}{r_h} - 2.\sqrt{5.0016 - 0.57\tilde{m}^2}\right) + c_2 L^{1}_{\frac{-1.\sqrt{5.0016-0.57\tilde{m}^2}-0.01\tilde{m}^2+1}{\sqrt{5.0016-0.57\tilde{m}^2}}} \times \left(\frac{2r\sqrt{5.0016 - 0.57\tilde{m}^2}}{r_h} - 2.\sqrt{5.0016 - 0.57\tilde{m}^2}\right)\right]. \tag{159}$$

Imposing the Neumann boundary condition at $r = r_h$ yields

$$\lim_{z\to 0}\frac{1}{r_h}\left\{\mathrm{e}^{-\sqrt{5.0016-0.57\tilde{m}^2}}\left[0.140858c_1 r_h U \times \left(\frac{0.01\tilde{m}^2}{\sqrt{5.0016 - 0.57\tilde{m}^2}} - \frac{1}{\sqrt{5.0016 - 0.57\tilde{m}^2}} + 1, 2, z\right) + 0.140858c_2 r_h L^{1}_{-\frac{0.01\tilde{m}^2}{\sqrt{5.0016-0.57\tilde{m}^2}}+\frac{1}{\sqrt{5.0016-0.57\tilde{m}^2}}-1}(z)\right]\right\}. \tag{160}$$

Considering $p = \frac{0.01\tilde{m}^2}{\sqrt{5.0016-0.57\tilde{m}^2}} - \frac{1}{\sqrt{5.0016-0.57\tilde{m}^2}} + 1$ and setting $c_2 = 0$ in (160), and then using $\lim_{z\to 0} U(p, 2, z \sim 0) \sim \frac{z^{-1}\,{}_1F_1(p-1;0;z)}{\Gamma(p)}$, one notes that one can satisfy the Neumann boundary condition at $r = r_h$ provided $\lim_{z\to 0}\,{}_1F_1(p-1;0;z) = \lim_{b\to 0}\lim_{z\to 0}\,{}_1F_1(p-1;b;z)$ (i.e. first set z to 0 and then b), $p = -n \in \mathbb{Z}^-$. Hence,

$$\begin{aligned} m^{1^{++}}(T) &= 2.6956\pi T, \\ m^{1^{+++}}(T) &= 2.8995\pi T, \\ m^{1^{++++}}(T) &= 2.9346\pi T, \\ m^{1^{+++++}}(T) &= 2.9467\pi T. \end{aligned} \tag{161}$$

One can show that one obtains the same spectrum as (161) even upon imposing the Dirichlet boundary condition: $G(r = r_h) = 0$.

(b) *Spectrum using the WKB method*: Following [32], the 'potential' V in the Schrödinger-like equation working with the dimensionless mass variable $\tilde{m}$ defined via $m = \tilde{m}\frac{r_h}{L^2} = \tilde{m}\frac{\sqrt{y_h}}{L^2}$, in the IR region, can be shown to be given by

$$V_{\mathrm{IR}}(z) = \mathrm{e}^{2z}(0.15\tilde{m}^2 - 1.52) + \mathrm{e}^{z}(1 - 0.01\tilde{m}^2) - \frac{1}{4} + \mathcal{O}\left(\mathrm{e}^{3z}, \frac{1}{N}\right). \tag{162}$$

The zeros of the potential, as a function of e^z, in (162) are given by

$$\frac{-1.8765\times 10^{14}\tilde{m}^2 \pm 6.022232598554301\times 10^{-7}\sqrt{9.70917\times 10^{40}\tilde{m}^4 + 1.26219\times 10^{44}\tilde{m}^2 - 5.04877\times 10^{44}} + 1.8765\times 10^{16}}{5.70456\times 10^{16} - 5.6295\times 10^{15}\tilde{m}^2} = -\frac{25}{\tilde{m}^2} + \mathcal{O}\left(\frac{1}{\tilde{m}^2}\right),$$

$0.07 + \mathcal{O}\left(\frac{1}{\tilde{m}^2}\right)$; the first not being permissible. Now, in the IR $r \in [r_h, \sqrt{3}a \approx 0.6\sqrt{3}r_h]$ or in terms of z : $(-\infty, -2.526]$. Therefore the allowed domain of integration is $[\log(0.07), -2.526]$. Thus, in the IR region

$$\int_{z=-2.704}^{z=-2.526}\sqrt{\mathrm{e}^{2z}(0.15\tilde{m}^2 - 1.52) + \mathrm{e}^{z}(1 - 0.01\tilde{m}^2) - \frac{1}{4}} \approx 0, \tag{163}$$

implying a null contribution to the WKB quantization condition in the IR region.

In the UV region, the potential is given by

$$V_{\mathrm{UV}}(z) = \frac{\mathrm{e}^{3z}(-3b^2 + \tilde{m}^2 + 10) + \mathrm{e}^{2z}(-3b^2(\tilde{m}^2 + 2) + 2\tilde{m}^2 + 9) + \mathrm{e}^{z}((1 - 3b^2)\tilde{m}^2 + 1) + 4\mathrm{e}^{4z} - 2}{4(\mathrm{e}^{z} + 1)^3(\mathrm{e}^{z} + 2)}, \tag{164}$$

by which for $b = 0.6$ one obtains

$$V(N_f = M = 0, \text{UV}) = \mathrm{e}^{-2z}(6.56 - 1.02\tilde{m}^2) + (0.25\tilde{m}^2 - 2.77)\mathrm{e}^{-z} + 1 + \mathcal{O}(\mathrm{e}^{-3z}). \quad (165)$$

The zeros of the potential in the UV region, as a function of e^z, in (165) are given by $-0.125\tilde{m}^2 \pm 0.005\sqrt{625.\tilde{m}^4 + 26950.\tilde{m}^2 - 185671.} + 1.385 = (-0.25\tilde{m}^2 - 1.31, 4.08 + \mathcal{O}(\frac{1}{\tilde{m}^2}))$; the former not being permissible. Hence, the allowed domain of integration, over which the potential is positive, is $([\log(4.08), \infty)$. Performing a large-$\tilde{m}$ expansion, one obtains

$$\int_{\log(4.08)}^{\infty} \sqrt{\mathrm{e}^{-2z}(6.56 - 1.02\tilde{m}^2) + (0.25\tilde{m}^2 - 2.77)\mathrm{e}^{-z} + 1} = \int_{z=\log(4.08)}^{\infty} \mathrm{e}^{-z}\sqrt{0.25\mathrm{e}^z - 1.02} + \mathcal{O}\left(\frac{1}{\tilde{m}}\right) = 0.389\tilde{m} = \left(n + \frac{1}{2}\right)\pi, \quad (166)$$

yielding

$$m_n^{1^{++}}(T) = 4.04(1 + 2n)\frac{r_h}{L^2}. \quad (167)$$

6.3.2 M-theory background with an IR cut-off r_0

(a) *Neumann/Diriclet boundary condition at $r = r_0$*: Considering the limit of $(r_h, a) \to 0$ in Eq. (157) up to LO in N and imposing the Neumann boundary condition at the IR cut-off $r = r_0$, yields isospectrality with the 2^{++} glueball spectrum at $r_h = 0$.

(b) *Spectrum using the WKB method*: Using the redefinition of [32], the 'potential' up to leading order in N is given by

$$V(z) = \frac{(\tilde{m}^2 + 2)\mathrm{e}^{2z} - 3\mathrm{e}^z + 4\mathrm{e}^{3z} - 1}{4(\mathrm{e}^z + 1)^3} + \mathcal{O}\left(\frac{g_s M^2}{N}\right). \quad (168)$$

$$\int_{-\log\tilde{m}}^{\log(\delta^2-1)} \sqrt{V_{\text{IR}}(z)} = \frac{(\delta^2 - 1)}{2}\tilde{m} - \frac{\pi}{4} = \left(n + \frac{1}{2}\right)\pi. \quad (170)$$

Therefore,

$$m_n^{1^{++}}(\text{IR}, r_h = 0) = m_n^{2^{++}}(\text{IR}, r_h = 0) = m_n^{0^{--}}(\text{IR}, r_h = 0). \quad (171)$$

Further, in the UV region:

$$V_{\text{UV}}(z) = \frac{1}{4}(\tilde{m}^2 - 10)\mathrm{e}^{-z} - \frac{3}{4}(\tilde{m}^2 - 5)\mathrm{e}^{-2z} + 1 + \mathcal{O}(\mathrm{e}^{-3z}), \quad (172)$$

implying that $V_{\text{UV}}(z) > 0$ for $z \in [\log\left(\frac{1}{8}\right(- \tilde{m}^2 + \sqrt{\tilde{m}^4 + 28\tilde{m}^2 - 140} + 10\right) = \log\left(3 + \mathcal{O}(\frac{1}{\tilde{m}^2})\right), \infty)$. This yields the following WKB quantization condition:

$$\int_{\log 3}^{\infty} \sqrt{V_{\text{UV}}(z)} = \frac{\pi\tilde{m}}{4\sqrt{3}} = \left(n + \frac{1}{2}\right)\pi, \quad (173)$$

from which one obtains

$$m_n^{1^{++}}(\text{UV}, r_h = 0) = (3.46 + 6.93n)\frac{r_0}{L^2}. \quad (174)$$

(c) *NLO-in-N/non-conformal corrections using WKB method*: In the IR region, the 'potential' including NLO-in-N corrections in the $r_h = 0$ limit, is given by

$$V(\text{IR}, r_h = 0) = \frac{1}{4}\mathrm{e}^{2z}(\tilde{m}^2 + 5) + \frac{1}{512\pi^2 N}\{g_s M^2 \mathrm{e}^{2z}(\log(y_0)(g_s N_f(\tilde{m}^2(-12\log N + 72 + \log(4096) - 15\log(16)) + 720) + 96\pi\tilde{m}^2) + 60(8\pi - g_s N_f(\log N - 12 + \log(16))) + 72 g_s \tilde{m}^2 N_f \log^2(y_0))\} - \frac{1}{4}, \quad (175)$$

whose turning points are

$$\left[\log\left(\frac{1}{\tilde{m}}\left[1 - \frac{g_s M^2 \log(y_0)(g_s N_f(-12\log N + 72 + \log(4096) - 15\log(16)) + 72 g_s N_f \log(y_0) + 96\pi)}{256\pi^2 N}\right]\right), \log(\delta^2 - 1)\right],$$

In the IR region we get the potential as

$$V_{\text{IR}}(z) = -\frac{1}{4} + \frac{1}{4}(5 + \tilde{m}^2)\mathrm{e}^{2z} + \mathcal{O}(\mathrm{e}^{3z}), \quad (169)$$

giving the turning points $z \in [\log\left(\frac{1}{\tilde{m}} + \mathcal{O}(\frac{1}{\tilde{m}^3})\right) \approx -\log\tilde{m}, \log(\delta^2 - 1)]$ and the WKB quantization condition becomes

and the integral of $\sqrt{V(\text{IR}, r_h = 0)}$ between these turning points yields isospectrality with the 0^{--} and 2^{++} NLO-in-N spectrum.

7 2^{++} Glueball masses from type IIB

7.1 $r_h \neq 0$

The 10-dimensional type IIB supergravity action in the low energy limit is given by

$$\frac{1}{2k_{10}^2}\left\{\int \mathrm{d}^{10}x\, \mathrm{e}^{-2\phi}\sqrt{-G}\left(R-\frac{1}{2}H_3^2\right) - \frac{1}{2}\int \mathrm{d}^{10}x\sqrt{-G}\left(F_1^2+\widetilde{F_3^2}+\frac{1}{2}\widetilde{F_5^2}\right)\right\}, \tag{176}$$

where ϕ is the dilaton, G_{MN} is the 10-d metric and F_1, H_3, $\widetilde{F}_3$, $\widetilde{F}_5$ are different fluxes.

The five-form flux $\widetilde{F}_5$ and the three-form flux $\widetilde{F}_3$ are defined by

$$\widetilde{F}_5 = F_5 + \frac{1}{2}B_2\wedge F_3, \quad \widetilde{F}_3 = F_3 - C_0\wedge H_3, \tag{177}$$

where F_5 and F_3 are sourced by the D_3 and D_5 branes, respectively. B_2 is the NS–NS two-form and C_0 is the axion. For the three-form fluxes $\widetilde{F}_3$, H_3, the two-form B_2 and the axion C_0 [27], see (9). Now varying the action in (176) with respect to the metric $g_{\mu\nu}$ one gets the following equation of motion:

$$\begin{aligned} R_{\mu\nu} &= \left(\frac{5}{4}\right)\mathrm{e}^{2\phi}\widetilde{F}_{\mu p_2 p_3 p_4 p_5}\widetilde{F}_{\nu}^{p_2 p_3 p_4 p_5} \\ &\quad -\left(\frac{g_{\mu\nu}}{8}\right)\mathrm{e}^{2\phi}\widetilde{F}_5^2+\left(\frac{3}{2}\right)H_{\mu\alpha_2\alpha_3}H_{\nu}^{\alpha_2\alpha_3} \\ &\quad -\left(\frac{g_{\mu\nu}}{8}\right)H_3^2+\left(\frac{3}{2}\right)\mathrm{e}^{2\phi}\widetilde{F}_{\mu\alpha_2\alpha_3}\widetilde{F}_{\nu}^{\alpha_2\alpha_3} \\ &\quad -\left(\frac{g_{\mu\nu}}{8}\right)\mathrm{e}^{2\phi}\widetilde{F}_3^2+\left(\frac{1}{2}\right)\mathrm{e}^{2\phi}F_\mu F_\nu, \end{aligned} \tag{178}$$

and we consider the following linear perturbation of the metric:

$$g_{\mu\nu} = g_{\mu\nu}^{(0)} + h_{\mu\nu}, \tag{179}$$

where as before $\mu,\nu = \{t, x_1, x_2, x_3, r, \theta_1, \theta_2, \phi_1, \phi_2, \psi\}$. Here the only non-zero component according to the tensor mode of metric fluctuation is $h_{x_2x_3}$. Since the non-zero components of F_1, $\widetilde{F}_3$ and H_3 have no indices as $\{x_2, x_3\}$, the final equation of motion gets simplified and can be shown to be given as

$$\begin{aligned} R_{x_2x_3}^{(1)} &= \left(\frac{5}{4}\right)\mathrm{e}^{2\phi}(4\widetilde{F}_{x_2x_3p_3p_4p_5}\widetilde{F}_{x_2x_3q_3q_4q_5}g^{p_3q_3}g^{p_4q_4}g^{p_5q_5}h^{x_2x_3}) \\ &\quad -\left(\frac{h_{x_2x_3}}{8}\right)\mathrm{e}^{2\phi}\widetilde{F}_5^2-\left(\frac{h_{yz}}{8}\right)H_3^2-\left(\frac{h_{x_2x_3}}{8}\right)\mathrm{e}^{2\phi}\widetilde{F}_3^2. \end{aligned} \tag{180}$$

Working at a particular value of θ_1 and θ_2 given as $\theta_1 = N^{-1/5}$ and $\theta_2 = N^{-3/10}$, the square of different fluxes figuring in (180) at the lowest-order in N, are given in (A1). Writing the perturbation $h_{x_2x_3}$ as $h_{x_2x_3} = \frac{r^2}{2(g_s\pi N)^{1/2}}H(r)\mathrm{e}^{ikx_1}$, Eq. (180) reduces to the following second order differential equation in $H(r)$:

$$\begin{aligned} &H''(r)+\left(\frac{5r^4-{r_h}^4}{r(r^4-{r_h}^4)}-\frac{9a^2}{r^3}+\left\{\frac{3}{256\pi^2N^{2/5}r^3}\right.\right. \\ &\times[-54a^2{g_s}^2M^2N_f-72\pi a^2g_sM^2+768\pi^2a^2 \\ &+12{g_s}^2M^2N_fr^2+9a^2{g_s}^2M^2N_f\log(16) \\ &-2{g_s}^2M^2N_fr^2\log(16)+16\pi g_sM^2r^2 \\ &+{g_s}^2M^2N_f(9a^2-2r^2)\log(N)-24{g_s}^2M^2N_f \\ &\left.\left.\times(9a^2-2r^2)\log(r)]\right\}\right)H'(r)+\left(\frac{1}{4\pi r^4(r^4-{r_h}^4)}\right. \\ &\times\{8\pi(a^2(6\pi g_sNq^2r^2-9r^4+9{r_h}^4) \\ &-2\pi g_sNq^2r^4+4r^6)+3{g_s}^2M^2q^2r^2(r^2-3a^2) \\ &\times\log(r)(g_sN_f\log(16N)-6g_sN_f-8\pi) \\ &-36{g_s}^3M^2N_fq^2r^2(r^2-3a^2)\log^2(r)\} \\ &-\frac{{g_s}^2}{512\pi^3}\left\{\frac{34992a^2g_sM^2\left(\sqrt[5]{N}+3\right)N_f{}^2\log(r)}{r^3}\right. \\ &+9a^2g_sN_f\left(\frac{7831552\pi^5}{(r^4-{r_h}^4)(g_sN_f\log(16N)-3g_sN_f\log(r)+4\pi)^3}\right. \\ &\left.\left.-\frac{81M^2\left(7\sqrt[5]{N}-1\right)N_f}{r^4}\right) \\ &\left.\left.+\frac{2\left(243g_sM^2\left(\sqrt[5]{N}+1\right)N_f{}^2+\frac{3915776\pi^5r^4}{\left(r^4-{r_h}^4\right)(g_sN_f\log(16N)-3g_sN_f\log(r)+4\pi)^2}\right)}{r^2}\right\}\right) \\ &\times H(r)=0. \end{aligned} \tag{181}$$

7.1.1 Mass spectrum from Neumann boundary condition at $r = r_h$

To get a sensible answer, one has to perform a small-T expansion when one rewrites and solves (181) around $r = r_h$. This time the analog of (93) becomes

$$0.5-\frac{0.174071m^2\left(1-\frac{3.(g_sM^2(2.\log(N)+11.8963)+4.g_sM^2\log(T)+0.6N)^2}{N^2}\right)}{T\sqrt{-m^2\left(4-7\left(1-\frac{3.(g_sM^2(2.\log(N)+11.8963)+4.g_sM^2\log(T)+0.6N)^2}{N^2}\right)\right)}} = -n, \tag{182}$$

which for $g_s = 0.8$, $N = g_s^{-39} \sim 6000$, $M = 3$ yields

$$\begin{aligned} m_{2^{++}} &= 4.975T, \\ m_{2^{++}}^{*} &= 14.925T, \\ m_{2^{++}}^{**} &= 24.876T, \\ m_{2^{++}}^{***} &= 34.826T, \\ m_{2^{++}}^{****} &= 44.776T. \end{aligned} \tag{183}$$

Thus, one obtains an approximate match between the ground state 2^{++} mass from M-theory and type IIB string theory.

7.1.2 WKB quantization method

Using the variables of [32], the 'potential', defining $m = \tilde{m}\frac{\sqrt{y_h}}{L^2}$, yields

$$V(2^{++}, \text{IIB}, r_h \neq 0) = \frac{1}{4(e^z+1)^3(e^z+2)^2} \times\{e^z(3b^2(e^z+2)(-(\tilde{m}^2-6)e^z - \tilde{m}^2 + 3e^{2z} + 6) + (-e^z-1)((25-3\tilde{m}^2)e^z - (\tilde{m}^2-18)e^{2z} - 2(\tilde{m}^2-6) + 4e^{3z}))\} + \mathcal{O}\left(\frac{g_s M^2}{N}\right). \quad (184)$$

In the IR region, the potential is given by

$$V(\text{IR}, T) = e^z((0.15\tilde{m}^2 - 1.3375)e^z - 0.01\tilde{m}^2 + 0.06) + \mathcal{O}(e^{3z}), \quad (185)$$

and in the IR region, for $\tilde{m} > 2.986$, $V(\text{IR} < T) > 0$ for $z \in [\log\left(0.067 + \mathcal{O}\left(\frac{1}{\tilde{m}^2}\right)\right) \approx -2.708, -2.526]$ and $\int_{2.708}^{-2.526}\sqrt{V(\text{IR}, T)} \approx 0$ – hence the IR region provides no contribution to the WKB quantization.

In the UV region,

$$V(\text{UV}, T) = \frac{1}{4}(\tilde{m}^2 + 9.24)e^{-z} - \frac{3}{4}(\tilde{m}^2 + 0.36(\tilde{m}^2+9) + 3) + \mathcal{O}(e^{-3z}), e^{-2z} - 1, \quad (186)$$

the turning points for $\tilde{m} > 7.141$ are $\left(\log(4.08 + \mathcal{O}\left(\frac{1}{\tilde{m}^2}\right), 0.25\tilde{m}^2 - 1.77\right)$. Hence,

$$\int_{1.406}^{\log(0.25\tilde{m}^2-1.77)}\sqrt{V(\text{UV}, T)} = \int_{1.406}^{\log(0.25\tilde{m}^2-1.77)}\frac{e^{-z}}{2}\sqrt{e^z - 4.08}\tilde{m} + \mathcal{O}\left(\frac{1}{\tilde{m}}\right) = 0.389\tilde{m} - 2 = \left(n+\frac{1}{2}\right)\pi, \quad (187)$$

from which one obtains

$$m_n^{2^{++}}(T) = (9.18 + 8.08n)\frac{r_h}{L^2}. \quad (188)$$

Hence, the string theory 2^{++} glueball is isospectral with 0^{++}; in the large-n limit of the spectrum, M-theory and type IIB spectra coincide.

7.2 $r_h = 0$

7.2.1 WKB method

Once again defining $r = \sqrt{y}, r_h = \sqrt{y_0}, y = y(1+e^z)$ analogous to their $r_h \neq 0$ redefinitions of [32], the 'potential' in the IR region, is given by

$$V(r_h = 0) = -\frac{1}{4} + \frac{1}{4}(1+\tilde{m}^2)e^{2z} + \mathcal{O}(e^{-3z}). \quad (189)$$

The domain in the IR region over which $V(r_h = 0) >$ is $[-\frac{1}{2}\log(5+\tilde{m}^2), \log(\delta^2-1)]$ and

$$\int_{-\frac{1}{2}\log(5+\tilde{m}^2)}^{-2.526}\sqrt{-\frac{1}{4} + \frac{1}{4}(1+\tilde{m}^2)e^{2z}} = \frac{(\delta^2-1)}{2}\tilde{m} - \frac{\pi}{4} = \left(n+\frac{1}{2}\right)\pi, \quad (190)$$

yielding

$$m_n^{2^{++}}(\text{IR}, \text{IIB}, r_h = 0) = m_n^{2^{++}}(\text{IR}, M \text{ theory}, r_h = 0). \quad (191)$$

In the UV region,

$$V(\text{UV}, r_h = 0) = \frac{1}{4}(\tilde{m}^2 - 10)e^{-z} - \frac{3}{4}(\tilde{m}^2 - 5)e^{-2z} + 1 + \mathcal{O}(e^{-3z}), \quad (192)$$

the zeros of which, as functions of e^z, are at $(\frac{1}{8}(-\tilde{m}^2 \pm \sqrt{\tilde{m}^4 + 28\tilde{m}^2 - 140} + 10) = (-\frac{\tilde{m}^2}{4} - \frac{1}{2}, 3 + \mathcal{O}(\frac{1}{\tilde{m}^2}))$. Hence the domain of integration over which $V(\text{UV}, r_h = 0) > 0$ is $[\log 3, \infty)$. Therefore,

$$\int_{\log 3}^{\infty}\sqrt{V(\text{UV}, r_h = 0)} = \frac{1}{2}\int_{\log 3}^{\infty}e^{-z}\sqrt{e^z - 3}\tilde{m} + \mathcal{O}\left(\frac{1}{\tilde{m}}\right) = \frac{\tilde{m}\pi}{4\sqrt{3}} = \left(n+\frac{1}{2}\right)\pi, \quad (193)$$

yielding

$$m_n^{2^{++}}(r_h = 0) = (3.464 + 6.928n)\frac{r_0}{L^2}. \quad (194)$$

7.2.2 NLO-in-N/non-conformal corrections in the IR region in the $r_h = 0$ limit

The 'potential' inclusive of the NLO-in-N corrections in the IR region in the $r_h = 0$ limit, reads

$$V(\text{IR}, r_h = 0) = e^{2z}\left(\frac{g_s M^2\left(\frac{1}{N}\right)^{2/5}(g_s N_f(6\log N - 72 + \log(16777216)) - 72 g_s N_f \log(y_0) - 48\pi)}{512\pi^2} + \frac{1}{4}(\tilde{m}^2 - 3)\right) - \frac{1}{4} + \mathcal{O}(e^{-3z}), \quad (195)$$

Table 1 Summary of glueball spectra: $m = \tilde{m}\frac{r_h}{L^2}$ from type IIB, IIA and M-theory using WKB quantization condition for $r_h \neq 0$, and $m = \tilde{m}\frac{r_0}{L^2}$ for $r_h = 0$ (equalities in the $r_h = 0$ column, are valid up to NLO in N); the colored triangles/square in the third column correspond to the colored triangles/square that appear in Fig. 2 in the combined plot of $r_h \neq 0$ supergravity calculations of glueballs

S. no.	Glueball	$\tilde{m}$ using WKB $r_h \neq 0$ (units of πT, up to LO in N) (large-$\tilde{m}$ limit)	$\tilde{m}$ using WKB $r_h = 0$ (units of $\frac{r_0}{L^2}$, up to NLO in N) (large-$\tilde{m}$ limit)
1	0^{++}	(M-theory)	(M-theory)
	(Fluctuations: $h_{00,rx_1,rr}$ in M-theory metric)	$\frac{\sqrt{35+70n}}{\sqrt{\mathcal{PL}(13.15+26.31n)}}$ ▲	No turning points
	0^{++}	(Type IIB)	(Type IIB)
	(Dilaton fluctuations)	$9.18 + 8.08n$ ▲	$\frac{(4.64+6.28n)}{(\delta^2-1)}\left[1 - 0.01\frac{g_s M^2}{N}(g_s N_f)\log N \log r_0\right]$
2	0^{-+}	(Type IIA)	(Type IIA)
	(One-form fluctuation a_{θ_2})	$11.12\left(n+\frac{1}{2}\right), n = 0$ ■	$\frac{3.72+4.36n}{(\delta^2-1)}, n = 0$
		$(6.22 + 4.80n), n \in \mathbb{Z}^+$ ▲	$4.8\left(n+\frac{1}{2}\right), n \in \mathbb{Z}^+$
3	0^{--}	(Type IIB)	(Type IIB)
	Two-form fluctuation A_{23}	$= m_n^{0^{++}}$ (dilaton, T)	$\frac{6.28n+4.71}{(\delta^2-1)}\left(1 + \frac{0.01 g_s{}^2 \log N M^2 N_f \log(r_0)}{N}\right), n = 0$
		▲	$(7.87 + 6.93n), n \in \mathbb{Z}^+$
4	1^{++}	(M-theory)	(M-theory)
	(Fluctuations: $h_{it} = h_{ti}, i = x_{2,3}$ in M-theory metric)	$8.08\left(n+\frac{1}{2}\right)$	$m_n^{1^{++}}(n = 0, r_h = 0) = m_n^{0^{--}}(n = 0, r_h = 0)$
		▲	$(3.46 + 6.93n), n \in \mathbb{Z}^+$
5	2^{++}	(M-theory)	(M-theory)
	(Fluctuations: $h_{x_2x_3} = h_{x_3x_2}, h_{x_2x_2} = h_{x_3x_3}$ in M-theory metric)	$8.08\left(n+\frac{1}{2}\right) = m_n^{1^{++}}(T)$	$= m_n^{1^{++}}(r_h = 0)$
		▲	
	2^{++}	(Type IIB)	(Type IIB)
	(Fluctuation $h_{x_2x_3} = h_{x_3x_2}$ in type IIB metric)	$9.18 + 8.08n = m_n^{0^{++}}$ (IIB, T)	$= m_n^{1^{++}}(r_h = 0)$
		▲	

whose turning points, in the large-$\tilde{m}$ limit, are $[\log\{\frac{1}{\tilde{m}} + \mathcal{O}(\frac{1}{\tilde{m}^3})\}, \log(\delta^2 - 1)] \approx [-\log\tilde{m}, \log(\delta^2 - 1)]$. Now,

$$\int_{-\log\tilde{m}}^{\log(\delta^2-1)} \sqrt{V(\mathrm{IR}, r_h = 0)} = \frac{(\delta^2-1)}{2}\tilde{m} - \frac{\pi}{4} + \mathcal{O}\left(\frac{1}{\tilde{m}}\right) = \left(n + \frac{1}{2}\right), \tag{196}$$

which yields the same *LO* spectrum as 0^{--}, 1^{++} and the 2^{++} spectrum obtained from M-theory. Hence, the type IIB at $r_h = 0$ is unable to capture the non-conformal NLO-in-N corrections in the 2^{++} corrections, as the same either precisely cancel out or are $\frac{1}{\tilde{m}}$-suppressed in the large-$\tilde{m}$ limit, in a IIB computation.

8 Summary and discussion

Supergravity calculations of glueball spectra in top–down holographic duals of large-N thermal QCD at *finite string/gauge coupling* and not just $g_s N \gg 1$, have thus far been missing in the literature. Such a limit is particularly relevant to sQGP [3]. This work fills in this gap by working out the spectra of $0^{++}, 0^{-+}, 0^{--}, 1^{++}, 2^{++}$ glueballs in a type IIB/delocalized SYZ IIA mirror/(its) M-theory (uplift) model corresponding to the top–down holographic dual of [27] in the MQGP limit introduced in [28]. As discussed in Sect. 2.1, towards the end of a Seiberg-duality cascade in the IR region, despite setting $M (= N_c$ in the IR region) to three in the MQGP limit, due a flavor–color enhancement of the length scale as compared to the KS model, one can trust supergravity calculations without worrying about stringy corrections. Further, in the MQGP limit, all physical quantities,

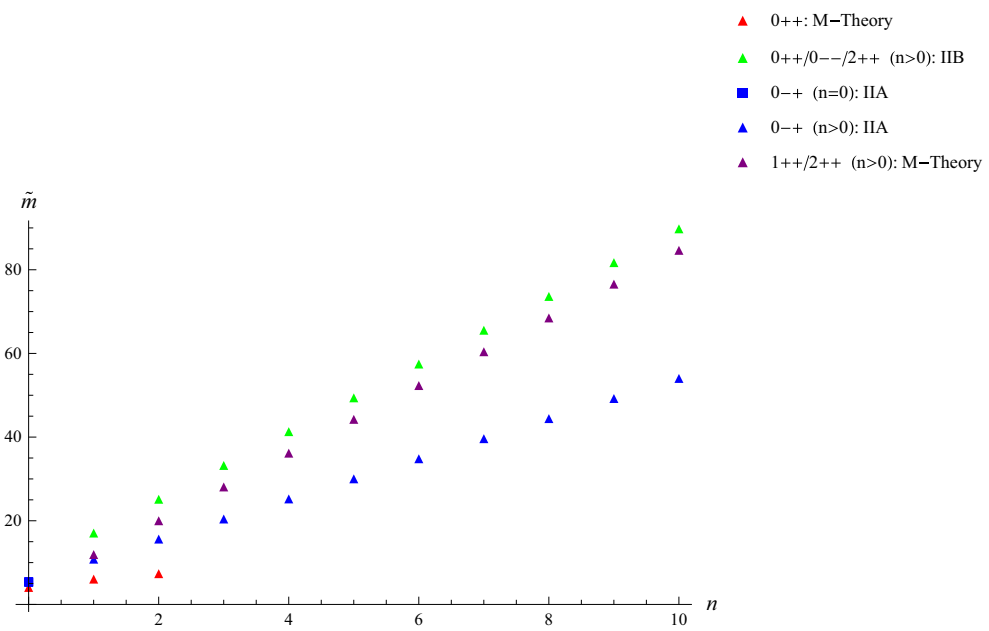

Fig. 2 Plots of supergravity 0^{++}, 0^{-+}, 0^{--}, 1^{++} glueball spectra for $r_h \neq 0$

Table 2 Comparison of [62]'s $N \to \infty$ lattice results for 0^{++} glueball with our supergravity results obtained using WKB quantization condition and redefinitions of [32] for M-theory scalar metric fluctuations

State	$N \to \infty$ entry in Table 34 of [62] in units of square root of string tension	M-theory scalar metric perturbations (Sect. 6.1.2 – in units of $\frac{r_h}{L^2}$)	Type IIB dilaton fluctuations of [60] in units of reciprocal of temporal circle's diameter
0^{++}	4.065 ± 0.055	4.267	4.07 (normalized to match lattice)
0^{++*}	6.18 ± 0.13	6.251	7.02
0^{++**}	7.99 ± 0.22	7.555	9.92
0^{++**}	–	8.588	12.80
0^{++***}	–	9.464	15.67

as seen in all calculations in [33], receive non-conformal corrections that appear at the NLO in N and display a universal $\frac{g_s M^2 (g_s N_f)}{N}$-suppression.

It should be noted that a numerical computation like the 'shooting computation' used in a lot of holographic glueball spectrum computations will not be feasible to use for the following reason. In the 'shooting method', like [60], one can first solve the EOMs in the UV using the infinite series/Frobenius method and then numerically (via Euler's method, etc.) obtain the solution at the horizon where one imposes a Neumann boundary condition. By matching the value obtained by numerically 'shooting' from the UV to the horizon in the IR region and matching the radial derivative of the solution so obtained to zero, one can obtain quantized values of the glueball masses. The caveat is that one should have at hand the exact radial profile of the effective number of fractional $D3$-branes ($D5$-branes wrapping the small two-cycle) and the number of flavor branes which would correctly interpolate between $(M, N_f) = (0, 0)$ in the UV and $(M = 3, N_f = 2)$ in the IR region. But we do not have this information – we know the values in the IR and the UV region but not for the interpolating region. Hence, numerical methods such as the 'shooting method' could at best be used, to obtain only the LO-in-N results, not the NLO-in-N results, which is one of the main objectives of our computations.

The summary of all calculations is given in Table 1 (and Fig. 2) and Table 3 – the former table/graph having to do with a WKB quantization calculation using the coordinate/field redefinitions of [32] and the latter table having to do with obtaining the mass spectrum by imposing Neumann/Dirichlet boundary condition at r_h/IR cut-off r_0. Some of the salient features of the results are given as separate bullets.

It should be noted that the last two columns in Tables 1 and 3 have been prepared in the same spirit as the last columns in Table 2 of [61].

Table 3 Summary of glueball spectra from Type IIB, IIA and M Theory for $r_h \neq 0/r_h = 0$ using Neumann/Dirichlet boundary conditions at the horizon r_h/IR cut-off r_0

S. no.	Glueball	Spectrum using N(eumann)/D(irichlet) b.c., $r = r_h$ (units of πT)	Spectrum using N(eumann)/D(irichlet) b.c., $r = r_0$ (units of $\frac{r_0}{L^2}$)
1	0^{++}	(M-theory)	(M-theory)
		(N) $12.25\sqrt{2+n}$	(N) 4.1
		(D) $12.25\sqrt{1+n}$	
2	0^{-+}	(Type IIA)	(Type IIA)
		(N/D) $\frac{3.1}{\pi}\sqrt{n}$	(N) $m^{0^{-+}}_{n=0} = 0, m^{0^{-+}}_{n=1} \approx 3.4, m^{0^{-+}}_{n=2} \approx 4.35$
			(D) $m^{0^{-+}}_{n=0} = 0, m^{0^{-+}}_{n=1} \approx 3.06, m^{0^{-+}}_{n=2} \approx 4.81$
3	0^{--}	(Type IIB)	(Type IIB)
		(N/D) $m^{0^{--}}_{n=0}(T) = 0, m^{0^{--}}_{n=1}(T) = \frac{32.46}{\pi}$,	(large n)
		$m^{0^{--}}_{n=2}(T) = \frac{32.88}{\pi}$	(N/D)
			$\frac{1}{2}5^{3/4}\sqrt[4]{\frac{2\left(\sqrt{6}\sqrt{\pi^2\left(16n^2+22n+7\right)}+6+6\right)+3\pi^2(2n+1)}{32-3\pi^2}}$
4	1^{++}	(M-theory)	(M-theory)
		(N/D) $m^{1^{++}}_{n=0}(T) = 2.6956, m^{1^{++}}_{n=1}(T) = 2.8995$	(N) $m^{1^{++}}_{n=0}(r_h = 0) \approx 1.137$
		$m^{1^{++}}_{n=2}(T) = 2.9346$	(D) $m^{1^{++}}_{n=0}(r_h = 0) \approx 0.665$
5	2^{++}	(M-theory)	(M-theory)
		(N) $m^{2^{++}}_{n=0}(T) = \frac{5.086}{\pi}, m^{2^{++}}_{n=1}(T) = \frac{5.269}{\pi}$	$= m^{1^{++}}_{n}(r_h = 0)$
		$m^{2^{++}}_{n=2}(T) = \frac{5.318}{\pi}$	
		$m^{2^{++}}_{n=0}(D,T) = 0, m^{2^{++}}_{n+1}(D,T) = m^{2^{++}}_{n}(N,T)$	

The $r_h \neq 0$ glueball spectrum is plotted in Fig. 2.

Some of the salient features of Table 1 and Fig. 2 are presented below:

1. Interestingly, via a WKB quantization condition using coordinate/field redefinitions of [32], the lightest 0^{++} glueball spectrum for $r_h \neq 0$ coming from scalar metric fluctuations in M-theory compares rather well with the $N \to \infty$ lattice results of [62] – refer to Table 2. Also, similar to [63], the 0^{++} coming from the scalar fluctuations of the M-theory metric is lighter than the 0^{++} coming from type IIB dilaton fluctuations. Furthermore, interestingly, one can show that by using the coordinate and field redefinitions of [64] when applied to the EOM for the dilaton fluctuation to yield a WKB quantization condition, for $a = 0.6 r_h$ – as in [33] – one obtains a match with the UV limit of the 0^{++} glueball spectrum as obtained in [32]. For our purpose, the method based on coordinate/field redefinitions of [64] is no good for obtaining the 0^{++} glueball ground state and was not used for any other glueball later on in subsequent calculations in this paper.
2. Also, from Table 1/Fig. 2, $m^{2^{++}}_{n>0} > m^{0^{++}}_{n>0}$ (scalar metric perturbations), similar to [63].
3. The higher excited states of the type IIA 0^{-+} glueball, for both $r_h \neq 0$ and $r_h = 0$, are isospectral. This is desirable because large n corresponds to the UV and that takes one away from the BH geometry, i.e., towards $r_h = 0$.
4. The non-conformal corrections up to NLO in N, have a semi-universal behavior of $\frac{(g_s M^2)(g_s N_f)\log r_0}{N}$ and turn out to be multiplied by a numerical pre-factor of $\mathcal{O}(10^{-2})$; we could disregard the same in the MQGP limit.
5. As per a more recent lattice calculation [65],[3] the 0^{++}-glueball has a mass $4.16 \pm 0.11 \pm 0.04$ (in units of the reciprocal of the 'hadronic scale parameter' of [66]), which compares rather well with $m^{0^{++}}_{n=0} = 4.267$ (in units of $\frac{r_h}{L^2}$) of Table 2 coming from scalar fluctuations of the M-theory metric. Similarly, the 0^{-+}-glueball in [65] has a mass $6.25 \pm 0.06 \pm 0.06$ and from Table 1, which matches rather nicely with $m^{0^{-+}}_{n=0}(\delta = 1.26) = 6.25$ (in units of $\frac{r_0}{L^2}$) of Table 1 coming from type IIA one-form fluctuation.
6. The ground state and the $n \gg 1$ excited states of 1^{++} and 0^{--} glueballs are isospectral.
7. The higher excited $r_h \neq 0$ 2^{++} glueball states corresponding to metric fluctuations of the M-theory metric

[3] We thank P. Majumdar for bringing this reference to our attention.

Table 4 Comparison of ratios of 0^{--} glueball masses obtained from Neumann/Dirichlet boundary conditions at the horizon, with [60]

Ratio	Our results	[60]'s results
$\frac{m^{*}_{0^{--}}}{m_{0^{--}}}$	1.0129	1.5311
$\frac{m^{**}_{0^{--}}}{m^{*}_{0^{--}}}$	1.0033	1.3244
$\frac{m^{***}_{0^{--}}}{m^{**}_{0^{--}}}$	1.0013	1.2393
$\frac{m^{****}_{0^{--}}}{m^{***}_{0^{--}}}$	1.0007	1.1588

and the ones corresponding to fluctuations of the type IIB metric, are isospectral. The $r_h = 0$ 2^{++} glueball states corresponding to metric fluctuations of the M-theory/type IIB string theory, are isospectral. Further, it turns out that due to internal cancellation of terms and $\frac{1}{\tilde{m}}$-suppression, a type IIB $r_h = 0$ 2^{++} glueball spectrum, unlike an M-theoretic computation, is unable to capture the NLO-in-N corrections to the LO-in-N type IIB 2^{++} glueball spectrum.

8. $m_n^{2^{++}}(\text{NLO}, r_h = 0) = m_n^{1^{++}}(\text{NLO}, r_h = 0) \xrightarrow{n\gg 1} m_n^{0^{--}}(\text{NLO}, r_h = 0)$, where the 'NLO' implies equality with the inclusion of NLO-in-N corrections.

Some salient features of Table 3 are presented below:

- The following is the comparison of ratios of 0^{--} glueball masses obtained in this work from Neumann/Dirichlet boundary conditions at the horizon, with [60]:
  Hence, for higher excited states, the ratio of masses of successive excited states approaches unity faster as per our results as compared to [60].
- From a comparison of results in Tables 1/2 or Fig. 2 with $N \to \infty$ lattice results, it appears that WKB quantization-based spectra are closer to $N \to \infty$ lattice results than the computations involving imposing the Neumann/Dirichlet boundary conditions at the horizon/IR cut-off. In particular, it is pleasantly surprising that the WKB quantization method applied to the 0^{++}, 0^{-+} glueball spectra, is able to provide good agreement (in fact, for the lightest 0^{++} glueball spectrum, better than the classic computations of [60]) with lattice results even for the ground and the lower excited states (Table 4).

Acknowledgements KS is supported by is supported by a senior research fellowship (SRF) from the Ministry of Human Re-source and Development (MHRD), Govt. of India. VY is supported by a junior research fellowship (JRF) from the University Grants Commission, Govt. of India. We would like to thank P. Majumdar and S. Gupta for useful communications, H. B. Filho for a useful clarification, and R. Das for participating in the material in Sect. 3.2.1 as part of his Masters' project work. One of us (AM) would like to dedicate this work to the memory of his father, the late R. K. Misra who was and (whose memory) still remains a true driving force and inspiration for him.

Funded by SCOAP[3].

Appendix A: $\widetilde{F_5^2}$, $\widetilde{F_3^2}$, H_3^2

The expressions of squares of various fluxes that figure in the EOM (180) are given below for ready reference:

$$\begin{aligned}
\widetilde{F_5^2} = &-\frac{8}{\sqrt{\pi}\sqrt{N}\sqrt{g_s}} - \frac{1}{254803968\pi^{13/2}N^{7/10}}[M^4 r^6 N_f^4 g_s^{11/2}(r^4 - r_h^4)(\phi_1+\phi_2-\psi)^2(N_f g_s \log(N)(2(r+1)\log(r)+1)\\
&+ 2\{-9(r+1)N_f g_s \log^2(r) - 2(r+1)\log(r)(2\pi - \log(4)N_f g_s) + \log(4)N_f g_s\})^2]\\
&+ a^2\left[+\frac{\pi^{3/2} r^{10} g_s^{3/2}}{956593800 N^{7/10}} - \frac{24}{\sqrt{\pi}\sqrt{N}\sqrt{g_s} r^2} - \frac{1}{84934656\pi^{13/2}N^{7/10}}\right.\\
&\times \{M^4 r^6 N_f^4 g_s^{11/2}(r^4 - r_h^4)(\phi_1+\phi_2-\psi)^2(24 r\log r - 1)(N_f g_s \log(N)(2(r+1)\log(r)+1)\\
&\left.+ 2\{-9(r+1)N_f g_s \log^2(r) - 2(r+1)\log(r)(2\pi - \log(4)N_f g_s) + \log(4)N_f g_s\})^2\}\right];\\
\widetilde{F_3^2} = &\frac{729 M^2 N_f^2 \sqrt{g_s}(r^4 - r_h^4)(72 a^2 N^{2/5}\log(r) + a^2(-(3N^{2/5}+4)) + 2N^{2/5} r^2)}{128\pi^{7/2} N^{11/10} r^6};\\
H_3^2 = &\frac{243 M^2 N_f^2 g_s^{5/2}(r^4 - r_h^4)(144 a^2(\sqrt[5]{N}+3) r\log(r) + a^2(9 - 15\sqrt[5]{N}) + 2\left(\sqrt[5]{N}+1\right)r^2)}{256\pi^{7/2}\sqrt{N} r^6};
\end{aligned}$$

$$\widetilde{F}_{x_2x_3p_3p_4p_5}\widetilde{F}_{x_2x_3q_3q_4q_5}g^{p_3q_3}g^{p_4q_4}g^{p_5q_5}h^{x_2x_3} = \frac{60r^4}{\pi^{3/2}N^{3/2}g_s^{3/2}} - \frac{1}{169869312\pi^{13/2}N^{7/10}}$$
$$\times[5M^4r^{10}N_f^4g_s^{9/2}(r^4-r_h^4)(\phi_1+\phi_2-\psi)^2(N_fg_s\log(N)(2(r+1)\log(r)+1)$$
$$+2\{-9(r+1)N_fg_s\log^2(r)-2(r+1)\log(r)(2\pi-\log(4)N_fg_s)+\log(4)N_fg_s\})^2]$$
$$+a^2\left[\frac{180r^2}{\pi^{3/2}N^{3/2}g_s^{3/2}}+\frac{1}{56623104\pi^{15/2}N^{17/10}}\{5M^4r^{10}N_f^4g_s^{9/2}(r^4-r_h^4)(\phi_1+\phi_2-\psi)^2\right.$$
$$\times(24r\log r-1)(N_fg_s\log(N)(2(r+1)\log(r)+1)+2\{-9(r+1)N_fg_s\log^2(r)-2(r+1)\log(r)$$
$$\left.\times(2\pi-\log(4)N_fg_s)+\log(4)N_fg_s\})^2\}\right]. \quad \text{(A1)}$$

References

1. J.M. Maldacena, The large N limit of superconformal field theories and supergravity. Adv. Theor. Math. Phys. **2**, 231–252 (1998). doi:10.1023/A:1026654312961. arXiv:hep-th/9711200
2. G. Boyd, J. Engels, F. Karsch, E. Laermann, C. Legeland, M. Luetgemeier, B. Petersson, Thermodynamics of SU(3) lattice gauge theory. Nucl. Phys. B **469**, 419–444 (1996). arXiv:hep-lat/9602007
3. M. Natsuume, String theory and quark-gluon plasma. arXiv:hep-ph/0701201 (2007)
4. P. Colangelo, F. Giannuzzi, S. Nicotri, Holographic approach to finite temperature QCD: the case of scalar glueballs and scalar and scalar mesons. Phys. Rev. D **80**, 094019 (2009). doi:10.1103/PhysRevD.80.094019. arXiv:0909.1534 [hep-ph]
5. S. Nicotri, Scalar glueball in a holographic model of QCD. Nuovo Cim. B **123**, 796, 851 (2008). doi:10.1393/ncb/i2008-10579-5. doi:10.1393/ncb/i2008-10580-0. arXiv:0807.4377 [hep-ph]
6. H. Forkel, Glueball correlators as holograms. PoS (CONFINEMENT8) 184 (2008). arXiv:0808.0304 [hep-ph]
7. H. Forkel, Holographic glueball structure. Phys. Rev. D **78**, 025001 (2008). doi:10.1103/PhysRevD.78.025001. arXiv:0711.1179 [hep-ph]
8. D. Li, M. Huang, Dynamical holographic QCD model for glueball and light meson spectra. JHEP **1311**, 088 (2013). doi:10.1007/JHEP11(2013)088. arXiv:1303.6929 [hep-ph]
9. E. Folco Capossoli, H. Boschi-Filho, Renormalized AdS_5 mass for even spin glueball and Pomeron trajectory from a holographic softwall model. arXiv:1611.09817 [hep-ph]
10. F. Jugeau, Holographic description of glueballs in a deformed AdS-dilaton background. AIP Conf. Proc. **964**, 151 (2007). doi:10.1063/1.2823842. arXiv:0709.1093 [hep-ph]
11. P. Colangelo, F. De Fazio, F. Jugeau, S. Nicotri, On the light glueball spectrum in a holographic description of QCD. Phys. Lett. B **652**, 73 (2007). doi:10.1016/j.physletb.2007.06.072. arXiv:hep-th/0703316
12. W.H. Huang, Holographic description of glueball and baryon in noncommutative dipole gauge theory. JHEP **0806**, 006 (2008). doi:10.1088/1126-6708/2008/06/006. arXiv:0805.0985 [hep-ph]
13. Y. Chen, M. Huang, Two-gluon and trigluon glueballs from dynamical holography QCD. Chin. Phys. C **40**(12), 123101 (2016). doi:10.1088/1674-1137/40/12/123101. arXiv:1511.07018 [hep-ph]
14. I. Gordeli, D. Melnikov, Calculation of glueball spectra in supersymmetric theories via holography. arXiv:1311.6537 [hep-ph]
15. K. Hashimoto, C.I. Tan, S. Terashima, Glueball decay in holographic QCD. Phys. Rev. D **77**, 086001 (2008). doi:10.1103/PhysRevD.77.086001. arXiv:0709.2208 [hep-th]
16. F. Brunner, A. Rebhan, Holographic QCD predictions for production and decay of pseudoscalar glueballs. Phys. Lett. B **770**, 124–130 (2017). arXiv:1610.10034 [hep-ph]
17. A. Rebhan, F. Brunner, D. Parganlija, Glueball decay patterns in top-down holographic QCD. PoS **EPS–HEP2015**, 421 (2015). arXiv:1511.01391 [hep-ph]
18. D. Parganlija, Scalar glueball in a top-down holographic approach to QCD. Acta Phys. Pol. Suppl. **8**(1), 219 (2015). doi:10.5506/APhysPolBSupp.8.219. arXiv:1503.00550 [hep-ph]
19. F. Brunner, D. Parganlija, A. Rebhan, Top-down holographic glueball decay rates. AIP Conf. Proc. **1701**, 090007 (2016). doi:10.1063/1.4938709. arXiv:1502.00456 [hep-ph]
20. F. Brunner, D. Parganlija, A. Rebhan, Holographic glueball decay. Acta Phys. Pol. Suppl. **7**(3), 533 (2014). doi:10.5506/APhysPolBSupp.7.533. arXiv:1407.6914 [hep-ph]
21. D. Paragnlija, Tensor glueball in a top-down holographic approach to QCD. Acta Phys. Pol. Suppl. **8**(2), 289 (2015). doi:10.5506/APhysPolBSupp.8.289. arXiv:1506.03000 [hep-ph]
22. E. Folco Capossoli, H. Boschi-Filho, Glueball spectra and Regge trajectories from a modified holographic softwall model. Phys. Lett. B **753**, 419 (2016). doi:10.1016/j.physletb.2015.12.034. arXiv:1510.03372 [hep-ph]
23. E. Witten, Anti-de Sitter space, thermal phase transition and confinement in gauge theories. Adv. Theor. Math. Phys. **2**, 505 (1998). arXiv:hep-th/9803131
24. J. Polchinski, M.J. Strassler, Hard scattering and gauge/string duality. Phys. Rev. Lett. **88**, 031601 (2002). arXiv:hep-th/0109174
25. K. Sil, A. Misra, On aspects of holographic thermal QCD at finite coupling. Nucl. Phys. B **910**, 754 (2016). arXiv:1507.02692 [hep-th]
26. M. Dhuria, A. Misra, Transport coefficients of black MQGP M3-branes. Eur. Phys. J. C **75**(1), 16 (2015). arXiv:1406.6076 [hep-th]
27. M. Mia, K. Dasgupta, C. Gale, S. Jeon, Five easy pieces: the dynamics of quarks in strongly coupled plasmas. Nucl. Phys. B **839**, 187 (2010). arXiv:0902.1540
28. M. Dhuria, A. Misra, Towards MQGP. JHEP **1311**, 001 (2013). arXiv:1306.4339
29. I.R. Klebanov, E. Witten, Superconformal field theory on three-branes at a Calabi–Yau singularity. Nucl. Phys. B **536**, 199 (1998). arXiv:hep-th/9807080
30. S.S. Gubser, Einstein manifolds and conformal field theories. Phys. Rev. D **59**, 025006 (1999). doi:10.1103/PhysRevD.59.025006. arXiv:hep-th/9807164
31. N. Kochelev, Ultralight glueballs in quark-gluon plasma. Phys. Part. Nucl. Lett. **13**(2), 149 (2016). doi:10.1134/S1547477116020138. arXiv:1501.07002 [hep-ph]
32. J.A. Minahan, Glueball mass spectra and other issues for supergravity duals of QCD models. JHEP **9901**, 020 (1999). doi:10.1088/1126-6708/1999/01/020. arXiv:hep-th/9811156

33. K. Sil, A. Misra, New insights into properties of large-N holographic thermal QCD at finite gauge coupling at (the non-conformal/next-to) leading order in N. Eur. Phys. J. C **76**(11), 618 (2016). doi:10.1140/epjc/s10052-016-4444-7. arXiv:1606.04949 [hep-th]
34. I.R. Klebanov, A. Tseytlin, Gravity duals of supersymmetric $SU(N) \times SU(M+N)$ gauge theories. Nucl. Phys. B **578**, 123–138 (2000). arXiv:hep-th/0002159
35. I.R. Klebanov, M.J. Strassler, Supergravity and a confining gauge theory: duality cascades and X SB-resolution of naked singularities. JHEP **0008**, 052 (2000). arXiv:hep-th/0007191
36. P. Ouyang, Holomorphic D7-branes and flavored N=1 gauge theories. Nucl. Phys. B **699**, 207–225 (2004). arXiv:hep-th/0311084
37. A. Buchel, Finite temperature resolution of the Klebanov–Tseytlin singularity. Nucl. Phys. B **600**, 219 (2001). arXiv:hep-th/0011146
38. S.S. Gubser, C.P. Herzog, I.R. Klebanov, A.A. Tseytlin, Restoration of chiral symmetry: a supergravity perspective. JHEP **0105**, 028 (2001). arXiv:hep-th/0102172
39. A. Buchel, C.P. Herzog, I.R. Klebanov, L.A. Pando Zayas, A.A. Tseytlin, Nonextremal gravity duals for fractional D-3 branes on the conifold. JHEP **0104**, 033 (2001). arXiv:hep-th/0102105
40. M. Mahato, L.A. Pando Zayas, C.A. Terrero-Escalante, Black holes in cascading theories: confinement/deconfinement transition and other thermal properties. JHEP **0709**, 083 (2007). arXiv:0707.2737 [hep-th]
41. B.A. Burrington, J.T. Liu, L.A. Pando Zayas, D. Vaman, Holographic duals of flavored N = 1 super Yang–Mills: beyond the probe approximation. JHEP **0502**, 022 (2005). arXiv:hep-th/0406207
42. M. Mia, F. Chen, K. Dasgupta, P. Franche, S. Vaidya, Non-extremality, chemical potential and the infrared limit of large N thermal QCD. Phys. Rev. D **86**, 086002 (2012). arXiv:1202.5321 [hep-th]
43. M. Mia, K. Dasgupta, C. Gale, S. Jeon, Toward large N thermal QCD from dual gravity: the heavy quarkonium potential. Phys. Rev. D **82**, 026004 (2010). arXiv:1004.0387 [hep-th]
44. A. Strominger, S.T. Yau, E. Zaslow, Mirror symmetry is T duality. Nucl. Phys. B **479**, 243 (1996). arXiv:hep-th/9606040
45. M. Ionel, M. Min-Oo, Cohomogeneity one special Lagrangian 3-folds in the deformed and the resolved conifolds. Ill. J. Math. **52**(3), 839–865 (2008)
46. S. Alexander, K. Becker, M. Becker, K. Dasgupta, A. Knauf, R. Tatar, In the realm of the geometric transitions. Nucl. Phys. B **704**, 231 (2005). arXiv:hep-th/0408192
47. F. Chen, K. Dasgupta, P. Franche, S. Katz, R. Tatar, Supersymmetric configurations, geometric transitions and new non-Kahler manifolds. Nucl. Phys. B **852**, 553 (2011). arXiv:1007.5316
48. D. Tong, NS5-branes, T duality and world sheet instantons. JHEP **0207**, 013 (2002). arXiv:hep-th/0204186
49. A. Sen, Dynamics of multiple Kaluza–Klein monopoles in M and string theory. Adv. Theor. Math. Phys. **1**, 115 (1998). arXiv:hep-th/9707042
50. F. Chen, K. Dasgupta, P. Franche, S. Katz, R. Tatar, Supersymmetric configurations, geometric transitions and new non-Kahler manifolds. Nucl. Phys. B **852**, 553 (2011). arXiv:1007.5316 [hep-th]
51. G. Lopes Cardoso, G. Curio, G. Dall'Agata, D. Lust, P. Manousselis, G. Zoupanos, NonKahler string backgrounds and their five torsion classes. Nucl. Phys. B **652**, 5 (2003). arXiv:hep-th/0211118
52. A. Butti, M. Grana, R. Minasian, M. Petrini, A. Zaffaroni, The baryonic branch of Klebanov–Strassler solution: a supersymmetric family of SU(3) structure backgrounds. JHEP **0503**, 069 (2005). arXiv:hep-th/0412187
53. S. Grigorian, Deformations of G2-structures with torsion. Asian J. Math. **20**, 123–156 (2016). arXiv:1108.2465
54. R.L. Bryant, Some remarks on G(2)-structures. Proceeding of Gokova Geometry-Topology Conference 2005, International Press, pp, 75–109. arXiv:math/0305124 [math-dg]
55. S. Karigiannis, Geometric flows on manifolds with G_2 structure. Commun. Math. Phys. **280**, 403–425 (2008). arXiv:math/0702077
56. P. Kaste, R. Minasian, M. Petrini, A. Tomasiello, Kaluza–Klein bundles and manifolds of exceptional holonomy. JHEP **0209**, 033 (2002). arXiv:hep-th/0206213
57. C. Csaki, Y. Oz, J. Russo, J. Terning, Large N QCD from rotating branes. Phys. Rev. D **59**, 065012 (1999). doi:10.1103/PhysRevD.59.065012. arXiv:hep-th/9810186
58. E. Kiritsis, *String Theory in a Nutshell* (Princeton University Press, Princeton, 2007)
59. R.C. Brower, S.D. Mathur, C.I. Tan, Discrete spectrum of the graviton in the AdS(5) black hole background. Nucl. Phys. B **574**, 219 (2000). doi:10.1016/S0550-3213(99)00802-0. arXiv:hep-th/9908196
60. C. Csaki, H. Ooguri, Y. Oz, J. Terning, Glueball mass spectrum from supergravity. JHEP **9901**, 017 (1999). doi:10.1088/1126-6708/1999/01/017. arXiv:hep-th/9806021
61. H. Boschi-Filho, N.R.F. Braga, Gauge/string duality and scalar glueball mass ratios. JHEP **0305**, 009 (2003). arXiv:hep-th/0212207
62. M.J. Teper, SU(N) gauge theories in (2+1)-dimensions. Phys. Rev. D **59**, 014512 (1999). doi:10.1103/PhysRevD.59.014512. arXiv:hep-lat/9804008
63. R.C. Brower, S.D. Mathur, C.I. Tan, Discrete spectrum of the graviton in the AdS_5 black hole background. Nucl. Phys. B **574**, 219 (2000). doi:10.1016/S0550-3213(99)00802-0. arXiv:hep-th/9908196
64. A.S. Miranda, C.A. Ballon Bayona, H. Boschi-Filho, N.R.F. Braga, Black-hole quasinormal modes and scalar glueballs in a finite-temperature AdS/QCD model. JHEP **0911**, 119 (2009). arXiv:0909.1790 [hep-th]
65. Y. Chen et al., Glueball spectrum and matrix elements on anisotropic lattices. Phys. Rev. D **73**, 014516 (2006). doi:10.1103/PhysRevD.73.014516. arXiv:hep-lat/0510074
66. R. Sommer, A new way to set the energy scale in lattice gauge theories and its applications to the static force and alpha-s in SU(2) Yang–Mills theory. Nucl. Phys. B **411**, 839 (1994). doi:10.1016/0550-3213(94)90473-1. arXiv:hep-lat/9310022